T.C. İSTANBUL KÜLTÜR UNIVERSITY

INSTITUTE OF GRADUATE STUDIES

SEISMIC PROTECTION OF STORAGE RACK SYSTEMS WITH BASE ISOLATION

Master of Applied Science Thesis

Mir Mohammad Amer Yahya

1700005179

Department: Civil Engineering

Programme: Structural Engineering

Supervisor: Assist. Prof. Dr. Gökhan YAZICI

July 2020

T.C. İSTANBUL KÜLTÜR UNIVERSITY

INSTITUTE OF GRADUATE STUDIES

SEISMIC PROTECTION OF STORAGE RACK SYSTEM WITH BASE ISOLATION

Master of Applied Science Thesis

Mir Mohammad Amer Yahya

1700005179

Department: Civil Engineering

Programme: Structural Engineering

Supervisor: Assist. Prof. Dr. Gökhan YAZICI

July 2020

T.C. İSTANBUL KÜLTÜR UNIVERSITY

INSTITUTE OF GRADUATE STUDIES

SEISMIC PROTECTION OF STORAGE RACK SYSTEM WITH BASE ISOLATION

Master of Applied Science Thesis

Mir Mohammad Amer Yahya
1700005179

Date of Submission: Civil Engineering
Date of defence examination: 2 July 2020

Supervisor and Chairperson:
Assist. Prof Dr. Gökhan YAZICI
Members of Examining Committee:
Assist. Prof Dr. Erdal COSKUN
Prof Dr. Cenk ALHAN (Istanbul University - Cerrahpasa)

July 2020

ACKNOWLEDGEMENT

I would like to express my sincere appreciation to Assist. Prof. Dr. Gökhan YAZICI for his guidance, time and patience throughout thesis meetings. I would also like to thank my family for their support and encouragement throughout my whole life.

University : **İstanbul Kültür University**
Institute : **Institute of Graduate Studies**
Department : **Civil Engineering**
Programme : **Structural Engineering**
Supervisor : **Assist. Prof. Dr. Gökhan YAZICI**
Degree Awarded and Date : **MSc Thesis – July 2020**

ABSTRACT

SEISMIC PROTECTION OF STORAGE RACK SYSTEMS WITH BASE ISOLATION

Mir Mohammad Amer Yahya

Steel storage rack systems are widely used in warehouses and stores for storing different types of products accessible for public and employees. Structural components of these systems consist of slender, thin-walled open section steel members, which are quite susceptible to buckling, and the live loads acting on these structures are much greater than the self-weight of these structures. These issues complicate the design and analysis of steel storage racks under earthquake loads. In addition, failure of these systems during earthquakes can result in the loss of lives of employees and customers in addition to economic losses due to damages to stored products and disruption of services. This study investigates the use of base isolation to improve the seismic response of steel storage racks. Seismic isolation system consists of friction pendulum bearings that support the floor slab underneath the storage racks. The model geometry and the loads supported by the steel storage rack has been adapted from the Seisracks 2 project. Finite element model of the fixed base storage racks was created using SAP 2000 and calibrated with the experimental results from the Seisracks 2 project. A parametric study which covered the variation of friction coefficients and distribution of live loads was conducted with a suite of 12 earthquakes to investigate the reductions in rack accelerations and drifts as well as the changes in bearing displacements. Results of the parametric study indicate that seismic isolation was effective for reducing the response parameters and distribution of live load as well as the friction coefficient of bearings can have a significant influence on the seismic response.

Keywords: Steel Storage Racks, Friction Pendulum System, Seismic Isolation, Earthquake Resistant Design

Üniversite	**:**	**İstanbul Kültür Üniversitesi**
Enstitüsü	**:**	**Lisansüstü Eğitim Enstitüsü**
Anabilim Dalı	**:**	**İnşaat Mühendisliği**
Programı	**:**	**Yapı (İngilizce)**
Tez Danışmanı	**:**	**Dr. Öğretim Üyesi Gökhan YAZICI**
Tez Türü ve Tarihi	**:**	**Yüksek Lisans – Temmuz 2020**

KISA ÖZET

DEPOLAMA RAF SİSTEMLERİNİN SİSMİK İZOLASYONLA DEPREMDEN KORUNMASI

Mir Mohammad Amer Yahya

Çelik raf sistemleri, depolar ve mağazalar gibi halka ve çalışanların erişimine açık yerlerde farklı tipte ürünleri depolamakta yaygın olarak kullanılmaktadır. Bu sistemlerin yapısal bileşenleri, burkulmaya maruz olabilecek ince cidarlı açık kesitli çelik elemanlardan oluşmaktadır ve bu sistemlere etkiyen hareketli yükler sistemin zati ağırlığından oldukça büyük olabilmektedir. Bu sebepler çelik raf sistemlerinin deprem yükleri etkisi altında analizini ve boyutlandırılmasını güçleştirmektedir. Buna ek olarak, bu sistemlerin deprem etkisiyle hasar görmesi, depolanan ürünlere gelebilecek hasarlar veya hizmetleri aksamasına bağlı oluşacak ekonomik kayıplara ek olarak çalışanların ve müşterilerin yaralanmaları veya ölümüne neden olabilmektedir. bu makalede, depolama raflarının tabanında Tek Sürtünme İzolatörlerinin kullanımı yapılmıştır. Yalıtılmış rafın yer değiştirmesi ve hızlanması sabit tabanlı rafla karşılaştırıldı. Ayrıca, 6 uzak saha ve 6 yakın saha depreminde farklı yükleme türlerinde raf yapısının davranışı gözlenmiştir. Raf yapısı SAP2000 ticari yazılımı kullanılarak modellenmiştir ve sonuçlar sunulmuştur.

Anahtar Kelimeler: Çelik Depolama Rafları, Sürtünmeli Sarkaç Sistemi, Sismik Yalıtım, Depreme Dayanıklı Tasarım

TABLE OF CONTENTS

ABBREVIATIONS

ASCE: American Society of Civil Engineers

PGA: Peak Ground Acceleration

PGV: Peak ground velocity

MFPS: Multi-Friction Pendulum Structures

SLE: Service Level Earthquake

DBE: Design Based Earthquake

MCE: Maximum Considered Earthquake

FEMA: Federal Emergency Management Agency

NHERP: National Earthquake Hazards Reduction Program

FNA: Non-linear Time History Analysis

PEER: Pacific Earthquake Engineering Research Centre

PTFE: Polytetrafluoroethylene

FPS: Single Friction Isolator

SEAONC: Structural Engineers Association of Northern California

UBC: Uniform Building Code

AASHTO: American Association of State Highway and Transportation Officials

EPS: Earthquake Protection Systems

TCL: Tool Command Language

THA: Time History Analysis

LIST OF TABLES

LIST OF FIGURES

LIST OF SYMBOLS

β: Damping ratio

β_s, β_b: Superstructure and base damping ratio

B_D, B_M: Design and maximum damping correction factor

c_s, c_b: Superstructure and base damping coefficients

C: Damping coefficient

d: Longest plan dimension (m)

d: Friction pendulum displacement capacities (m)

d_1, d_2, d_3, d_4: Friction pendulum displacement capacities 1, 2, 3 and 4 (m)

D_D, D_M: Design and maximum displacement (m)

D_{TD}, D_{TM}: Total design and total maximum displacement (m)

D: Bearing displacement (m)

Eh: Hysteretic damping energy (KN/m)

EDC: Energy dissipation circle (KN/m)

g: Acceleration due to gravity m/s^2

F: Lateral force (KN)

F_f: Frictional force (KN)

F_s: Story force (KN)

h: Friction pendulum height (m)

k: Lateral force distribution correction coefficient

K: Stiffness (KN/m)

K_d: Bearing stiffness (KN/m)

K_{eff}: Effective bearing stiffness (KN/m)

1. Introduction

Large-scale steel storage racks have become a significant component of warehouses, stores, and many other facilities. These systems are available in a variety of types, size and shapes and their configurations can be adjusted with ease. The height of storage rack structures can reach up to 35 meters. The components of a typical steel storage rack is shown in the Figure 1. A large number of steel storage racks use a moment frame in the down aisle direction and a braced frame in cross aisle direction to resist horizontal loads such as earthquakes and forklift impact loads [5]. Structural components of steel storage racks in use today are generally thin-walled open sections. Live loads acting on these structures are considerably high compared to their self-weight. All of these factors contribute to the susceptibility of the steel storage rack systems to earthquake related damages. During earthquakes, racks can collapse, overturn or the stored contents may slide off. Since these systems are often used in publicly accessible spaces, their failure can result in the injuries and casualties in addition to economic losses and disruption of services.

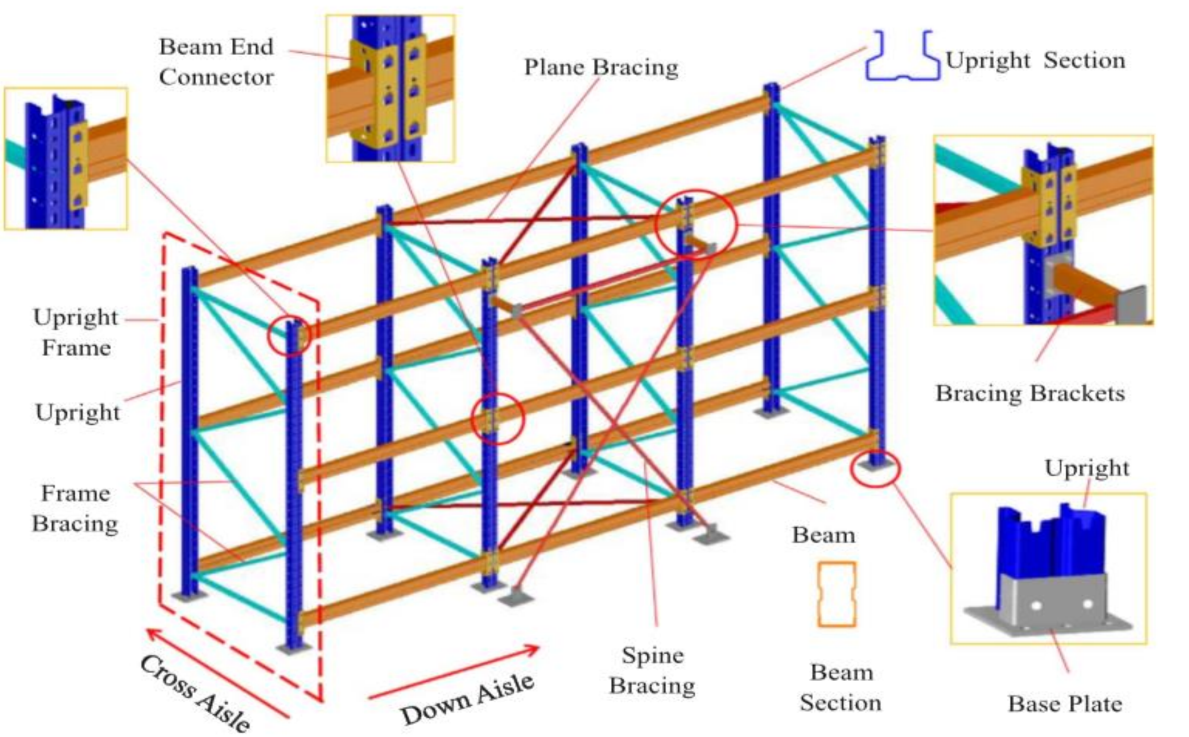

Figure 1: Typical racking system [5]

1.1 Steel Storage Racks

Design of steel storage racks under seismic loads require to understand the behavior of racks completely. Hence, in this section different parts of racks have been studied and explained.

1.1.1 Beam End Connectors

Steel storage racks consist of beams, uprights, base-plate and bracings. The connections between beam and upright are called beam end connectors. Beam end connectors have a significant effect on the global response of steel storage rack systems under external forces. Especially the seismic response of rack structure in the longitudinal direction significantly depends on the behavior of these connections. Many researchers have stated that taking into account the inelastic response of beam end connectors is crucial for modelling rack systems under seismic excitations [20,28].

There are different kinds of beam end connector types with various member geometries. The connection of beam to upright or beam end connectors can be established by bolts or hooks. The hook connections of beam to upright is done with tabs which are perforations on the uprights. Additionally, hooks have a semi-rigid behavior. Various types of beam end connectors make it impossible to a typical moment rotation behavior, therefore, several studies have been conducted regarding to beam end connections [20].

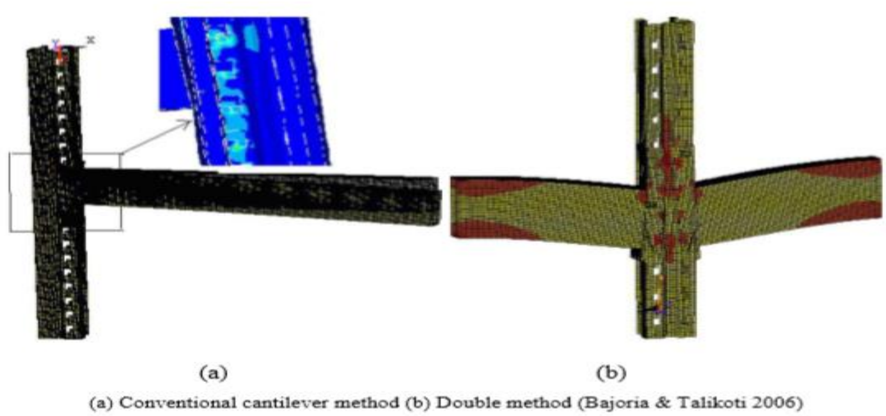

Figure 2: Modelled by ANSYS software for finite element analysis [28]

1.1.2 Upright and Base plate

Uprights are cold-formed steel members. Existence of perforation along its height is the main characteristic of an upright that allows assemblage of braces and other structural elements. Perforations along the height of an upright significantly influence the structural behavior of the upright and it is recommended to take it into account during design.

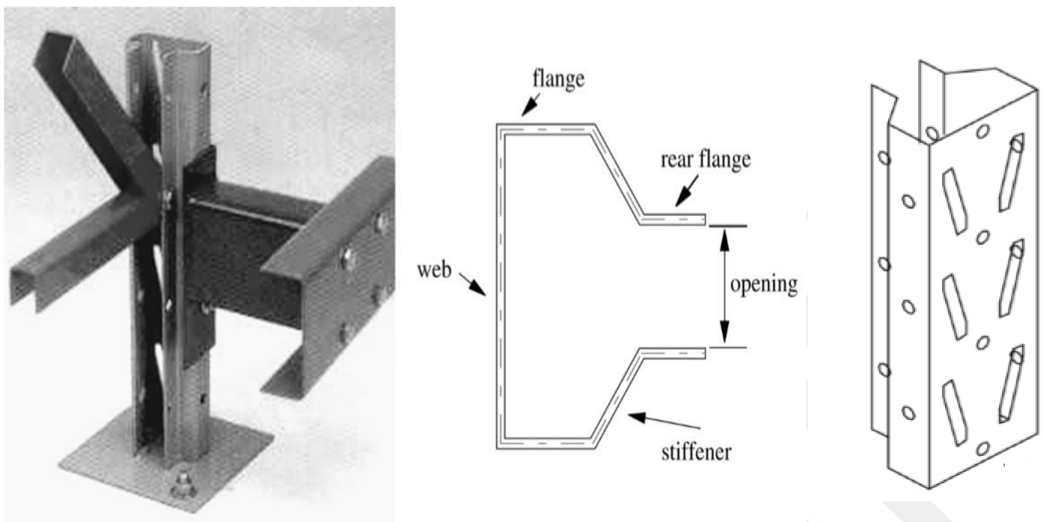

Figure 3: A typical upright with the cross section [29]

Uprights are connected to the base plates, where base plates are usually fixed to the ground. Performance of base plate connections depends on the level of axial loads applied to the upright.

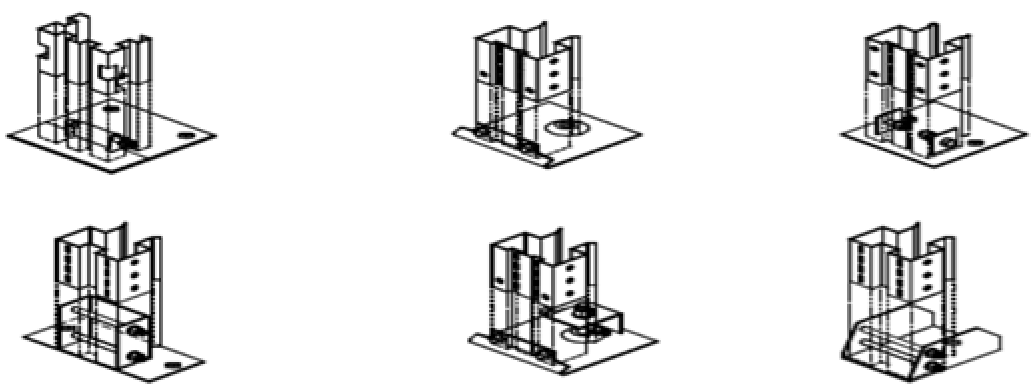

Figure 4: Typical base-plate connections [29]

At the University of Trento, the response of base-plate under axial eccentric load was studied. Results point out a notable non-linear behavior in base joints.[29]

Freitas and his colleagues conducted a study on perforations, material properties, collapse mode and ultimate strength of uprights when subjected to compression. Their numerical study results were compared to the experimental results pointing out that RMI codes considered conservative values (Freitas et al. 2005) [30].

1.1.3 Bracing

Braces are being used for providing of stability to steel storage racks mostly in cross-aisle direction. Braces are connected to uprights forming a hinge joint. Bracings can be applied as diagonal bracing, plane bracing and spine bracings in steel storage rack structures.

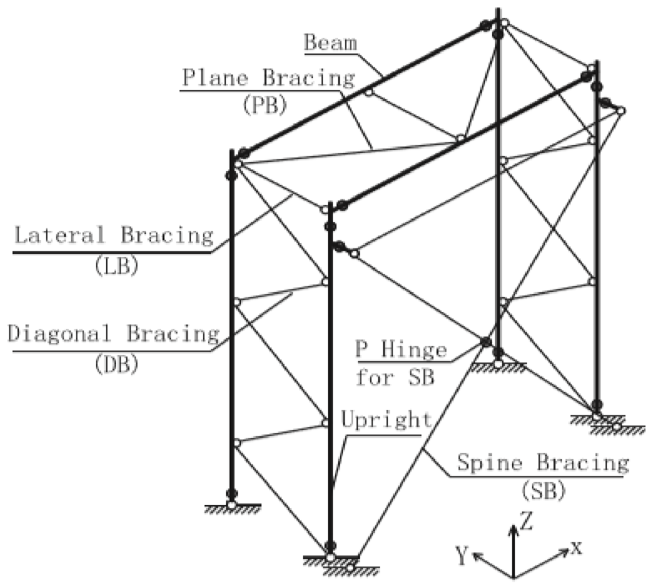

Figure 5: Typical rack structure with diagonal, plane and spine bracings [35]

During the 1992 Landers Earthquake, the storage racks at the Builders Emporium Store had broken away from their anchorages in the wall pilasters and in some places had battered their way through the walls. Storage racks at Santa Carlita Store failed during the 1994 Northridge Earthquake, as the load carrying capacity of the racks was inadequate to support the weight of stored goods and as a result, several bays of racks failed completely in the cross-aisle direction, which in turn caused considerable damages to the stored contents. The 2003 San Simeon Earthquake caused rack failure in a big-box store due to pallets with lower coefficient of friction. A small lawn tractor on a steel palleted slid off the top of a rack and cans of roofing tar fell off another rack from a significant height. Similarly, during the 2001 Nisqually Earthquake, Storage racks at Olympia store had rack damages due to element buckling of some diagonal braces. The mentioned rack damages during earthquakes are provided by FEMA 460 (2005) [2].

Figure 6: Collapse of a rack structure during earthquake at the Santa Clarita Store [2]

Figure 7: Collapse of a rack structure at the Santa Clarita Store [2]

Figure 8: Collapse of a rack structure at the Santa Clarita Store [2]

Crosier et. al. (2010) [3] surveyed the damages of Darfield Earthquake that occurred in New Zealand at 2010. According to their report, facilities and businesses such as a kitchen cabinet manufacturer, miscellaneous storage providers, a glass workshop, a milk distribution center, a food distribution center that were using steel storage rack structures were partially damaged and some were severely damaged. The damages included collapse of rack structures, damage of goods, failure in down-aisle direction of racks and extensive damage to products.

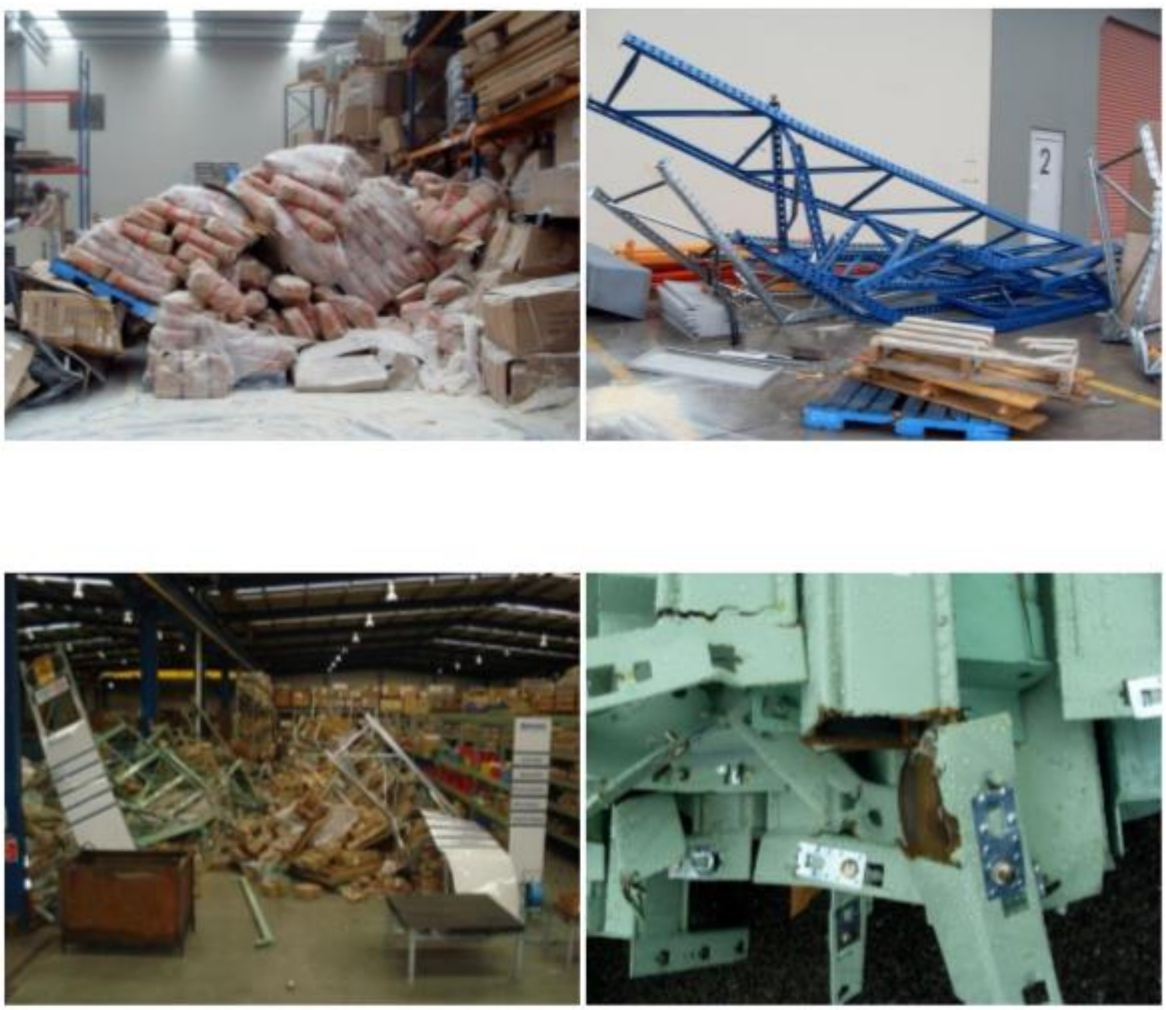

Figure 9: Damages from the 2010 Darfield Earthquake [3]

The susceptibility of steel storage racks have motivated research on the analysis and design procedures for the seismic design of these structures.

SEISRACKS [51] project, launched in 2004 and ended in 2007, was funded by the European Union and focused on the design of seismic pallet racking systems. Following this research project, the follow up project titled SEISRACKS 2 started in 2007 [52].

Freitas et al. (2005) analyzed steel storage rack columns; the results of analysis show that imperfections and material properties in stub columns have a strong influence on their structural performance [10].

Linfeng et al. (2012), investigated the effect of spine bracing and reported that the existence of spine bracing in the rack systems significantly improves the seismic performance of storage racks as unbraced pallet racks critically depend on the beam end connectors to resist lateral loading [6].

Baldassino et al. (2014) studied performance of beam to column joints and base-plate connections of steel storage racks with 61 different types of joints. The results of 238 tests show the actual response of beam-end connectors provide a non-negligible degree of lateral stiffness of the frame and as a consequence, semi-continuous frame model is always suggested for a more refined and "optimal" design analysis [9].

Zhao et al. (2014) studied the flexural behavior of beam end connections under hogging loading in a single cantilever test setup. They studied 17 types of beam end connections, where various parameters such as profile of the upright, thickness and number of tabs in connector were investigated. Experiment results stated that failure mode of beam end connectors depend on the relative thickness between the beam end connector and upright [23].

Giordanoa et al. (2014) investigated experimentally the behavior of three different types of beam end connections of steel storage racks and compared results of experimental tests under both monotonic and cyclic loads. Type A connector is with four hooks which is folded at its end, type B connector is with five hooks which is welded to the beam end with a double-sided welding, type C is formed by the same connection as type B but it is welded all around the beam end section. This study concluded that in monotonic tests, connections with the folded ends are more deformable. However, when the welding is done all around the beam end section, the connection failure may associate with the collapse of tabs with higher ultimate moments and rotations. Also, the cyclic test is confirming the various behavior of rack connections with comparisons to traditional steel joints [24].

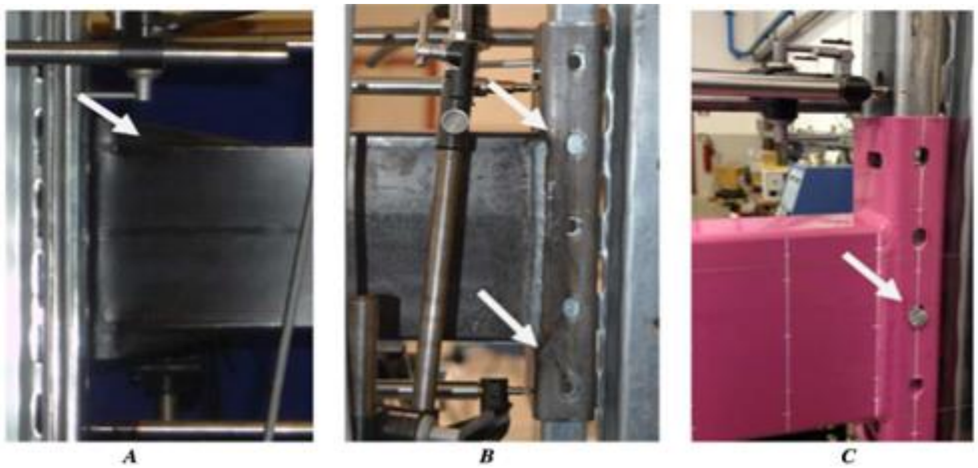

Figure 10: All three beam end connectors type [24]

Yin et al. (2018) studied a steel storage rack with spine bracing. It was observed that after applying lateral forces during pushover analysis, spine bracing bears the majority of shear force [35].

Around the world, codes of design for large scale steel storage racks are being developed. In the United States, RMI (Rack Manufacturers Institute) [48] published its first “Minimum Engineering Standards for Industrial Storage Racks.” in 1964. To reflect this rapid development and to assure adequate safety performance of modern rack structures, the RMI decided early in 1971 to replace its original standards by a more detailed and comprehensive specification. Continued testing and parametric studies of RMI during past years resulted in the 2002 Specification [49]. In 2004 the 2002 RMI Specification and Commentary were adopted in the American National Standard ANSI MH 16.1-2004 [49] which was again revised in 2008 [1].

FEMA-460 (2005) [2], a design guideline for the seismic considerations for steel storage racks developed for FEMA, addresses the issues regarding the mitigation of the life-safety risk posed by the storage racks in publicly accessible areas of retail stores.

In Canada\ Canadian Standard Associations building code for steel storage racks CSA A344 (2005) [53] went into effect in 2005. Priorly, RMI Specifications were used for the design of storage rack systems in Canada.

The first Australian Standard for Steel Storage Racks AS4084 was published in 1993. In 2009 [54] a new draft for steel storage rack structures was introduced and a new version of the Australian Standard AS 4084 was published in 2012 [55].

Widespread use of large-scale steel storage rack systems in seismically active regions have also motivated researchers to implement seismic isolation and energy dissipation systems to protect these structures and their contents from earthquake induced damages.

FEMA-460 suggested seismic isolators best option for the safety of storage rack systems in seismic zones.

Filiatrault et al. (2008) [45] studied experimentally the seismic behavior of storage racks which were isolated by an innovative base isolation (Figure 11). The isolated rack was designed to meet FEMA460 requirements. A series of uniaxial and triaxial tests with real merchandise on shake table have been conducted. Results displayed a significant improvement in behavior of a rack structure incorporating a new cross-aisle base isolation system. It was concluded that the rigid based racks did not meet the expected performance objectives recommended in the FEMA460 document.

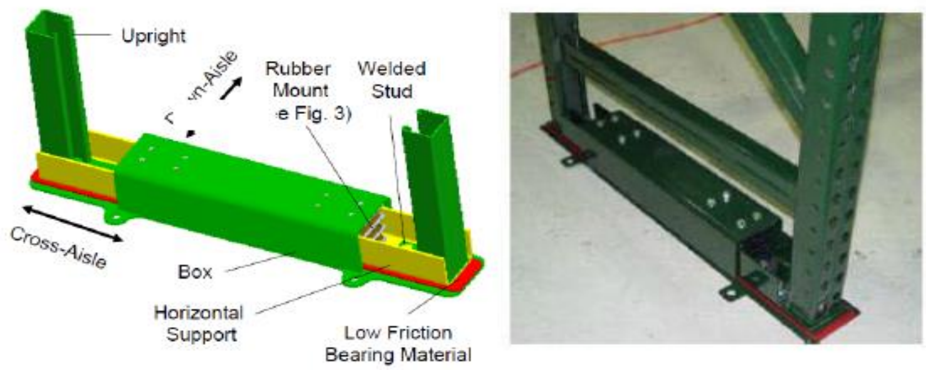

Figure 11: Innovative Base Isolation for steel storage rack [45]

Patent N0.: US 7,263,806 B2 (United States Patent Pellegrino et al.) (2007) is an invention of storage rack vibration isolators by Pellegrino and his colleagues. The effects of seismic forces on a storage rack system mounted on a floor are reduced through the use of the storage rack vibration isolators constructed according to this invention [12].

Robert et al. (2010) developed a new base isolation system and experimentally studied seismic response of a steel pallet storage rack. The experiment was done both on base isolated and rigid based storage racks and results were compared. Seismic test results observed that base isolated rack remained damage free up to 100% test level, however, rigid based rack faced severe local inelastic buckling in central upright and weld cracking at the central horizontal bracing member. After this damage seismic testing was stopped for rigid based rack for not being enough stable for 100% test level. Additionally, it is observed that merchandise spillage will not happen at this level of acceleration. But the rigid based rack under the same excitation lost almost all of its merchandise [11].

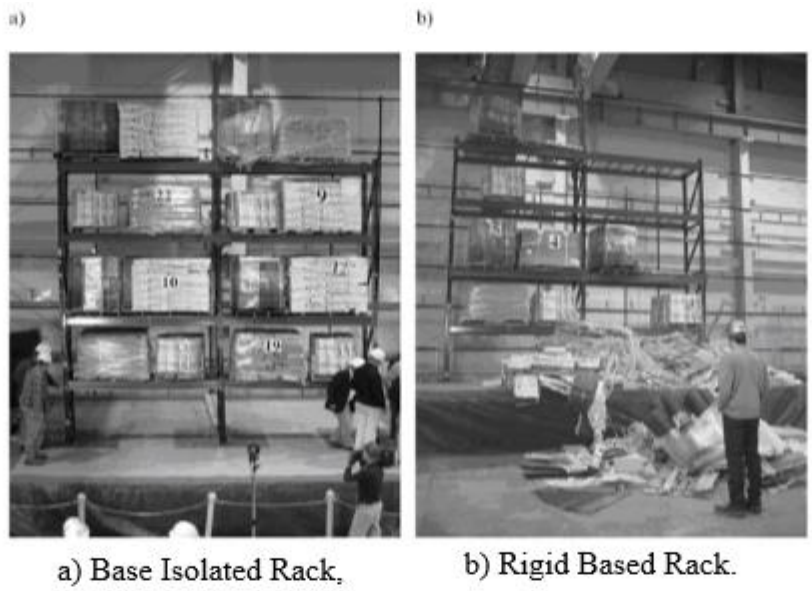

Figure 12: Base isolated and rigid based racks under Tri-Axial Seismic Excitations experiment [11].

Kilar et al. (2011) [46] investigated numerically the effect of asymmetry on fixed and isolated racks. They conducted several pushover analyses in which the results were compared with non-linear time history analyses. The results displayed that asymmetry increased the damage of the supports in the flexible side. In other words, racks which are fully loaded do not experience the worst-case scenario, while lower occupancy would case eccentricity in the range of 10% to 15% of the larger floor plan dimension. The study reported that using base isolation in storage racks has a positive effect on the performance of the frame even in the case of higher levels of loading and larger mass eccentricities.

1.2 Layout of the Thesis

This thesis is divided into 4 chapters and each chapter is divided into subsections to maintain the flow of chapters. Graphs, Tables and Figures are presented right after the paragraph for more essence and clear understanding.

CHAPTER 1: Provides introduction to the topic and an abroad overview to the background of base isolators. Plus, literature reviews.

CHAPTER 2: Discuss the Base Isolation and provides additional information on types of base isolators. Furthermore, explanations for FPS type isolators.

Chapter 3: Discuss briefly the SIESRACK 2 project model and simulations conducted by National Technical University of Athens. Also, Presents the numerical modelling of rack structure with the FPS. The work done in this thesis is briefly discussed and explained providing the results for all cases.

Chapter 4: Conclusion, provides summary and results of the isolated rack structure comparing to the fixed base. Furthermore, this chapter discusses the loading cases of a combined isolated rack structure under real earthquakes.

These chapter are followed by list of all references used in this thesis and appendixes.

2. Seismic Isolation

Seismic isolation is a technique used for reducing the effects of strong ground motions on structures and their components, to protect them from collapse and damages. Seismic isolation systems work by increasing the vibration period of the structure beyond the fundamental period of the earthquake, thereby reducing the amplification of the inertial loads due to resonance effect [56].

Base isolation components generally are horizontally flexible to allow lateral displacements, considering that they are also vertically stiff to safely carry gravitational loads like static weight of structure. The horizontally flexibility of base isolation cause an increase in period of the structure which lowers peak acceleration levels during an event. Structures with fixed base move with the ground motion during an earthquake which results in extensive damages but structures with base isolators will move a little or not at all during an earthquake (Figure13). Base isolators by reducing the seismic energy and forces cause the structure to not be affected directly by seismic forces. (P. Agarwal et al. 2006).

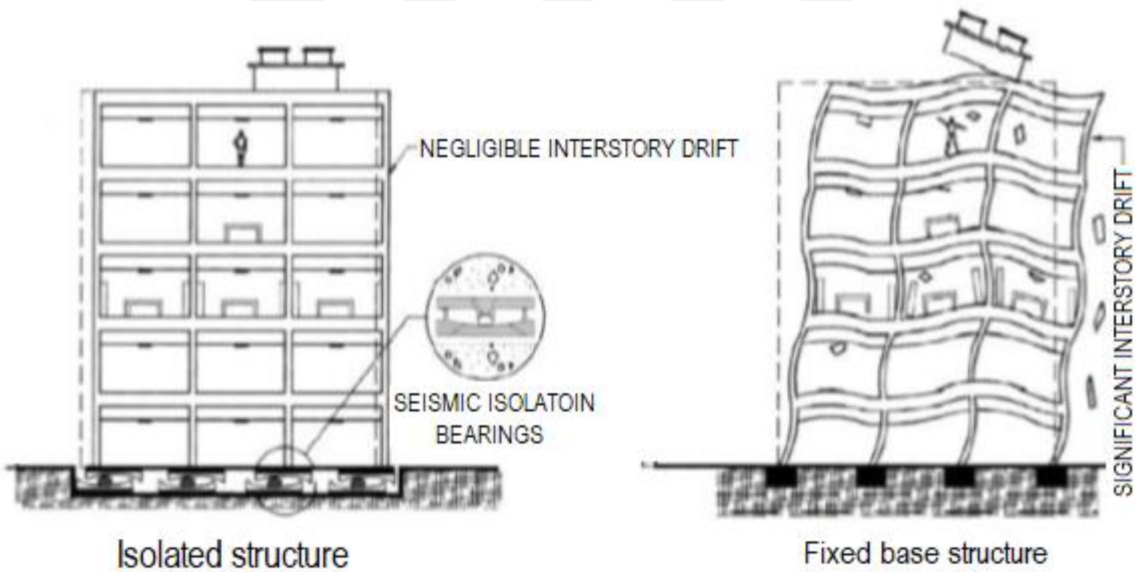

Figure 13: A multi-story structure with and without base isolator during an earthquake [13].

EUROCODE 8 [4] suggest the following objectives for base isolators:

The main type of isolation systems used up to now are based on flexibility with respect to the horizontal forces acting on the structure, such as:

- to increase the period of the fundamental mode to obtain a reduced spectral acceleration response.
- to force the fundamental modal shape to a pure translation, so much as possible.
- to make the higher modes response insignificant by concentrating the mass of the structure into the fundamental mode, thereby drastically decreasing the input energy.

The damping by energy dissipation has influence on response of displacement and acceleration (Figure 14). An increase in damping cause decrease in acceleration by lengthening the period, however in case of displacement vice versa will happen.

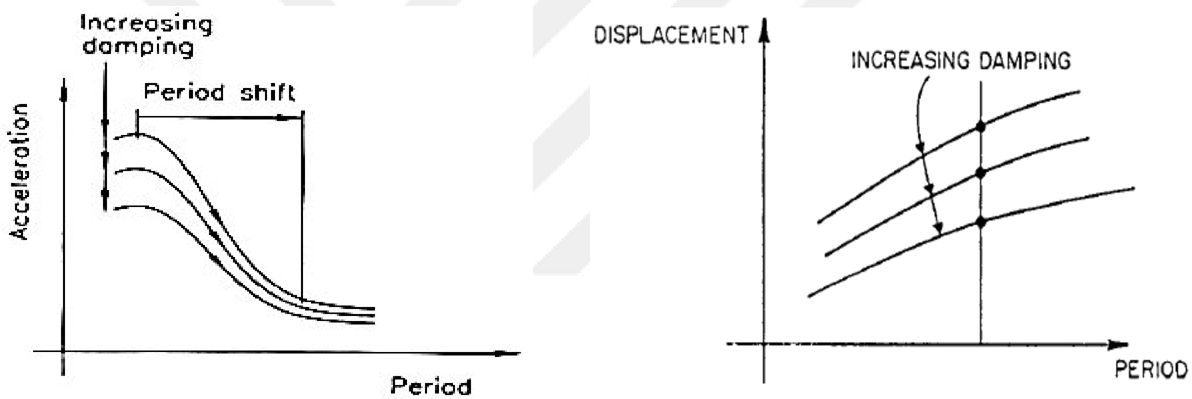

Figure 14: Effects of base isolation on acceleration and displacement by increasing damping [59]

Stiff soil conditions will cause reduction in spectral acceleration while in soft soil adverse occurs (Figure 15). Condition of soil has a significant effect on performance of base isolators (37).

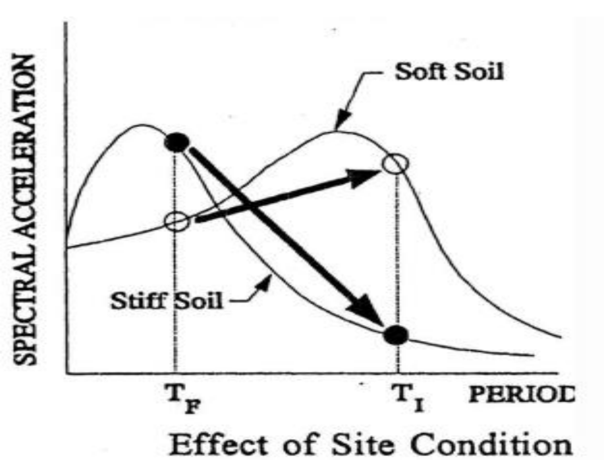

Figure 15: Effects of base isolation [60]

Energy dissipation devices may take many forms and dissipate energy through a variety of mechanisms including the yielding of mild steel, viscoelastic action in rubberlike materials, shearing of viscous fluid and sliding friction [44].

Hysteretic energy dissipation is one of the most effective means for providing a substantial level of additional damping. The term hysteretic refers to the offset in the loading and unloading curves cyclic loading. Figure 16 is a force-displacement curve where the enclosed area is a measure of the energy dissipated during cycles of motion. Work done during loading is not fully recovered during unloading and the difference is lost or dissipated as heat [59].

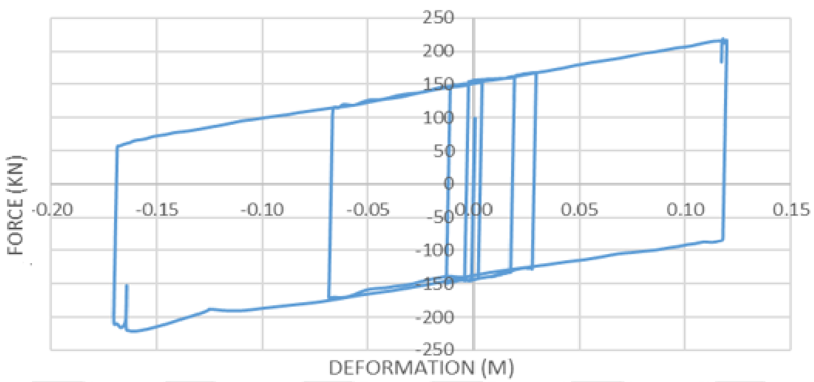

Figure 16: Hysteretic Energy

Viscous damping devices are based on material damping which may be assumed to behave linear viscous. However, it must be mentioned that most dampers classified as “viscous dampers” do not behave completely linear over the entire velocity range due to sealing friction and nonlinear material behavior which ends up in a nonlinear viscous behavior at small velocities [61].

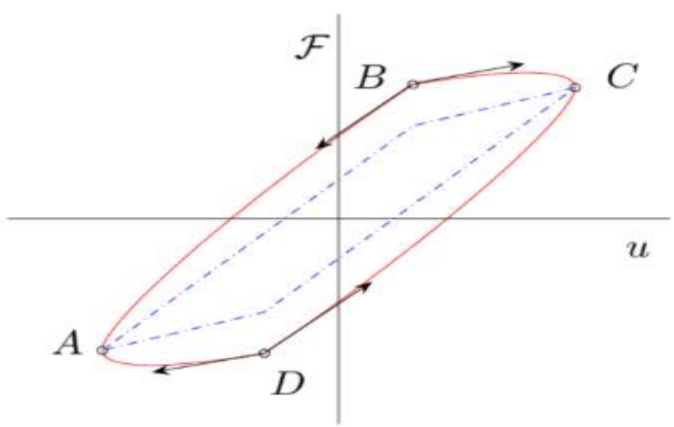

Figure 17: Viscous Damping Energy (Solid line) [61]

2.1 Types of Seismic Isolators:

There are 2 major types of base isolators in use today, namely, elastomeric isolators and sliding isolators.

Sliding isolators (Figure 18) works on principle of friction. This approach is based on the proposition that the lower the friction coefficient, the less the shear transmitted [57]. In sliding isolators, a stainless-steel plate or spherical surface and articulated friction slider will slide over each other during earthquake excitation. For initiation of sliding the intensity of exciting force must break away friction force of isolator. Hence during earthquake excitation, the frequency of which is not harmonic, the isolator displacement is of stick-slip nature (Girish et al. 2012)

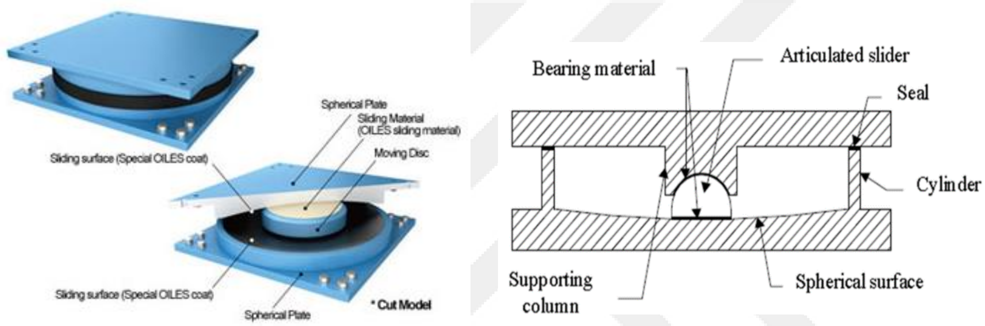

Figure 18: Sliding Isolators [36]

Sliding seismic isolation systems are provided in flat or curved surface. The separation between the two structural elements is important because efforts resulting from earthquake excitation will not transmit on the vertical upward to the superstructure. And in this type of isolation systems the mechanism which provides restoring force to return the structure to its equilibrium position are high-tension springs, laminated rubber bearings or by making the sliding surface curve [62].

Isolation systems with flat slider surface are used in combination with high-tension spring for restoring force, however curved surface sliders recover by the gravity force as a mechanism for restoring force.

2.1.1 Friction Pendulum Isolator

The friction pendulum system has been widely used for seismic protection of buildings, bridges and industrial structures. According to previous studies in the friction pendulum system, the coefficient of friction depends on several effects such as sliding velocity, apparent pressure, air temperature and cycling effect [57][58]. Friction isolators for rack systems can also be a significant approach for reducing merchandise shedding during earthquake.

By application of low coefficient of friction in bearings, it will reduce the acceleration of structure and decrease the transfer of force into structure. Additionally, low coefficient of friction causes reduced energy dissipation capacity, allowing supplemental dampers to provide the primary source of energy dissipation (Madden et al. 2002).

<u>For a friction pendulum isolator, the following variables must be considered carefully since they have significant influence on the behavior of isolator:</u>

3. Friction Coefficient

   It depends on the surface material that is used. This factor is the most important factor for a friction pendulum isolator.

4. Radius of curvature

   This parameter will influence the natural period of the friction isolator system. It is important to consider this parameter carefully during design of isolator in order to avoid the period which resonance with the ground acceleration.

5. Initial stiffness

   In the ideal condition, it can be assumed that initial stiffness is almost infinite because no movement will occur before the force surpasses the weight of the building x friction coefficient. However, in the real practice and computational model, there will be an initial slip thus it is needed to determine a value which should be far higher than the post-elastic stiffness to represent the condition properly.

For finding the Effective Stiffness, Effective damping ratio and the fundamental period of the structure the following formulas (2.1) (2.2) (2.3) respectively can be used [41]:

$$K = W/ R + \mu W/ D \tag{2.1}$$

Where,

K – Effective stiffness
W – The total weight of structure
R – Net pendulum Radius
μ - Friction Coefficient, Slow/Fast
D – Approximate estimated isolator displacement

$$\beta = 2 / \pi \, [\, \mu / \mu + D/R] \tag{2.2}$$

Where,

β – Effective Damping Ratio
R – Net pendulum Radius
μ - Friction Coefficient, Slow/Fast
D – Approximate estimated isolator displacement

$$T = 2\pi \sqrt{R/g} \tag{2.3}$$

Where,

T – The fundamental period of structure
R – Net pendulum Radius

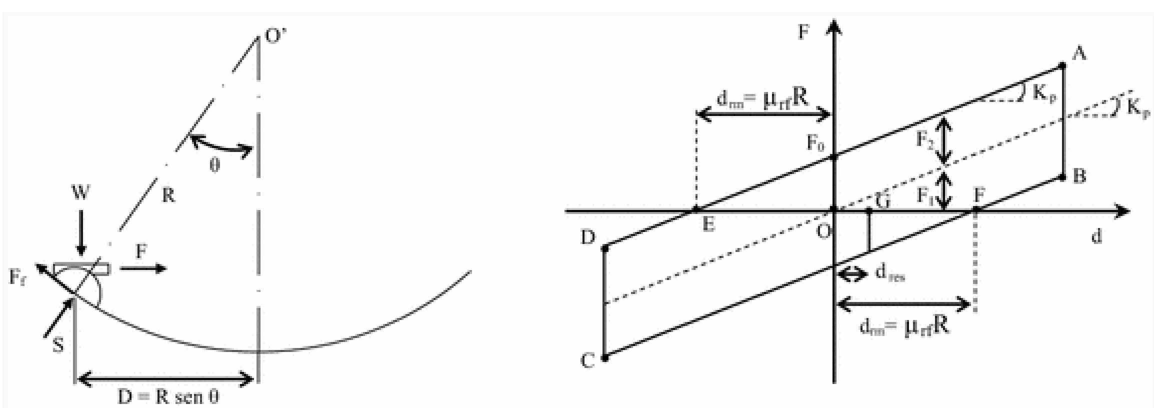

Figure 19: Working principles of Friction Pendulum System [63]

In the 1980s, Victor Zayas studied the idea for isolating the buildings with devices base on friction and on the response of a pendulum (patent filed on Dec. 12, 1985 and published on Feb. 24, 1987) [14]. The detailed concept, design and testing of the system which is referred to as Friction Pendulum System are explained in a report published in 1987 [15] and in a journal paper published in 1990 [16]. These documents show range of applications with velocities starting from 0 up to 0.9 m/s, load bearing capacities starting from 7 up to 210 MPa, friction coefficients starting from 5% up to 20% and radius of curvature starting from 0.9 up to 15m. Some of the ranges later shown to be technically impossible, but the choice for considering these ranges can be justified by the desire to cover all possible applications and developments (17).

The most significant factor for friction pendulum isolator is the sliding properties of the surface materials. The FPS has a spherical stainless-steel surface and a slider, covering by a Teflon-based composite material. During a strong earthquake, the slider moves on the spherical stainless-steel surface lifting the structure and dissipating the ground motion energy by friction between the spherical surface and the slider. The isolator uses the surface curvature for generating the restoring force from the pendulum action of the weight on the FPS [57].

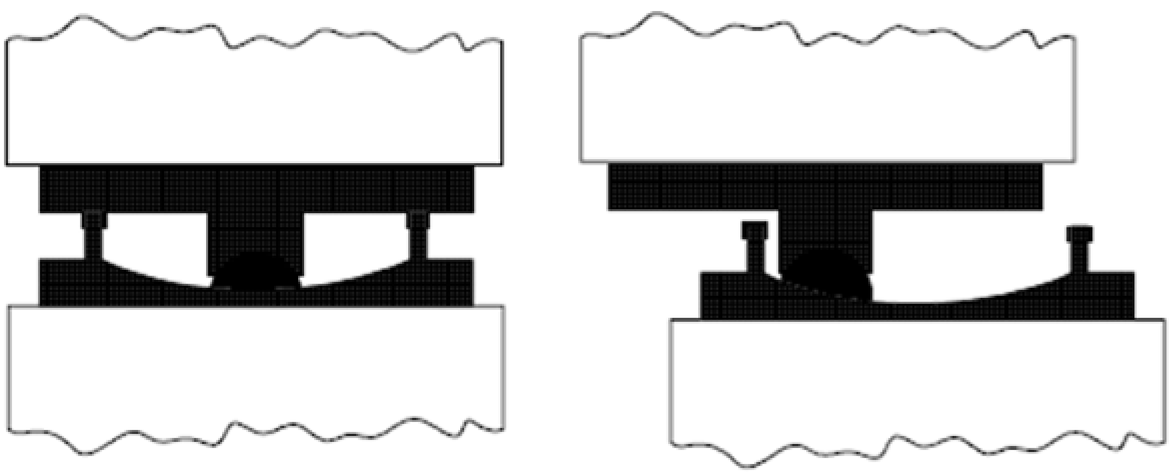

Figure 20: The motion of a Friction Pendulum Isolator [17]

According to the simplified Coulomb model, the frictional force is directly proportional to the applied load, independent on the apparent area of contact and sliding velocity. Also, tests in recent years documented the degradation of the frictional characteristics due to the generation of high temperatures at the sliding interface during reversal cycles of motion [64].

In structural engineering, the Bouc–Wen model of hysteresis is used to describe non-linear hysteretic systems. Force–displacement characteristics of seismic protection devices are of hysteretic type. Often, the experimental hysteretic loops are obtained by imposing cyclic relative motions between the device mounting ends on the structure rig and by recording the evolution of the developed force versus the imposed displacement. By fitting a Bouc–Wen model type to experimental data, one obtains a single non-linear first order equation which can describe the evolution of force developed by one device for almost any loading pattern (periodic, a-periodic or random).

The classical Bouc–Wen model used for approximation of hysteretic curves:

$$F(t) = \alpha k y(t) + (1 - \alpha) \; k \tilde{z}(t) \qquad \text{.... (2.4)}$$

where k is the stiffness coefficient, $\alpha \in [0, 1]$ a weighting parameter and $\tilde{z}$ an virtual displacement given by the Bouc–Wen equation:

$$\tilde{z} = A - \tilde{\beta} \, |\tilde{z}| \, n - \tilde{\gamma} \, |\tilde{z}| \, n \, \mathrm{sgn}\,(\tilde{z} \, \dot{y}) \, \dot{y} \qquad \text{.... (2.5)}$$

with the parameters $A > 0$, β, γ and n.

3. Numerical Modelling

3.1 Numerical Modelling of the Steel Storage Rack

The storage rack model which was used in this study is the storage rack model used in the SEISRACK 2 project. The finite element modelling aspects of this rack structure has been thoroughly explained in Seismic Performance of Steel Pallet Racks [42] and modelling of the rack structure for this study has been created accordingly.

This model has been tested in National Technical University of Athens, Laboratory of Metal Structure 2014. This chapter deals with the modelling of the storage rack components using SAP2000. The results of the experiment have been used to calibrate the finite element model.

Numerical model of the rack was developed in SAP2000 and the model was verified by comparison with experimental results. later on, the developed model used to conduct parametric studies with and without base isolation system. Also, various cases of loadings were studied.

3.1.1 Rack Geometry and its Properties:

The racking system used in the seisrack 2 project have four levels and six bays. The height of the rack structure is approximately 8.2 meters, the width without rear bracing is 1.1 meters and the length in down-aisle direction is approximately 17.2 meters. One single bay has the capacity for 12 pallets which means one compartment can carry 3 pallets. In total the racking system can carry up to 72 units of pallet goods [42]. The longitudinal view, Plain view, Cross-aisle view, Upright, Base-plate, Diagonal connections and Horizontal bracings of the rack system are given in figures 28, 29, 30, 31, 32, 33 and 34 respectively.

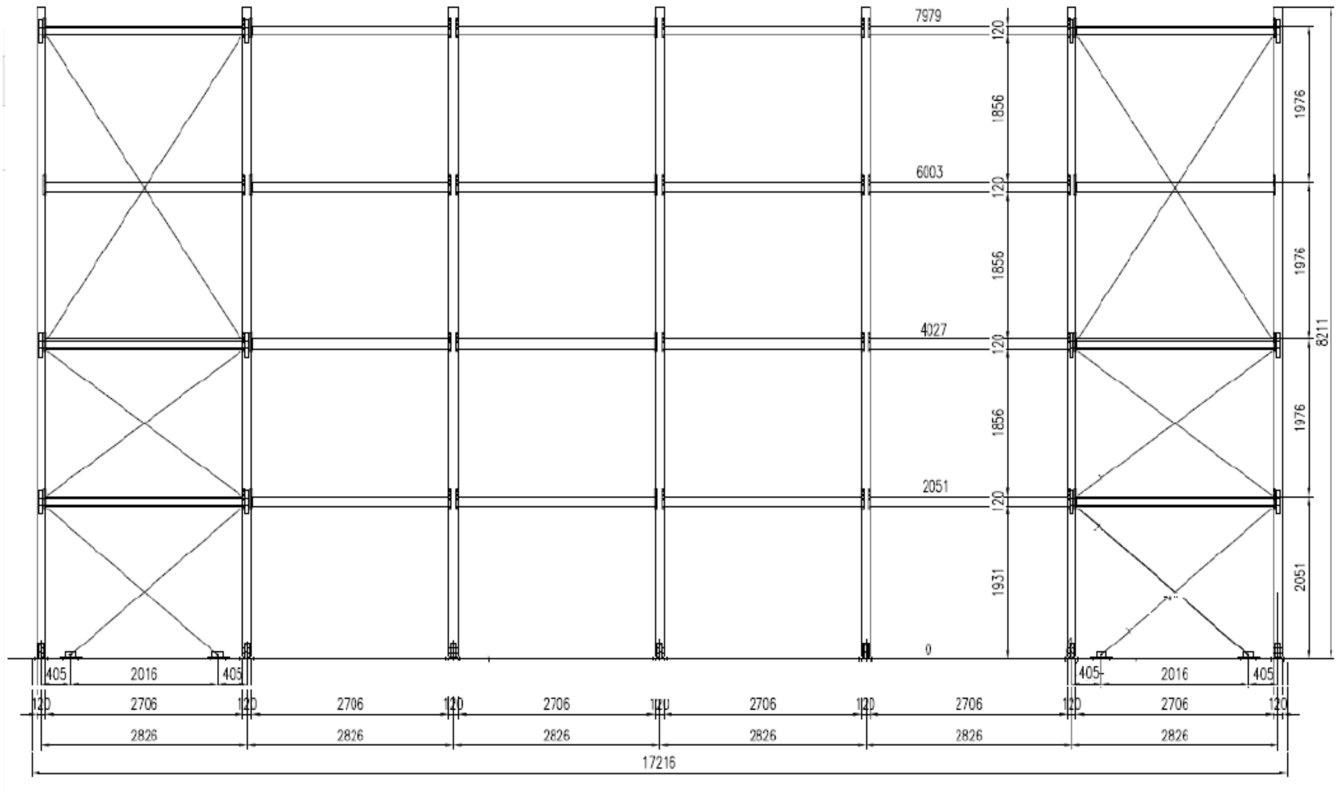

Figure 21: Longitudinal view of the rack model [42]

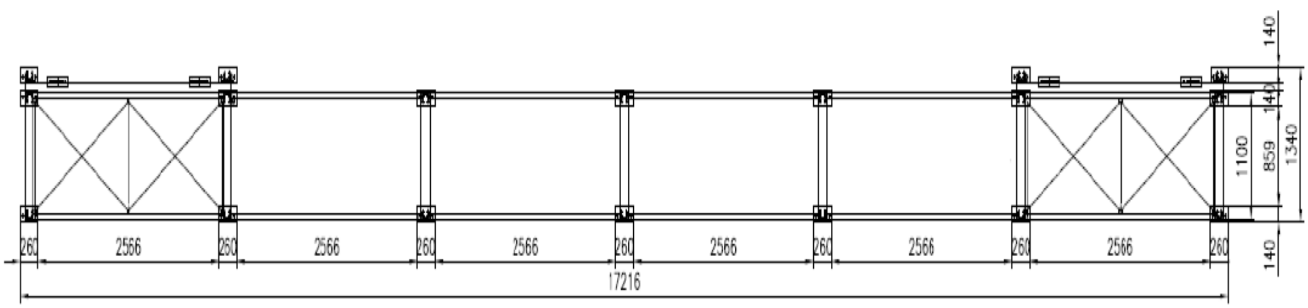

Figure 22: Plan view of the rack model [42]

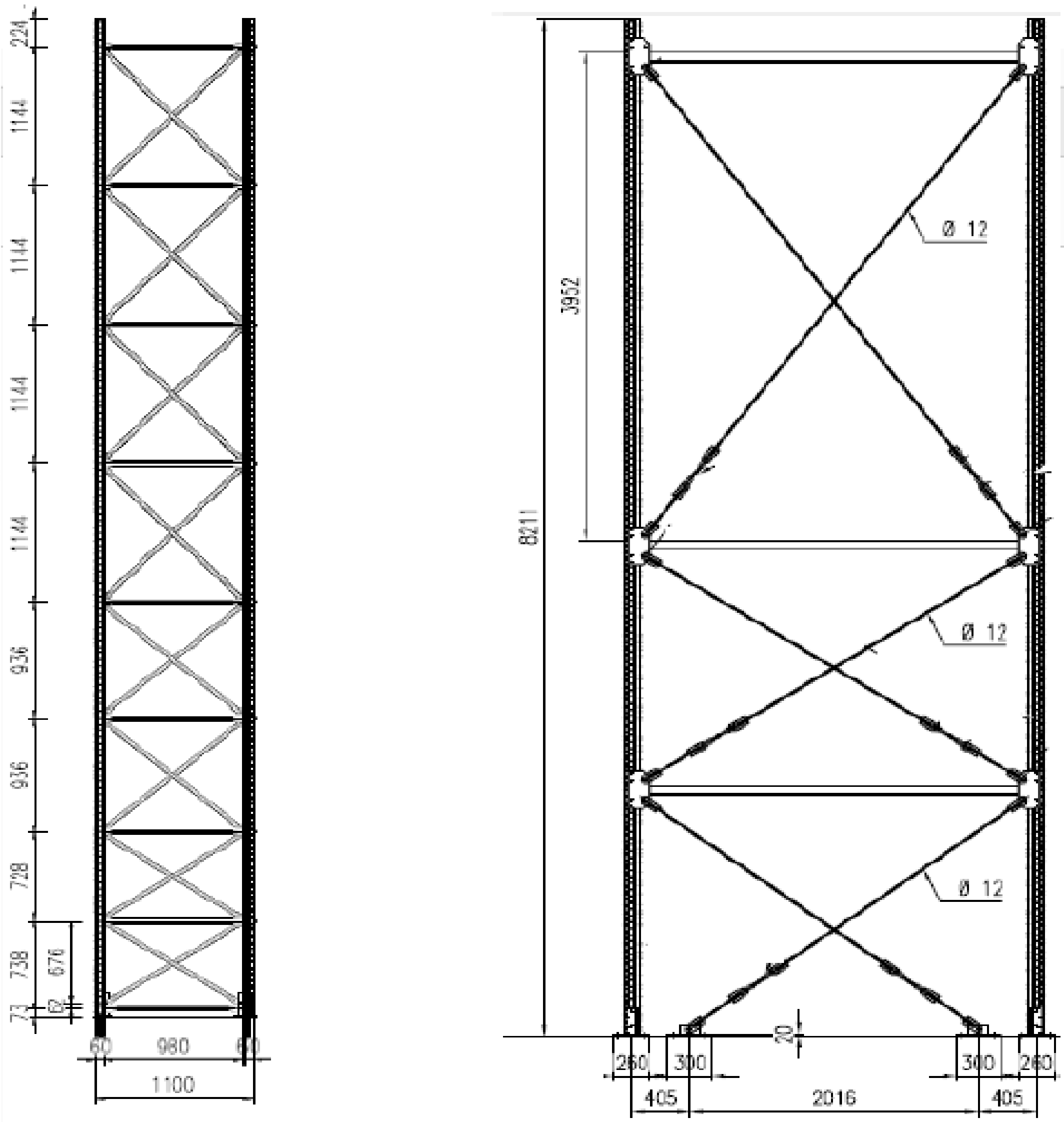

Figure 23: Cross-aisle view and Rear bracing view of the rack model [42]

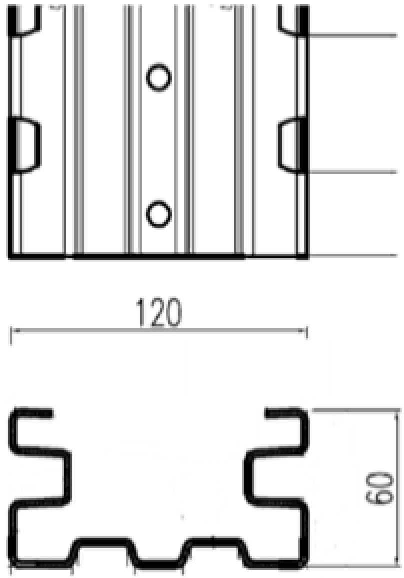

Figure 24: Upright of the rack model [42]

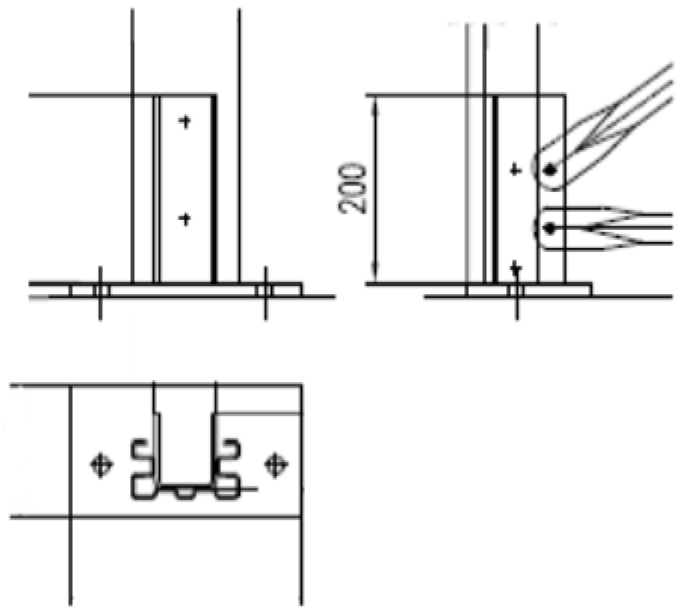

Figure 25: Base plate of the rack model [42]

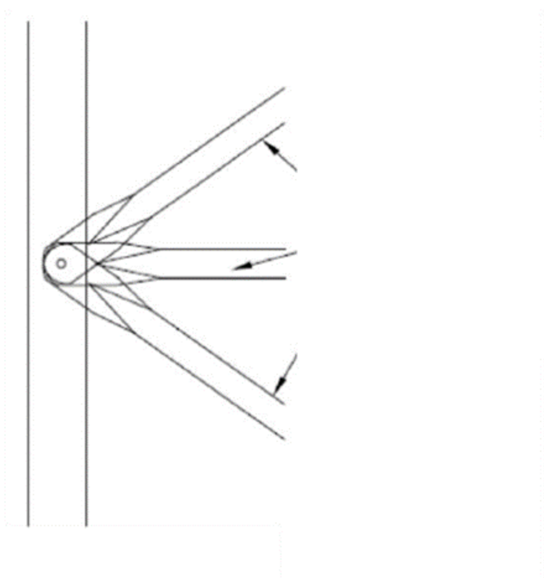

Figure 26: Diagonal of the rack model [42]

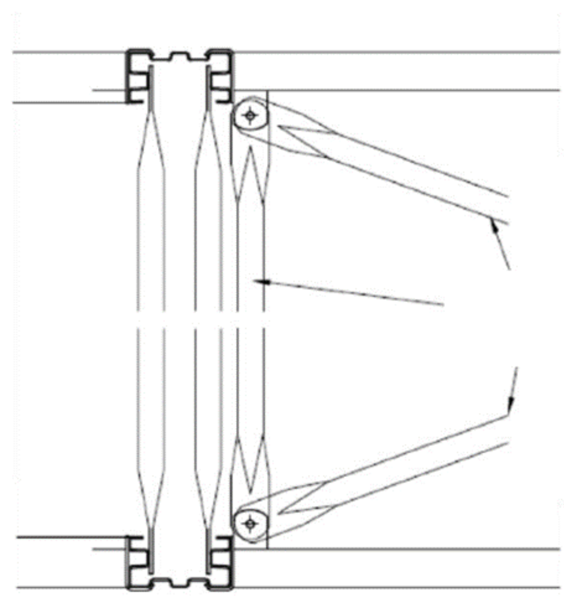

Figure 27: Horizontal bracing of the rack model [42]

3.1.2 Modelling of the storage rack in SAP2000

The software used for this thesis is SAP2000 version 19. The reason which this software was used for analysis purpose is the ability of elements design by section design tools, detailed options for links and non-linear time history analysis by several earthquakes. The loads, materials and section properties are presented in Table 1 [42].

Table 1: Loads, Materials and Section properties [42].

Materials	
Uprights	S420 MC
Bracings	S355 MC
Beams	S235 JRC
Loads	
Dead Loads (KN/m)	19.2
Live Pallet Loads (KN/m)	576
Section Properties	
Beams (mm)	45*120*1.5
Uprights (mm)	120*60
Bracings (mm)	45*45

3.1.3 Geometry

The finite element model geometry of the rack in axis X is the down-aisle direction and in axis Y is the cross-aisle direction (fig. 28). Bracings were modelled as truss elements by releasing all moments at both ends. Sap2000 section designer tool was used to design the uprights (fig. 29).

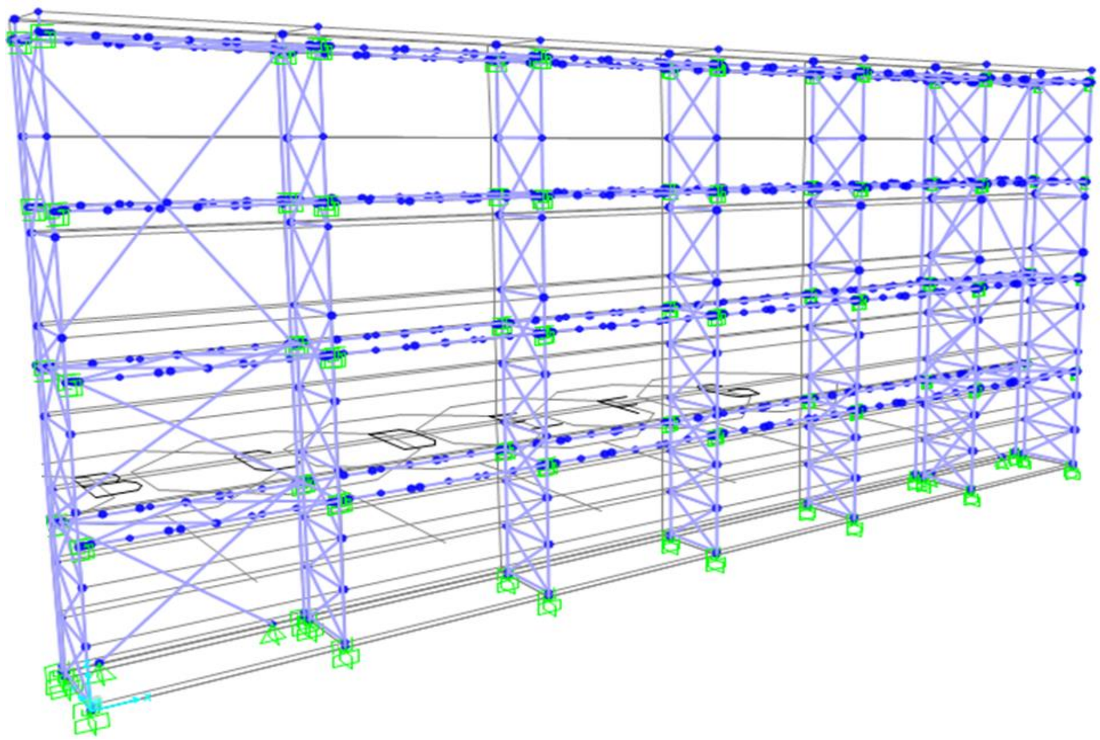

Figure 28: Grids in X, Y, Z axes

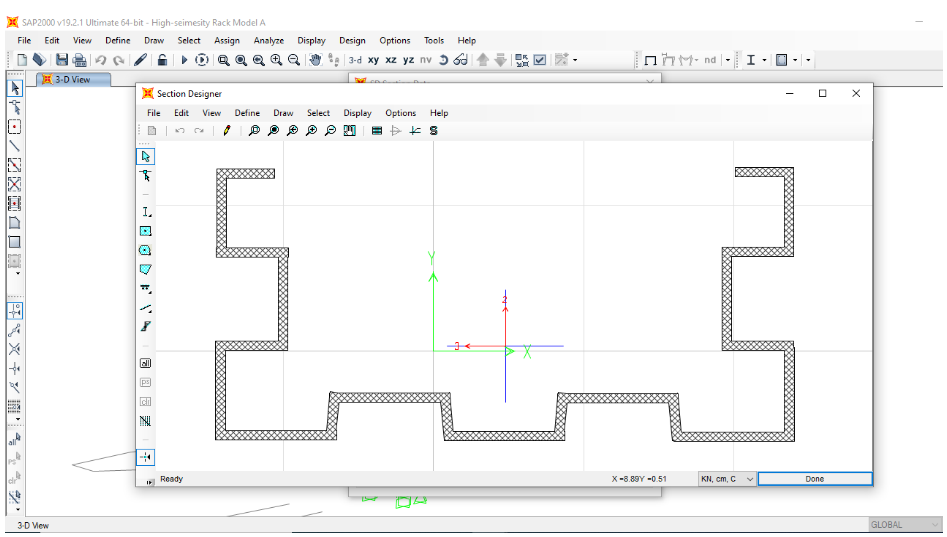

Figure 29: Section Designer tool

3.1.4 Uprights

All the uprights were fixed on the ground. A multilinear plastic link (fig. 30) was used between fixed support and uprights to simulate the plastic response of the base plate (fig. 31).

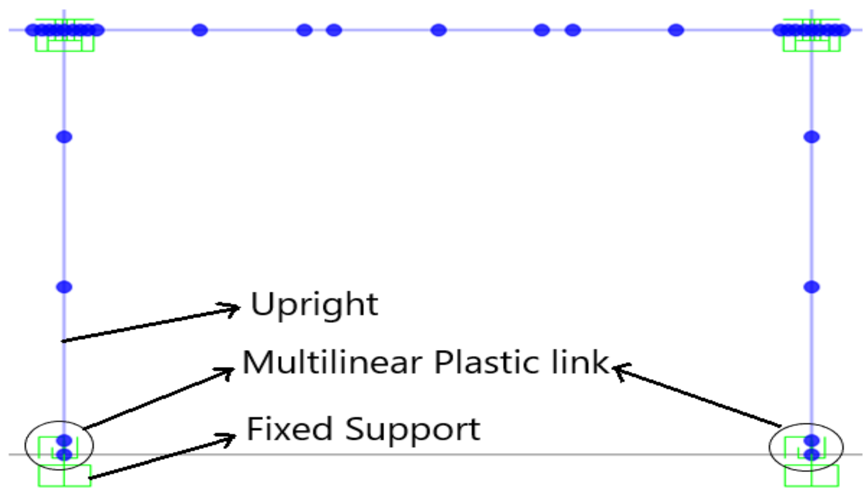

Figure 30: Detail of link assignments in the lowest level [42]

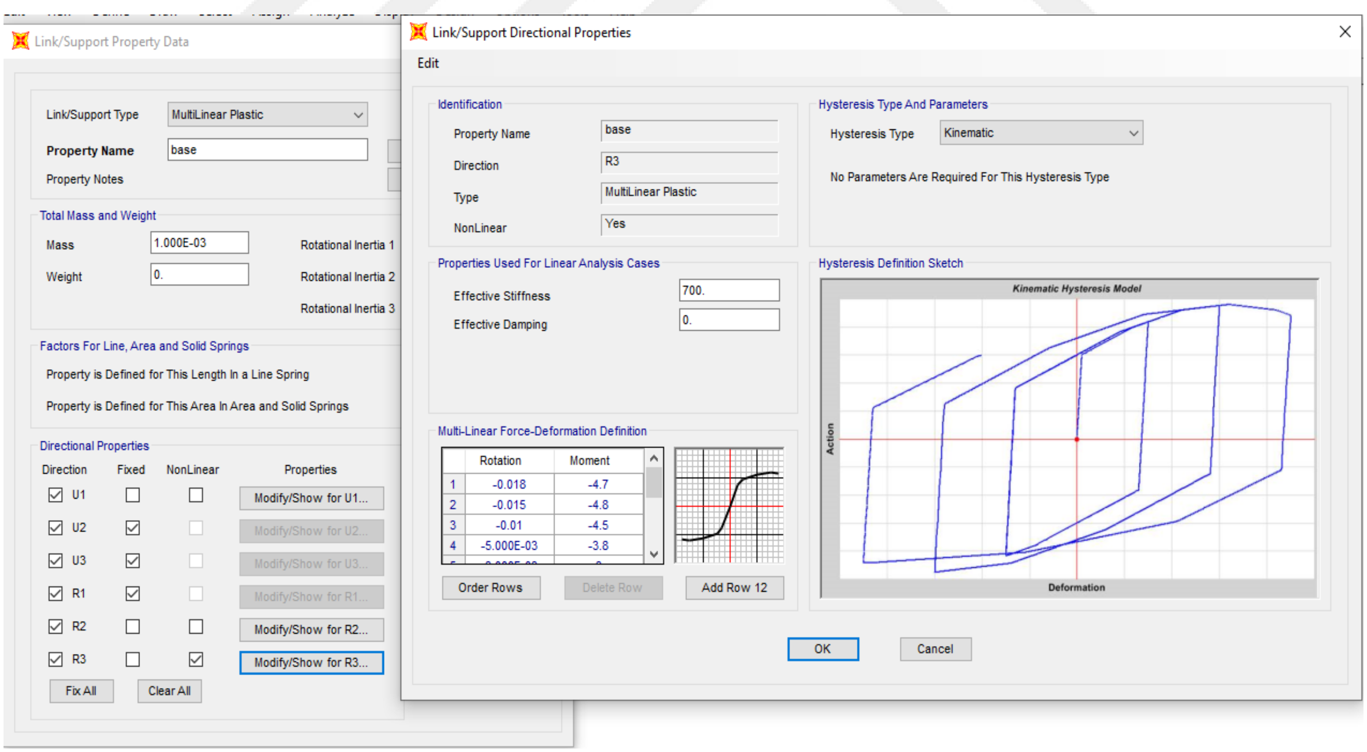

Figure 31: Link/Support properties of the base plate [42]

3.1.5 Beams

The capacity of each bay per level is 3 pallets (fig. 32). Hence, the internal nodes of the beams were drawn accordingly. Each pallet at each bay is presented with three nodes, two of the nodes at the end and one node at the middle. The distance between pallets in each bay is equally distributed. The loads of the pallets were considered as concentrated loads and it was imposed according to the geometry of the pallets. As Euro standards a typical pallet has a length of 800 mm in X direction and a total load of 8 KN [42].

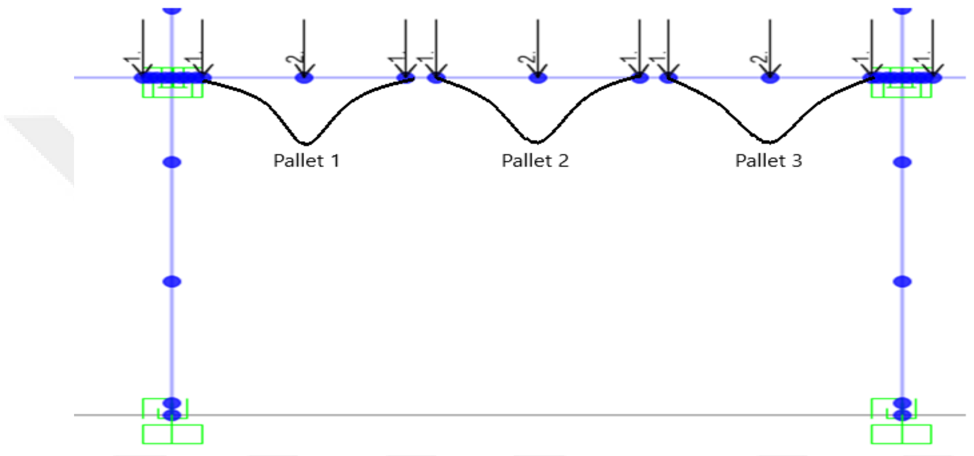

Figure 32: Detail of nodes and load assignments in beams [42]

Two types of links were used at the end of pallet beams: a rigid link connecting the upright and the beam for representing the geometrical eccentricity between the edge of beam and the centroid of upright. Also, a multi linear plastic link was used to simulate the non-linear behavior of beam end connector. The properties of links are again defined by experimental data provided by the construction companies and are used to explain the moment rotation relation with regard to the rotation around Y axis [42].

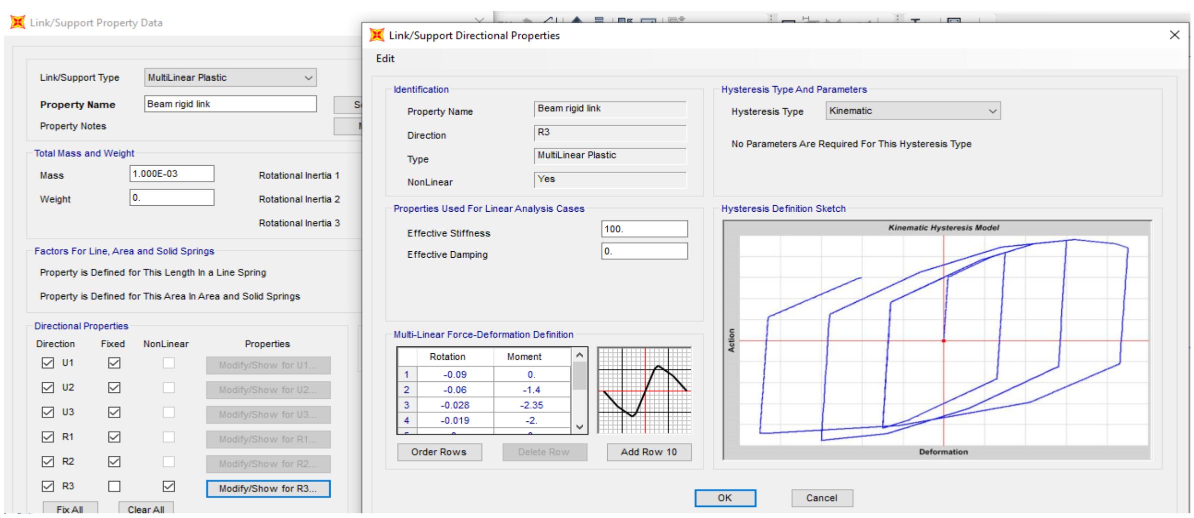

Figure 33: Link/Support properties of the beam end connector [42]

Figure 34: Following figures are behavior of Beam End Connector Link

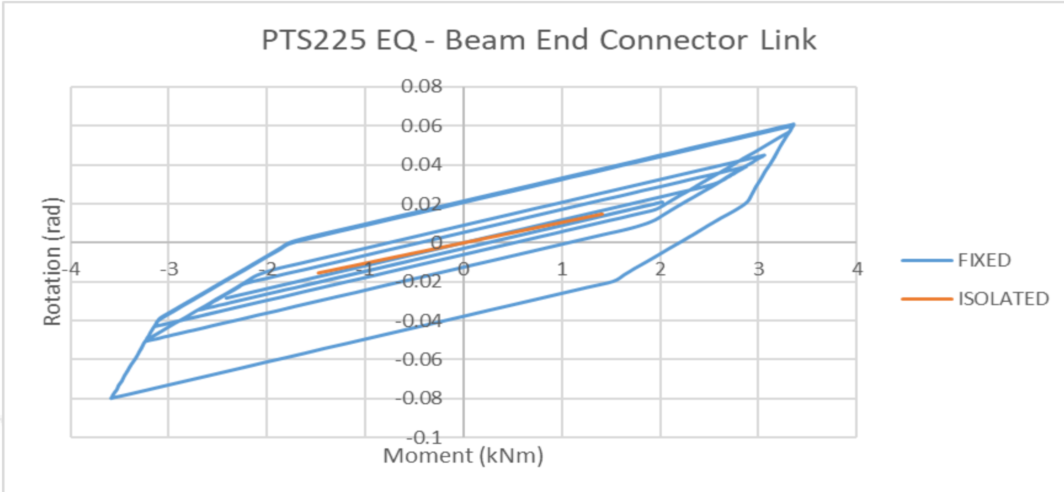

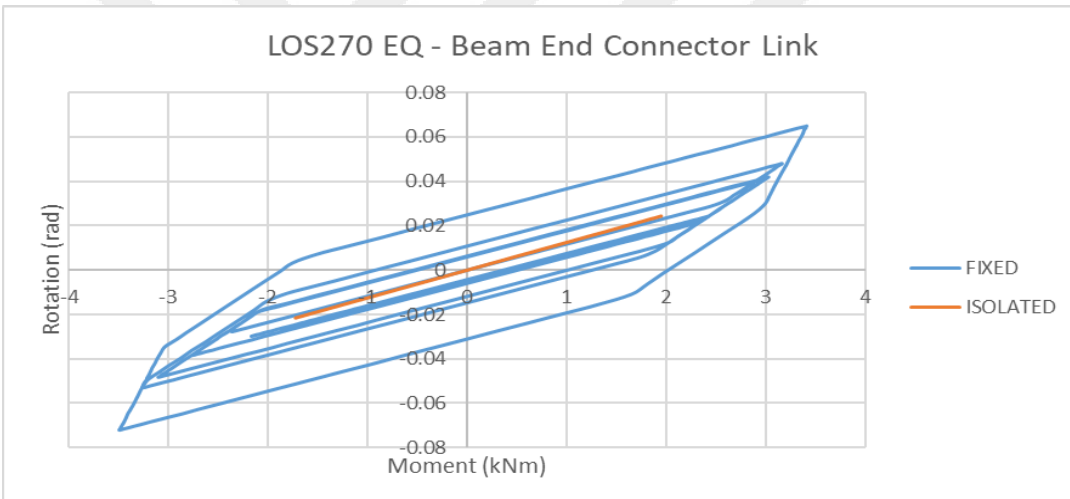

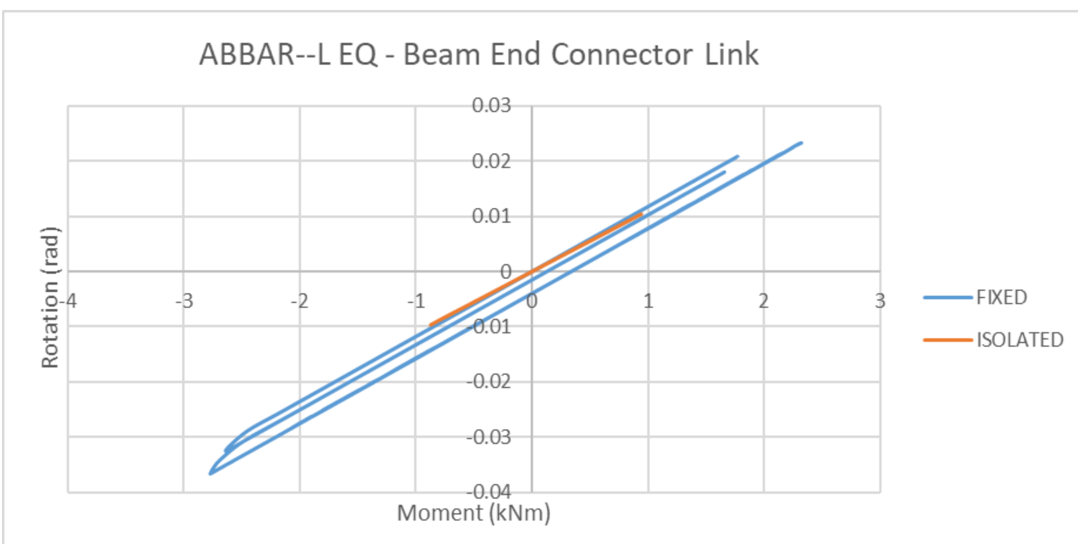

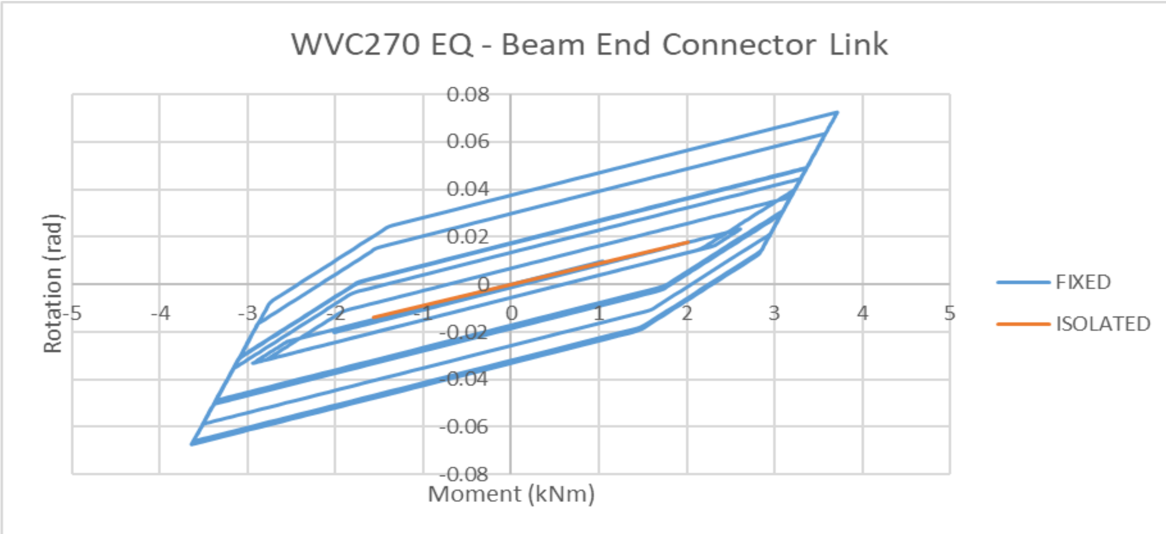
WVC270 EQ - Beam End Connector Link
Rotation (rad)
Moment (kNm)
0.08
0.06
0.04
0.02
0
-0.02
-0.04
-0.06
-0.08
-5
-4
-3
-2
-1
0
1
2
3
4
5
FIXED
ISOLATED

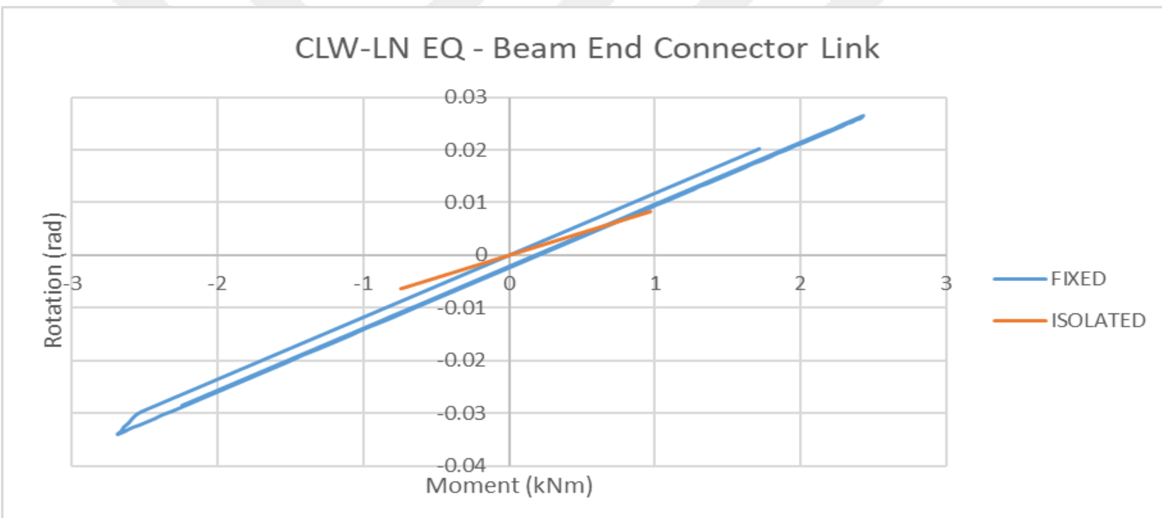
CLW-LN EQ - Beam End Connector Link
Rotation (rad)
Moment (kNm)
0.03
0.02
0.01
0
-0.01
-0.02
-0.03
-0.04
-3
-2
-1
0
1
2
3
FIXED
ISOLATED

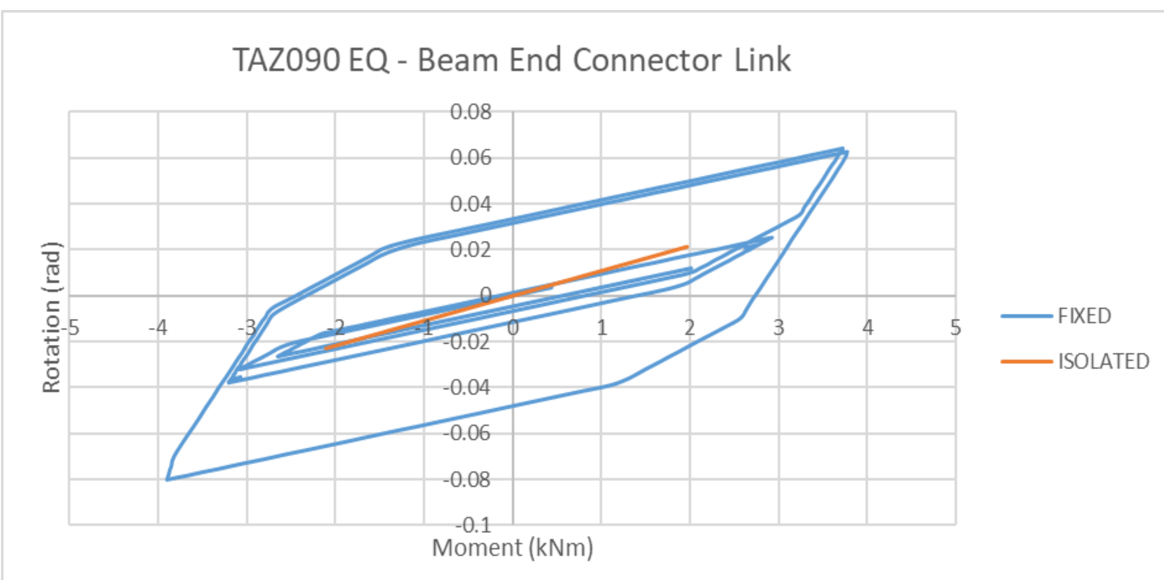
TAZ090 EQ - Beam End Connector Link
Rotation (rad)
Moment (kNm)
0.08
0.06
0.04
0.02
0
-0.02
-0.04
-0.06
-0.08
-0.1
-5
-4
-3
-2
-1
0
1
2
3
4
5
FIXED
ISOLATED

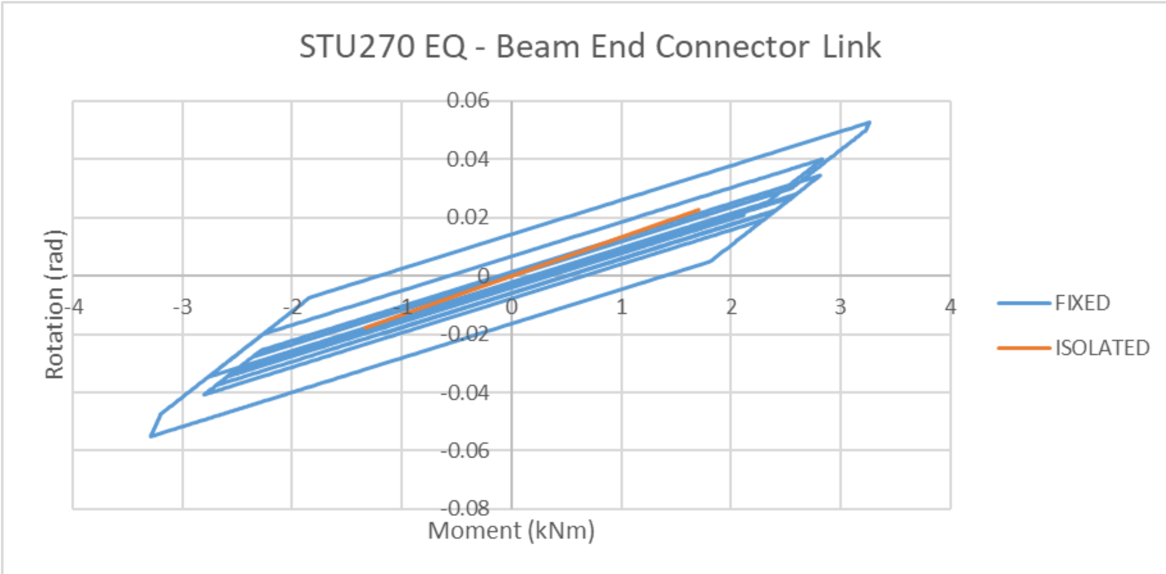
STU270 EQ - Beam End Connector Link
Rotation (rad)
Moment (kNm)
0.06
0.04
0.02
0
-0.02
-0.04
-0.06
-0.08
-4
-3
-2
-1
0
1
2
3
4
FIXED
ISOLATED

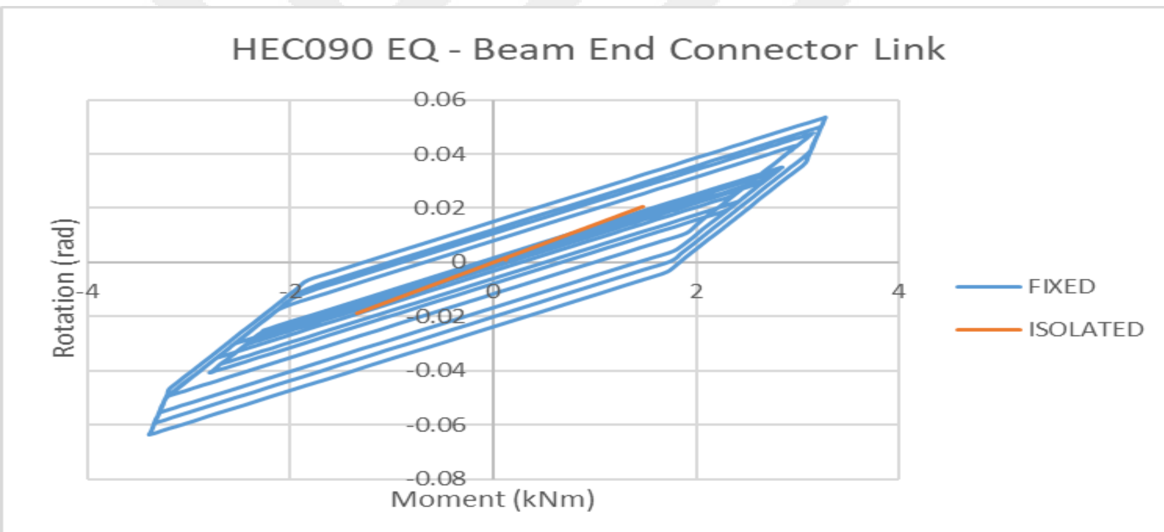
HEC090 EQ - Beam End Connector Link
Rotation (rad)
Moment (kNm)
0.06
0.04
0.02
0
-0.02
-0.04
-0.06
-0.08
-4
-2
0
2
4
FIXED
ISOLATED

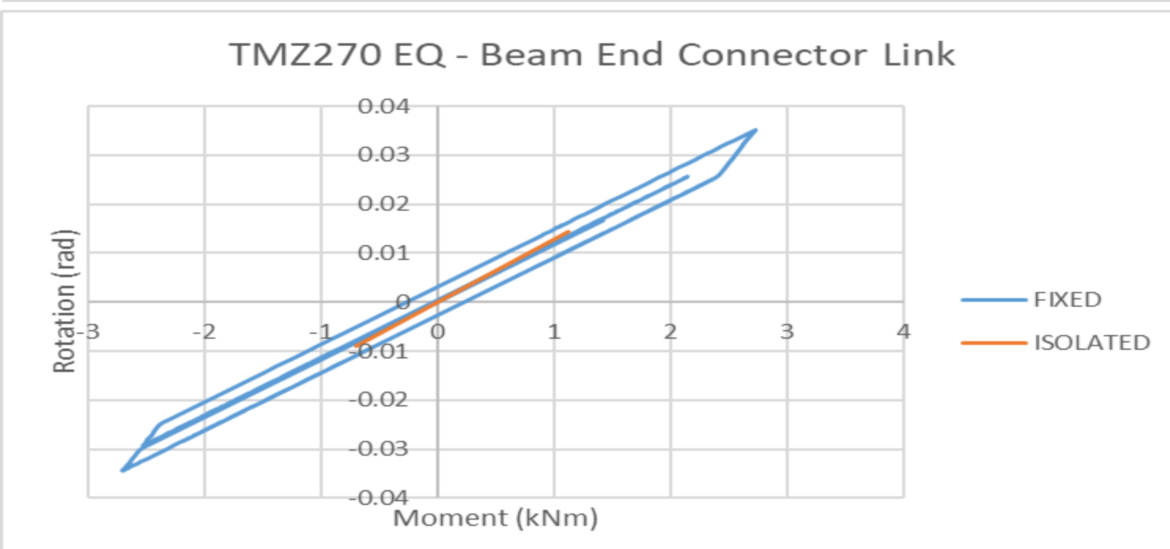
TMZ270 EQ - Beam End Connector Link
Rotation (rad)
Moment (kNm)
0.04
0.03
0.02
0.01
0
-0.01
-0.02
-0.03
-0.04
-3
-2
-1
0
1
2
3
4
FIXED
ISOLATED

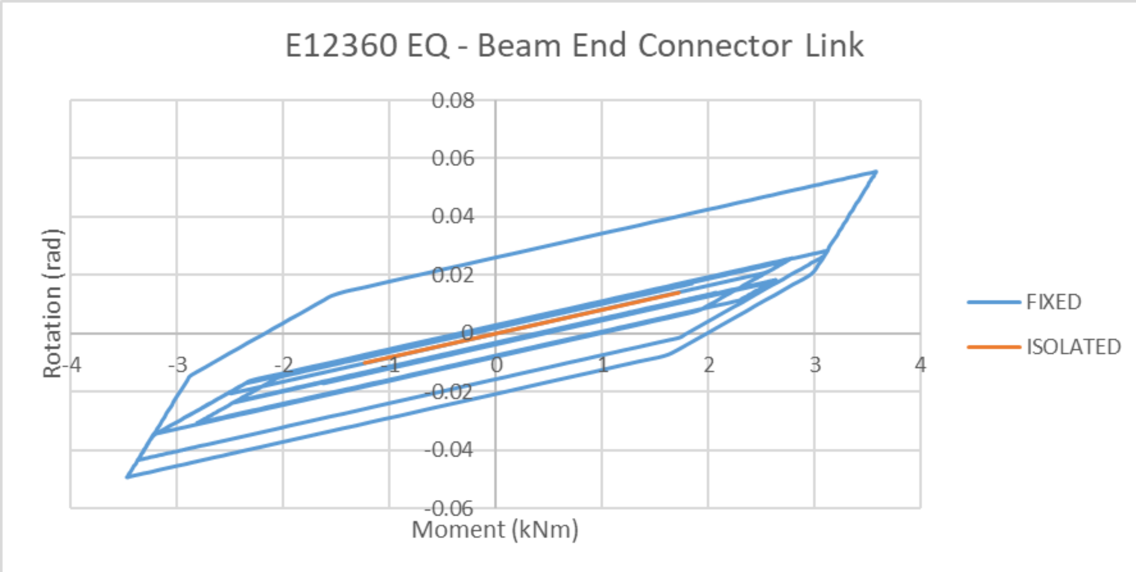
E12360 EQ - Beam End Connector Link
Rotation (rad)
Moment (kNm)
FIXED
ISOLATED
0.08
0.06
0.04
0.02
0
-0.02
-0.04
-0.06
-4
-3
-2
-1
0
1
2
3
4

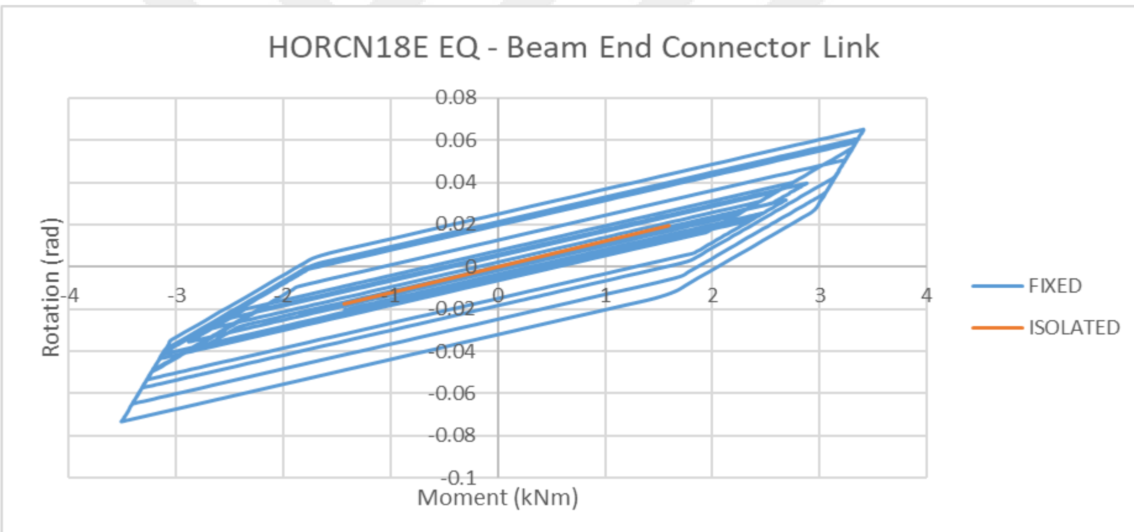
HORCN18E EQ - Beam End Connector Link
Rotation (rad)
Moment (kNm)
FIXED
ISOLATED
0.08
0.06
0.04
0.02
0
-0.02
-0.04
-0.06
-0.08
-0.1
-4
-3
-2
-1
0
1
2
3
4

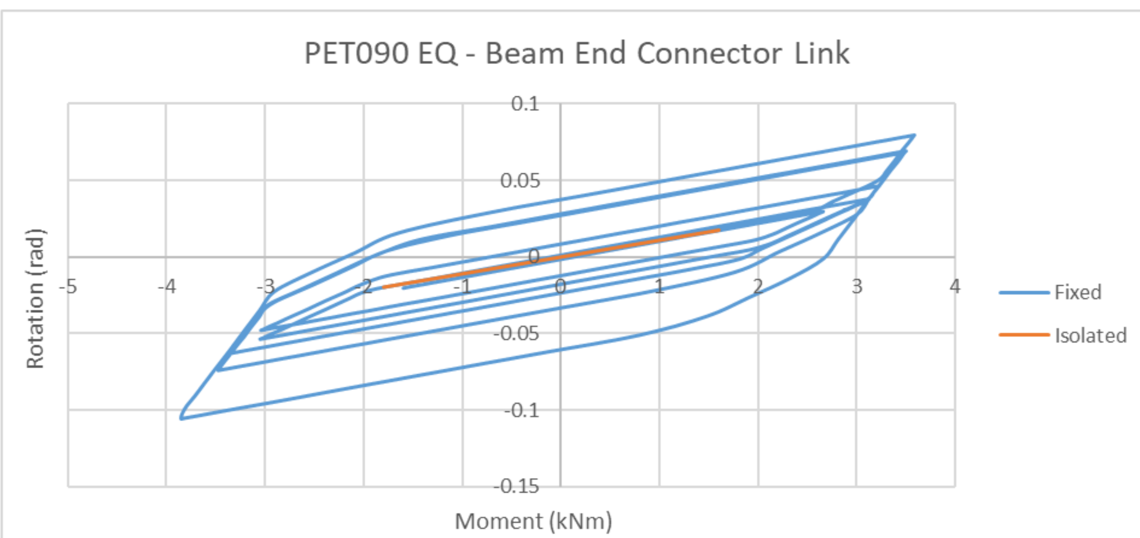
PET090 EQ - Beam End Connector Link
Rotation (rad)
Moment (kNm)
Fixed
Isolated
0.1
0.05
0
-0.05
-0.1
-0.15
-5
-4
-3
-2
-1
0
1
2
3
4

3.1.6 Diagonals

In this study diagonals are modelled truss elements with open symmetric sections. In order diagonals behave as trusses all moments were released in both ends.

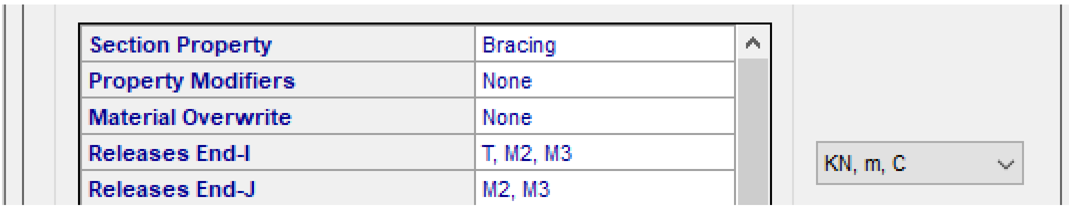

Figure 35: Moment releases in Diagonals [42]

3.2 Modal Analysis Results

As mentioned before, the experimental data provided by rack manufacturer companies were used for the simulation of the rack structure as reference for this thesis. The geometry of the structure as well as loads, elements and assignments of nodes with inelastic behavior has already been explained. The modal analysis of model is presented in here. In the following table, 20 modes of the fixed base structure is shown.

Table 2: Modal Analysis Results for fixed base Structure

Mode No.	Numerical - Fixed Base Period (s)	Experimental - Fixed Base Period (s)
1	1.291	1.261
2	1.202	1.225
3	1.151	1.003
4	0.901	0.977
5	0.851	0.841
6	0.562	0.615
7	0.551	0.594
8	0.532	0.538
9	0.489	0.526
10	0.477	0.516
11	0.465	0.498
12	0.451	0.485
13	0.448	0.481
14	0.441	0.476
15	0.437	0.468
16	0.431	0.461
17	0.436	0.456
18	0.433	0.431
19	0.431	0.421
20	0.422	0.417

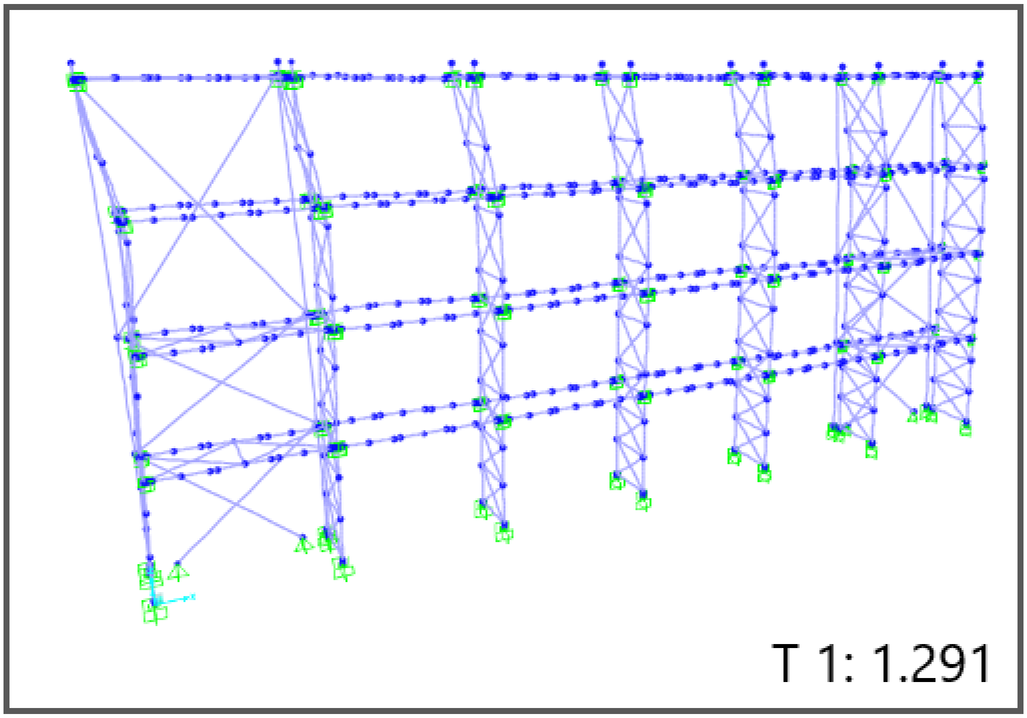

Figure 36: Mode 1

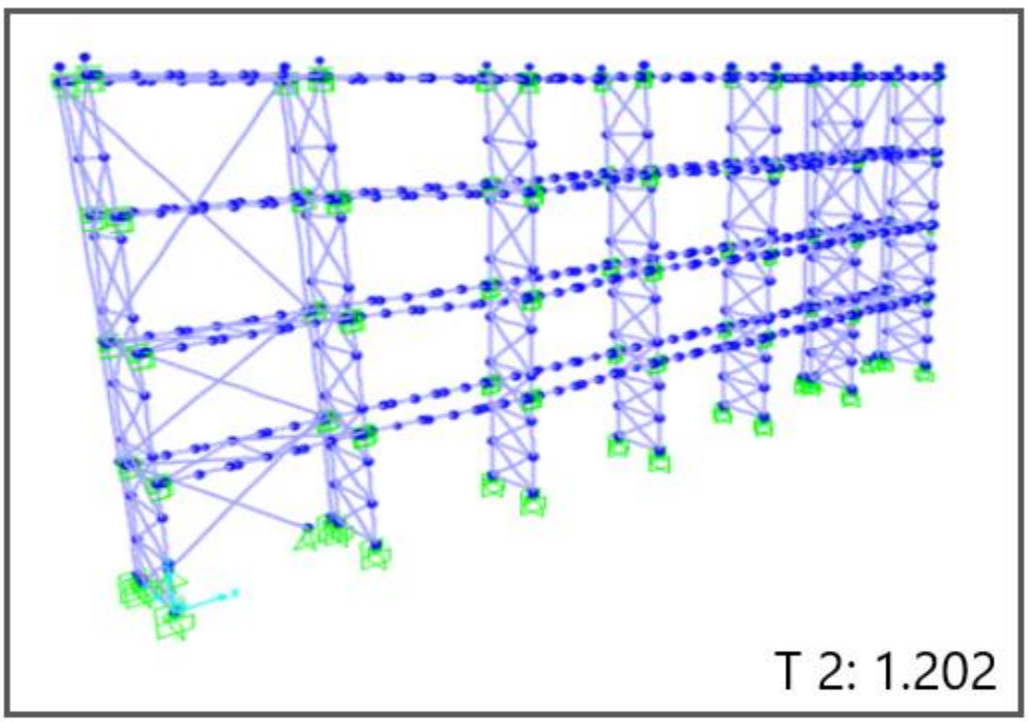

Figure 37: Mode 2

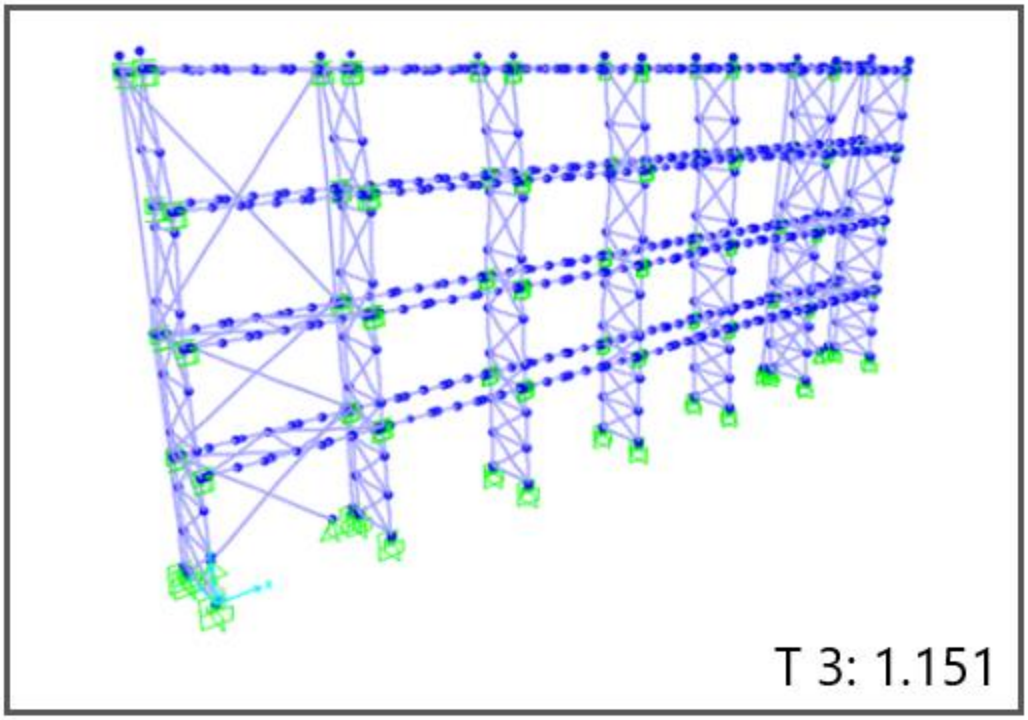

Figure 38: Mode 3

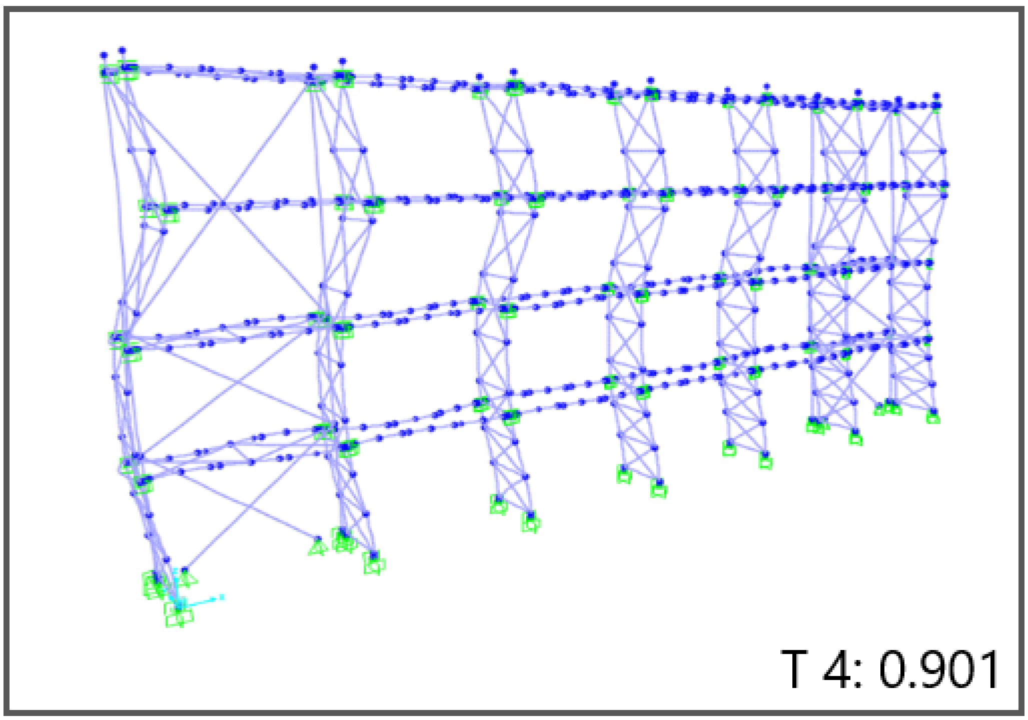

Figure 39: Mode 4

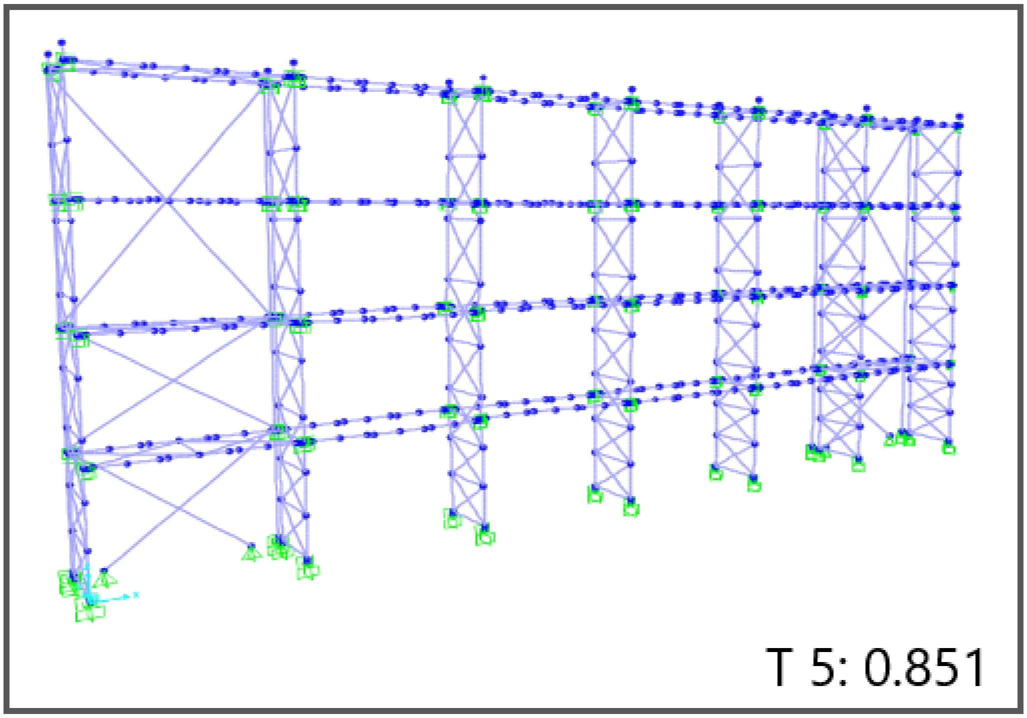

Figure 40: Mode 5

3.3 Numerical Modelling of the Seismically Isolated St. Storage Rack

The fixed base structure was isolated with single friction isolators at the base. A concrete slab of 45-cm thick was placed under the structure to control the acceleration of rack structure during earthquakes. Later on, the isolators were applied under the concrete slab at the bearings (Fig. 41).

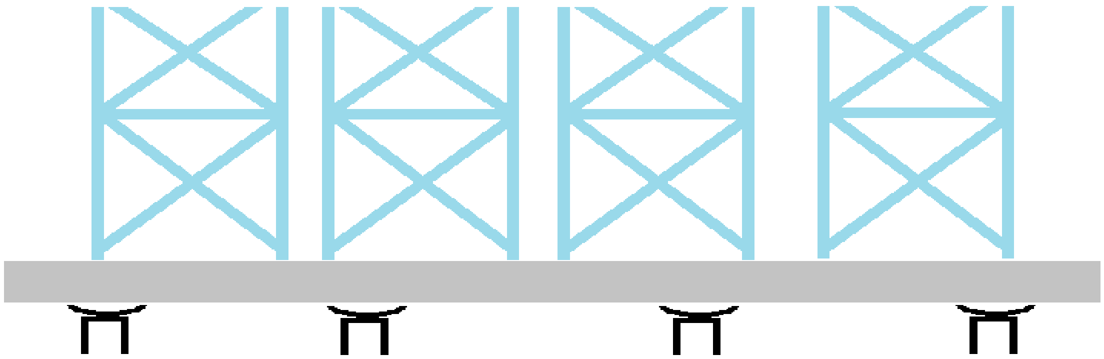

Figure 41: Combined steel isolated rack structure

Main characteristics of single friction isolators are taken from a commercial catalogue which are presented in Table 3. The stiffness of isolators was calculated according to the weight of the structure (Fig. 42,43).

Table 3: Main characteristics of the commercial FPSs considered in the analysis [47]

FPS type	R (mm)	Max Displacement Capacity	Nsd/Ned	μfast	μslow	drm (mm)
Medium-type friction	3,700	400	1	0.055	0.022	81.4
Medium-type friction	2,500	100	0.8	0.062	0.025	62.36
Medium-type friction	2,500	150	0.8	0.062	0.025	62.36
Medium-type friction	3,100	200	0.8	0.062	0.025	77.33
Medium-type friction	3,100	250	0.8	0.062	0.025	77.33
Medium-type friction	3,700	300	0.8	0.062	0.025	92.3
Medium-type friction	3,700	350	0.8	0.062	0.025	92.3
Medium-type friction	3,700	400	0.8	0.062	0.025	92.3
Medium-type friction	2,500	100	0.6	0.073	0.029	73.33
Medium-type friction	2,500	150	0.6	0.073	0.029	73.33
Medium-type friction	3,100	200	0.6	0.073	0.029	90.93
Medium-type friction	3,100	250	0.6	0.073	0.029	90.93
Medium-type friction	3,700	300	0.6	0.073	0.029	108.52
Medium-type friction	3,700	350	0.6	0.073	0.029	108.52
Medium-type friction	3,700	400	0.6	0.073	0.029	108.52
Medium-type friction	2,500	100	0.4	0.092	0.037	92.13
Medium-type friction	2,500	150	0.4	0.092	0.037	92.13
Medium-type friction	3,100	200	0.4	0.092	0.037	114.24
Medium-type friction	3,100	250	0.4	0.092	0.037	114.24
Medium-type friction	3,700	300	0.4	0.092	0.037	136.35
Medium-type friction	3,700	350	0.4	0.092	0.037	136.35
Medium-type friction	3,700	400	0.4	0.092	0.037	136.35

Effective Stiffness - $K = W/R + \mu W/D$ (3.1)

(Case One)

W = 4523.8 KN

R = 3.1

$\mu = 0.062$

D = 0.2 (m)

K1 (Linear case) = 4523.8 / 3.1 + (0.062*4523.8) / 0.2

K1 = 2861.6 KN/m

K2 (Nonlinear case) = 4523.8 / 3.1 + (0.062*4523.8) / 0.0014

K2 = 201799 KN/m

(Case Two)

W = 3947.8 KN (For FPS under loaded rack)

W = 3743 KN (For FPS under unloaded rack)

R = 3.1

$\mu = 0.062$

D = 0.2 (m)

K1 (Linear case) = 3947.8 / 3.1 + (0.062*3947.8) / 0.2 (For FPS under loaded rack)

K1 = 2497 KN/m

K1 (Linear case) = 3743 / 3.1 + (0.062*3743.8) / 0.2 (For FPS under unloaded rack)

K1 = 2367.8 KN/m

K2 (Nonlinear case) = 3947.8 / 3.1 + (0.062*3947.8) / 0.0014 (For FPS under loaded rack)

K2 = 176113.4 KN/m

K2 (Nonlinear case) = 3743 / 3.1 + (0.062*3743) / 0.0014 (For FPS under unloaded rack)

K2 = 165761.4 KN/m

(Case Three)

W = 3372 KN (For FPS under loaded rack)

W = 3211 KN (For FPS under unloaded rack)

R = 3.1

μ = 0.062

D = 0.2 (m)

K1 (Linear case) = 3372 / 3.1 + (0.062*3372) / 0.2 (For FPS under loaded rack)

K1 = 2133 KN/m

K1 (Linear case) = 3211 / 3.1 + (0.062*3211) / 0.2 (For FPS under unloaded rack)

K1 = 2031.5 KN/m

K2 (Nonlinear case) = 3372 / 3.1 + (0.062*3372) / 0.0014 (For FPS under loaded rack)

K2 = 150419 KN/m

K2 (Nonlinear case) = 3211 / 3.1 + (0.062*3211) / 0.0014 (For FPS under unloaded rack)

K2 = 143237.4 KN/m

(Case Four)

W = 2796 KN (For FPS under loaded rack)

W = 2510 KN (For FPS under unloaded rack)

R = 3.1

μ = 0.062

D = 0.2 (m)

K1 (Linear case) = 2796 / 3.1 + (0.062*2796) / 0.2 (For FPS under loaded rack)

K1 = 1769 KN/m

K1 (Linear case) = 2510 / 3.1 + (0.062*2510) / 0.2 (For FPS under unloaded rack)

K1 = 1587.7 KN/m

K2 (Nonlinear case) = 2796 / 3.1 + (0.062*2796) / 0.0014 (For FPS under loaded rack)

K2 = 124725 KN/m

K2 (Nonlinear case) = 2510 / 3.1 + (0.062*2510) / 0.0014 (For FPS under unloaded rack)

K2 = 111966.7 KN/m

Effective Damping - $\beta = 2\,\mu / [\,\mu + (D/R)\,\pi]$ (3.2)

= (2*0.062) / 3.14(0.2/3.1) + 0.062= 0.47

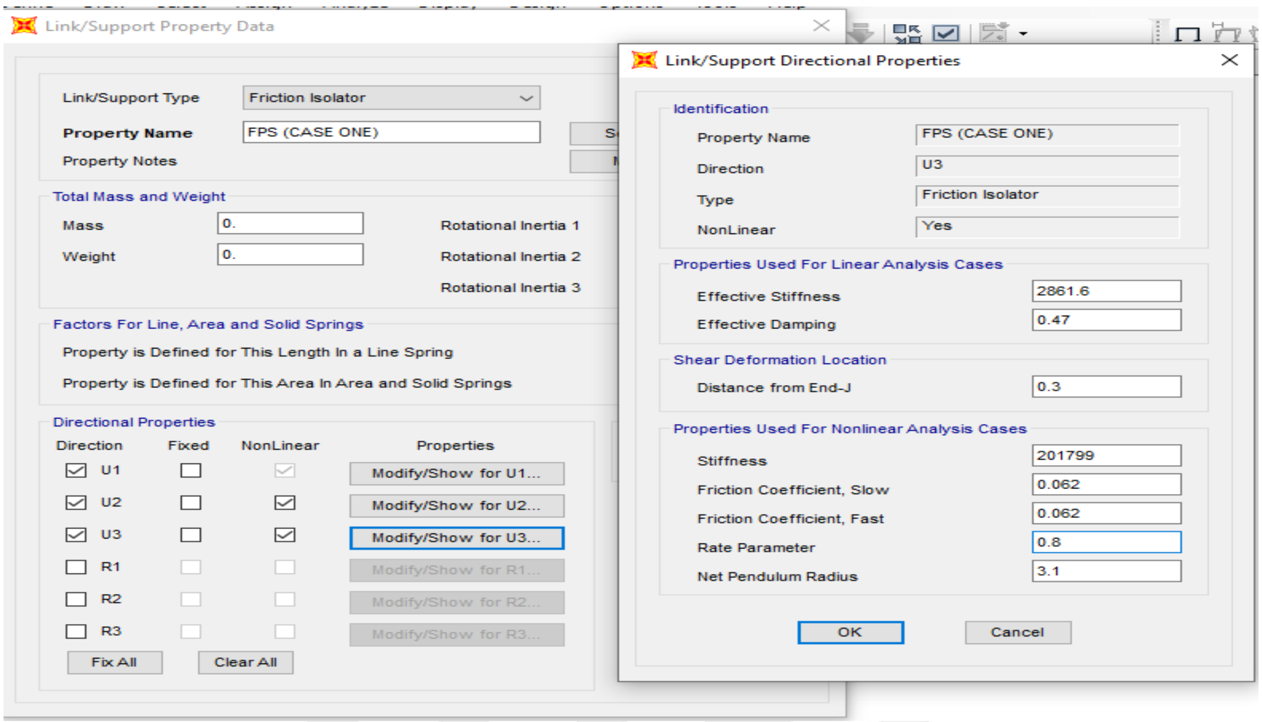

Figure 42: FPS properties in SAP2000 (Case One)

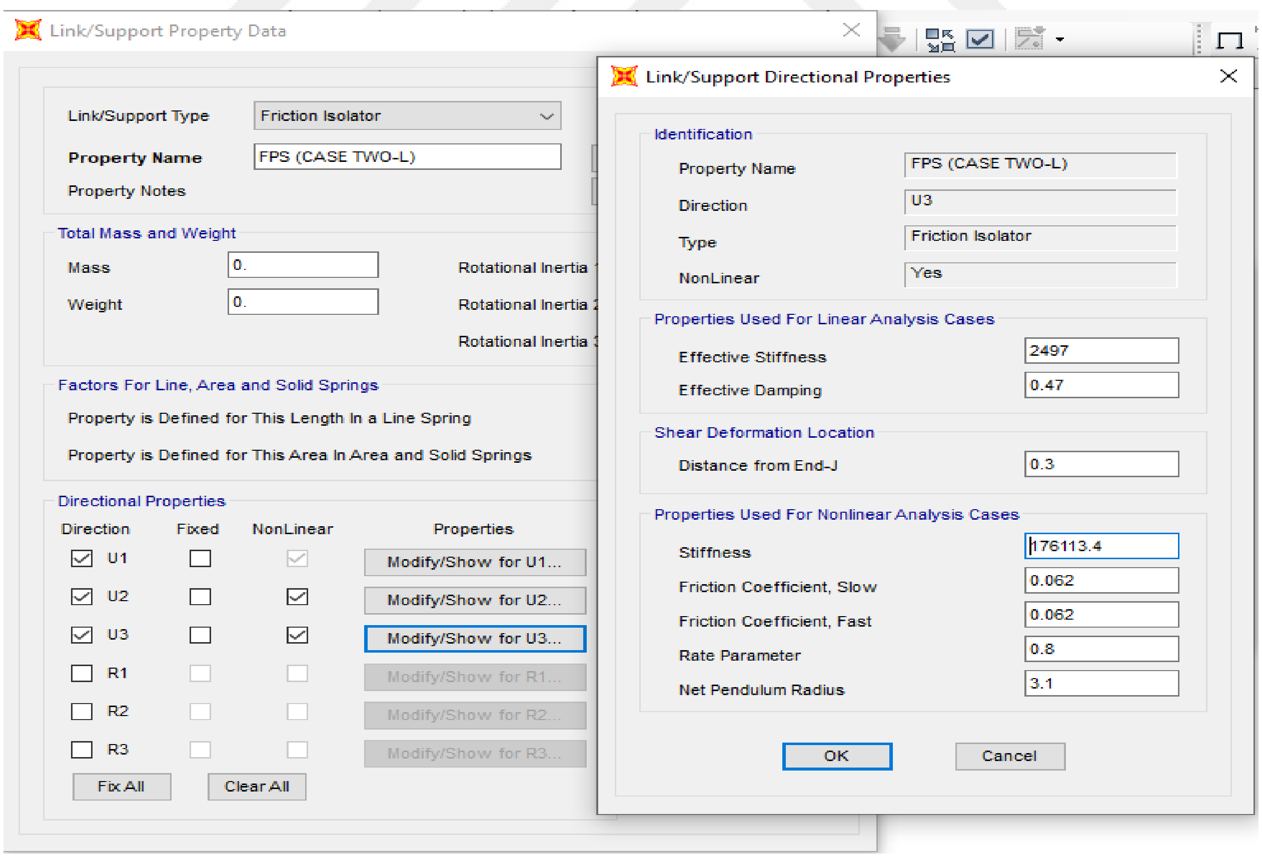

Figure 43: FPS properties in SAP2000 (Case Two)

A non-linear Time History analysis was done on the isolated steel storage racks with FPS to find out the effect of isolator application in steel storage racks. Acceleration and Relative Displacements of isolated steel storage rack was observed and compared to the fixed base steel storage rack. Both in fixed base and isolated base steel storage rack structures the acceleration and displacements were observed at top joint of the model. The natural frequency period of the isolated model showed a significant increase which resulted in decrease of acceleration. The decrease in acceleration of rack structure can cause to prevent shedding of contents from beams and a well-controlled steel storage rack during earthquakes.

Six near-field and six far-field earthquakes with various magnitudes were used [43]. The following table present the details of all 12 earthquakes, record is available from the PEER NGA database.

Table 4: Earthquake Records for different kinds of loadings [43]

No.	Name and Station	Component	Year	Magnitude	Distance
1	Darfield New Zealand - HORC	HORCN18E	2010	7.3	Near-Field
2	Loma Prieta -Saratoga	WVC270	1989	6.9	Near-Field
3	Cape Mendocino - Petrolia	PET090	1992	7.1	Near-Field
4	Irpinia, Italy-01 - Sturno	STU270	1980	6.9	Near-Field
5	Superstition Hills-02 - PTS	PTS225	1987	6.5	Near-Field
6	Kobe Japan - Takarazuka	TAZ090	1995	6.9	Near-Field
7	Landers - Coolwater	CLW-LN	1992	7.3	Far-Field
8	Northridge - Canyon Country WLC	LOS270	1994	6.7	Far-Field
9	Manjil Iran - Abbar	ABBAR—L	1990	7.4	Far-Field
10	Firuli, Italy - Tolmezzo	TMZ270	1976	6.5	Far-Field
11	Hector Mine - Hector	HEC090	1999	7.1	Far-Field
12	El Mayor-Cucapah - El Centro	E12360	2010	7.1	Far-Field

3.3.1 Modal Analysis

For finding fundamental natural period a modal analysis was performed on a single isolated and fixed steel storage rack. Vibration modes of a structures is good for understanding of the system's behavior. The results obtained from modal analysis of isolated steel storage rack with FPS show reasonably good increase in period of the structure in comparison to fixed based steel storage rack.

Table 5: Vibration modes of SAP model for single rack

Mode No.	Numerical - Fixed Base	Experimental - Fixed Base	Numerical - Isolated Base
	Period (s)	Period (s)	Period (s)
Mode 1	1.291	1.261	3.131
Mode 2	1.202	1.225	2.552
Mode 3	1.15	1.003	2.011

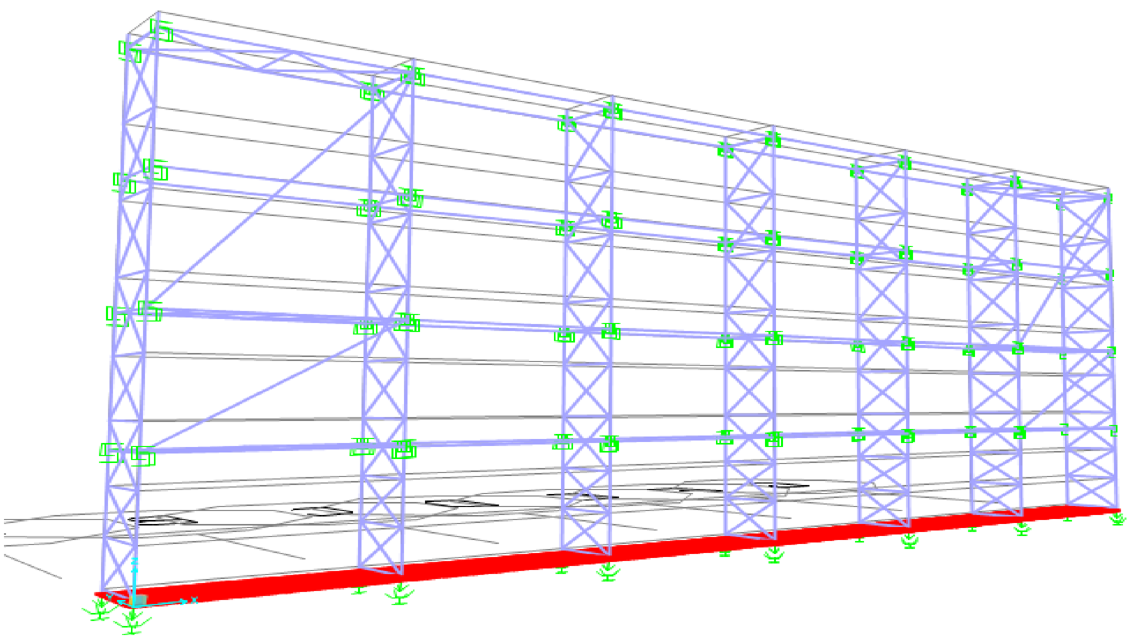

Figure 44: 3D View of the Model

3.3.2 Seismic Time History Analysis

Time history analysis was performed for simulation of seismic loads. Time history analysis use dynamic loading to apply on the rack system step by step and then it starts recoding the corresponding response. In this analysis, time history analysis is performed step by step by Nonlinear Modal History (FNA). FNA time depends on the size of the structure and the number of time steps to follow which each analysis may lead to a long time. Time history in this part of analysis was conducted with earthquake records of Table 4 on the combined steel storage rack structure with FPS (The periods of combined St. storage rack structure are T1: 2.01, T2: 1.61 and T3: 1.21) (fig. 41).

Numerical Results of isolated steel storage rack with 100% of the applied earthquakes are compared with fixed base steel storage rack. In this section results of Acceleration and Relative Displacement of the analysis is presented and discussed (fig. 45) (fig. 46).

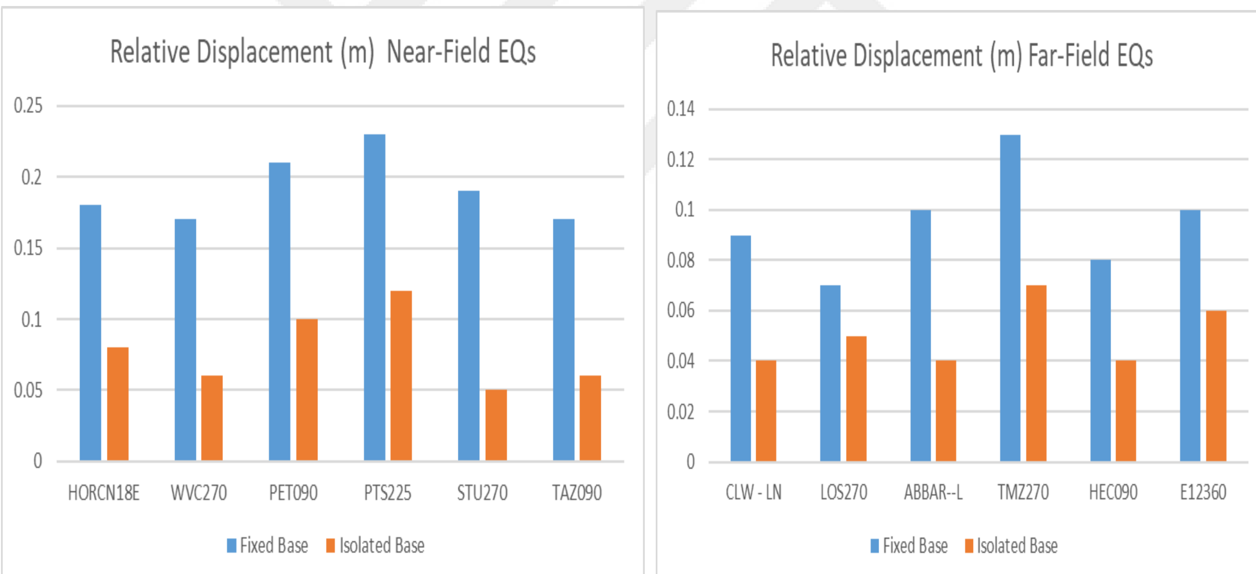

Figure 45: Isolated Base and Fixed Base results of relative displacement

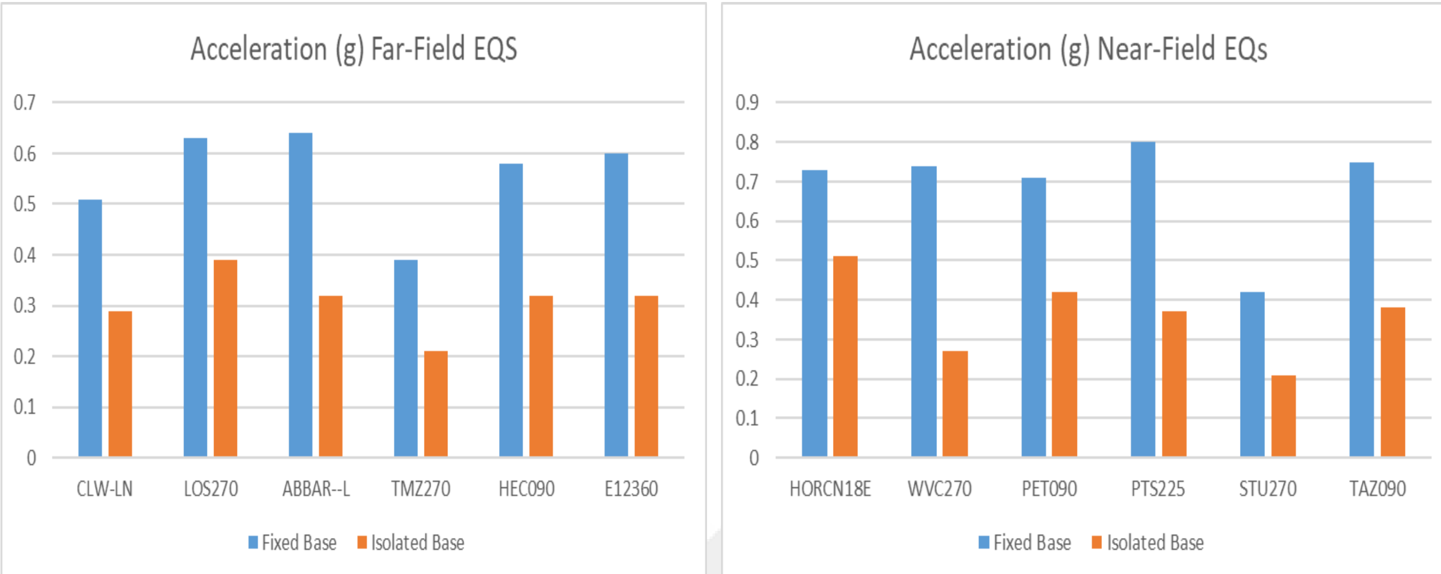

Figure 46: Isolated Base and Fixed Base results of acceleration

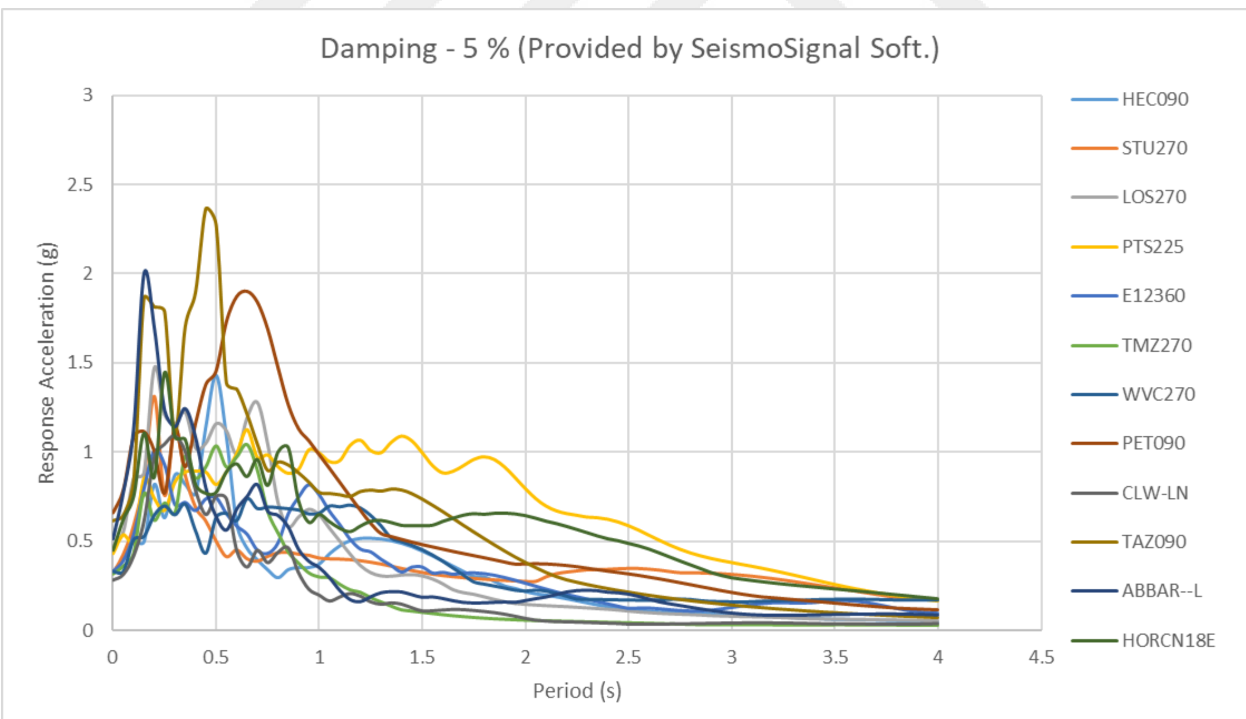

Figure 47: Response Acceleration of earthquakes (5% Damping)

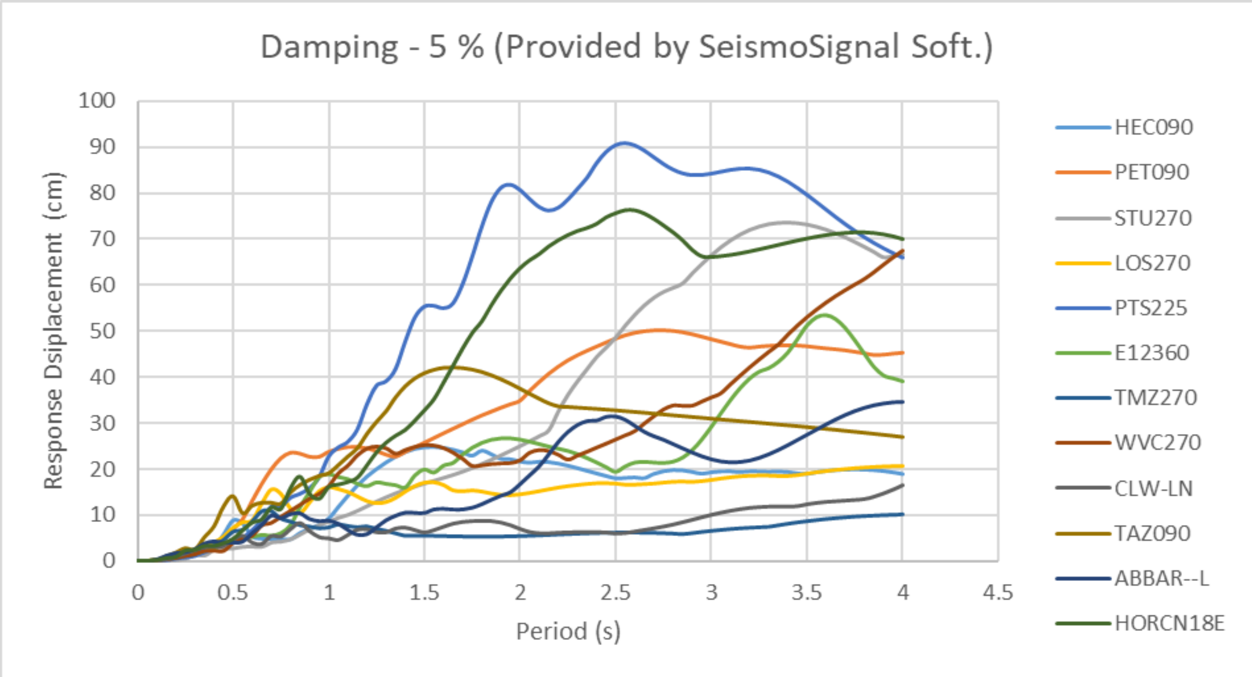

Figure 48: Response Displacement of earthquakes (5% Damping)

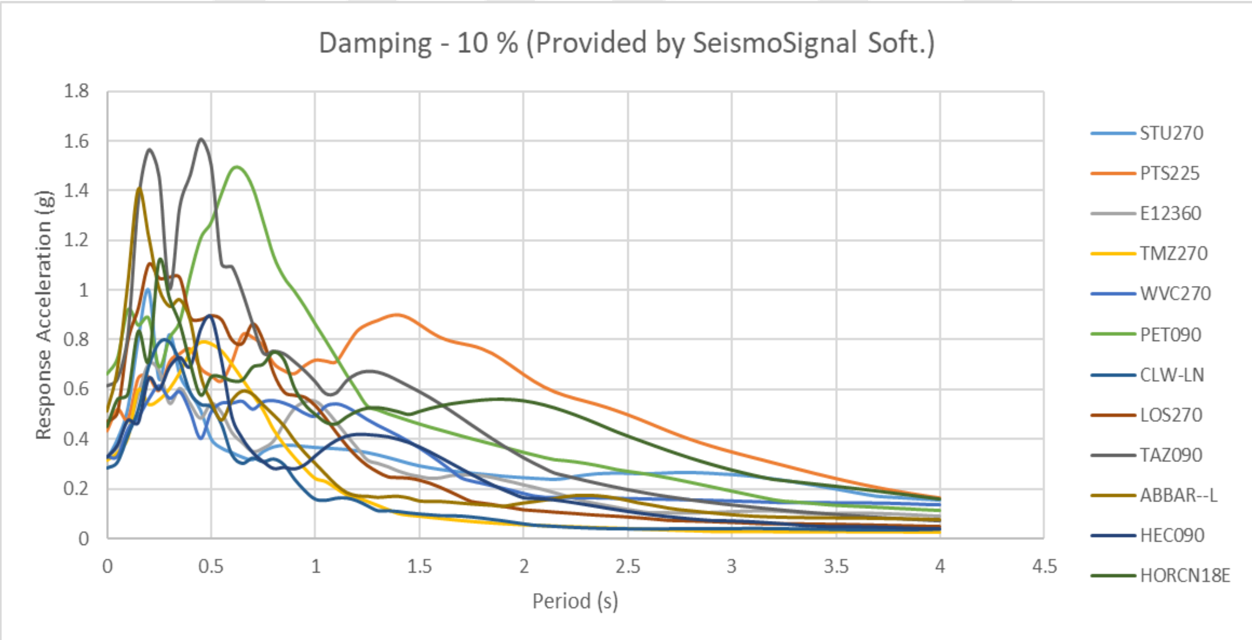

Figure 49: Response Acceleration of earthquakes (10% Damping)

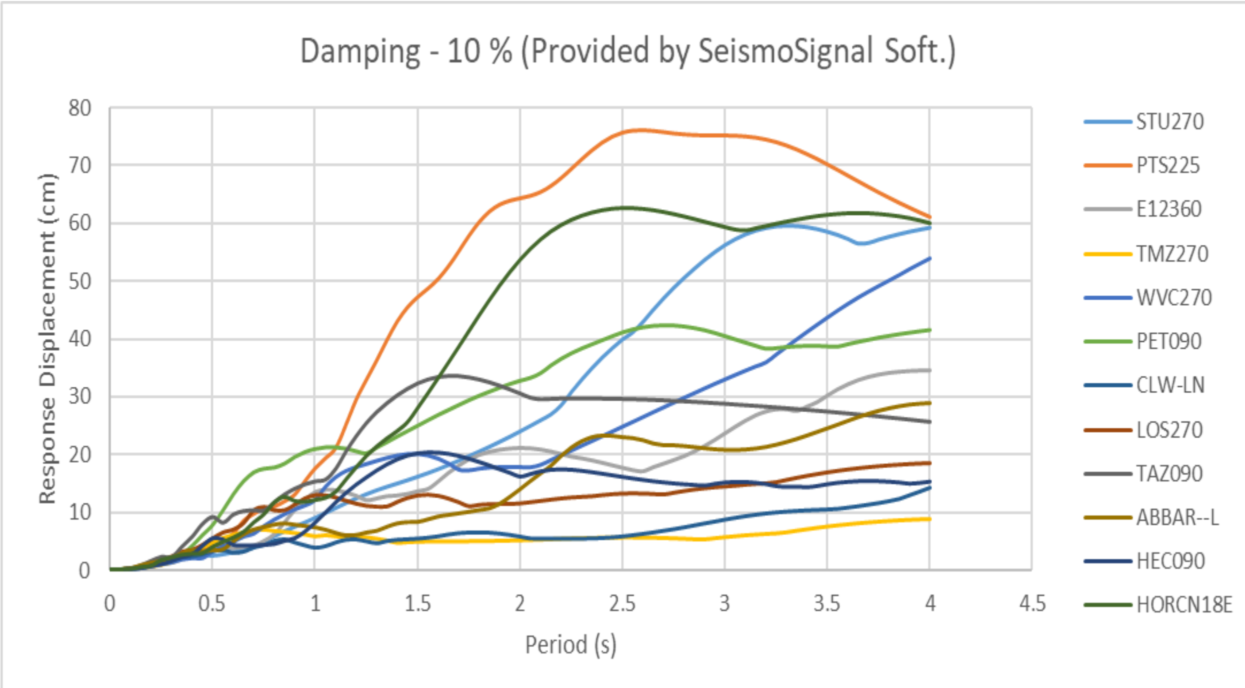

Figure 50: Response Displacement of earthquakes (10% Damping)

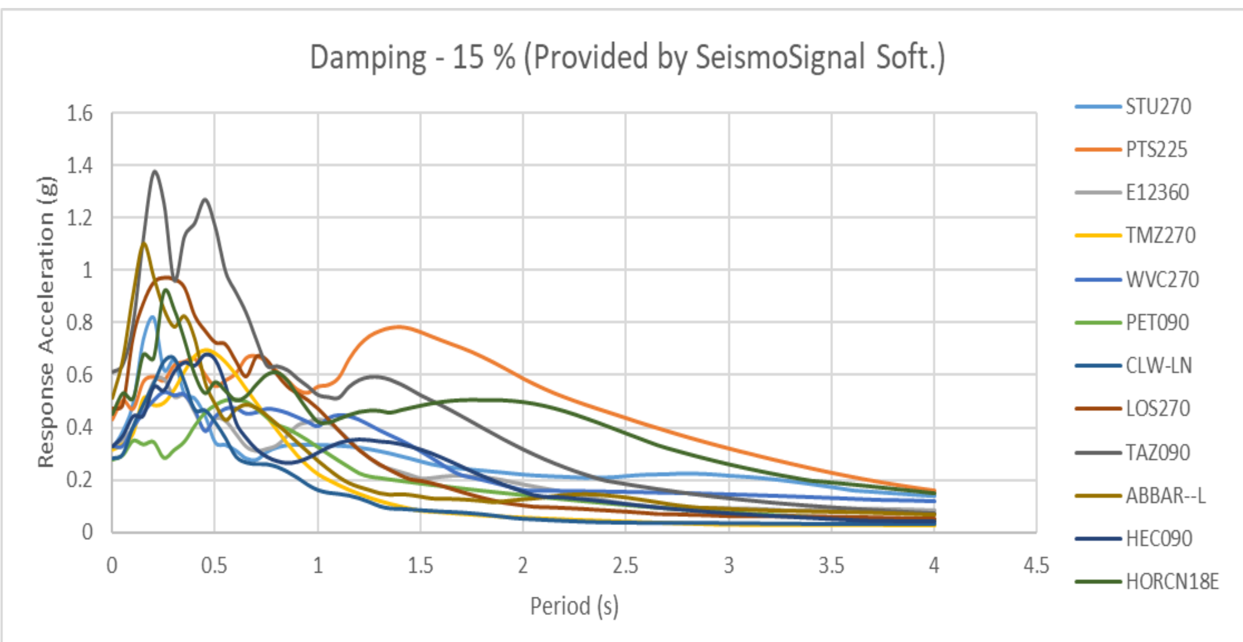

Figure 51: Response Acceleration of earthquakes (15% Damping)

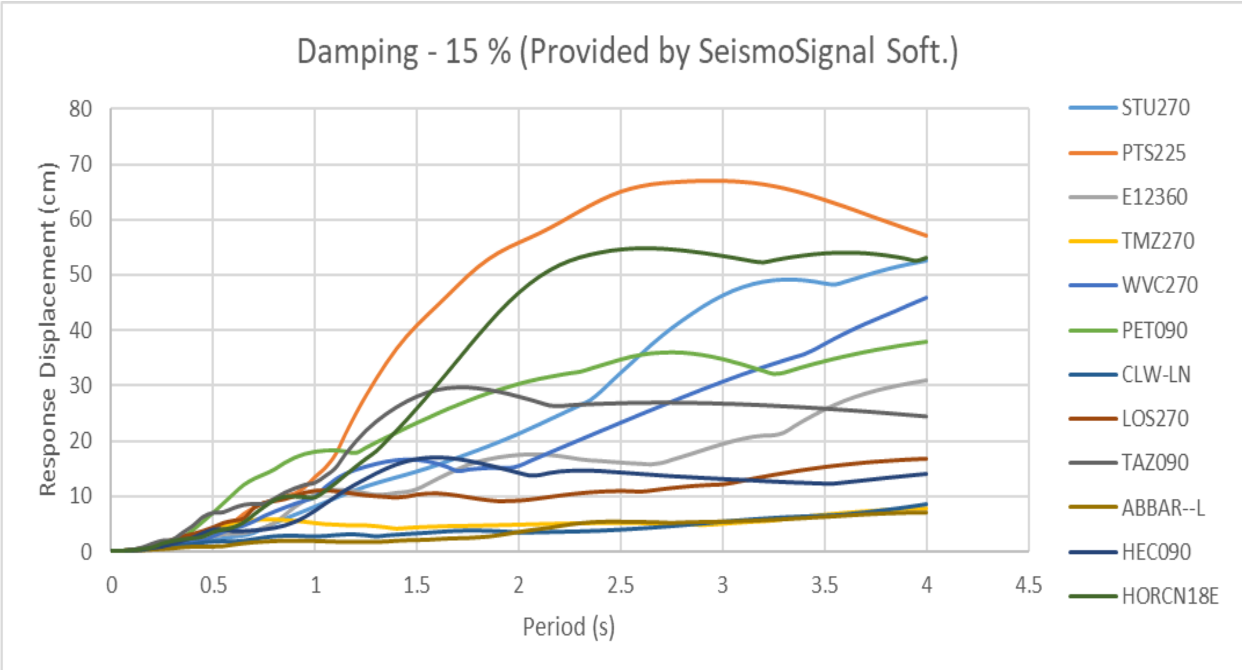

Figure 52: Response Displacement of earthquakes (15% Damping)

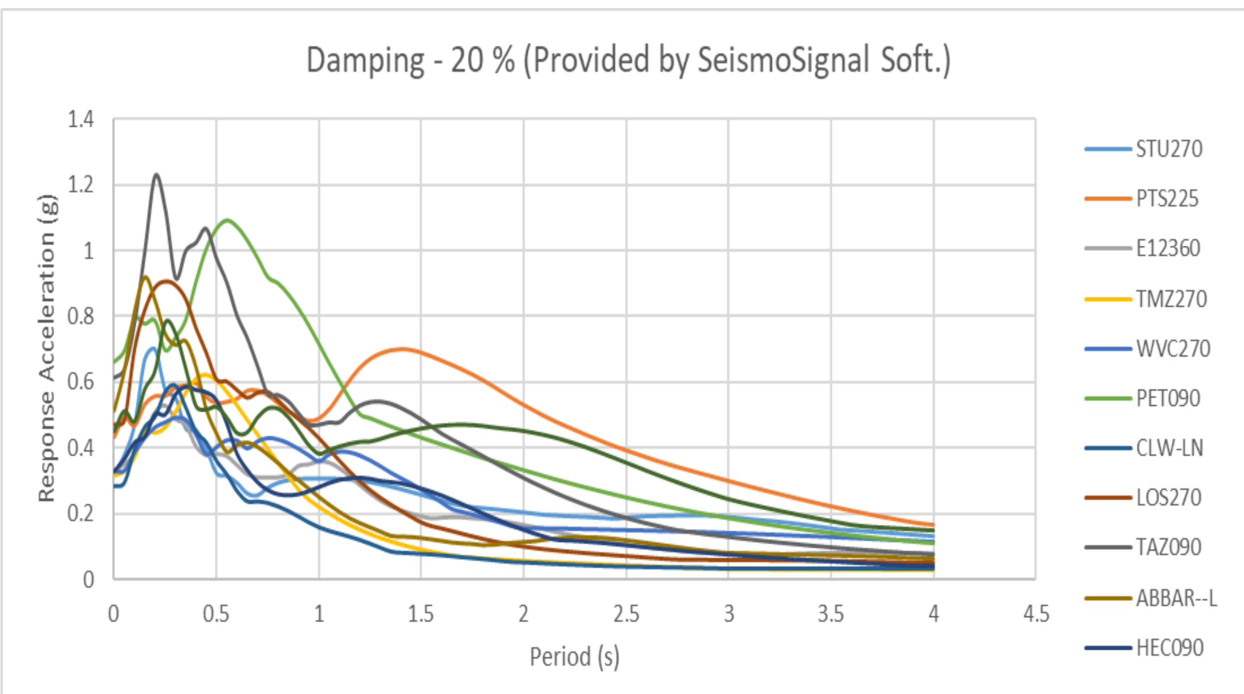

Figure 53: Response Acceleration of earthquakes (20% Damping)

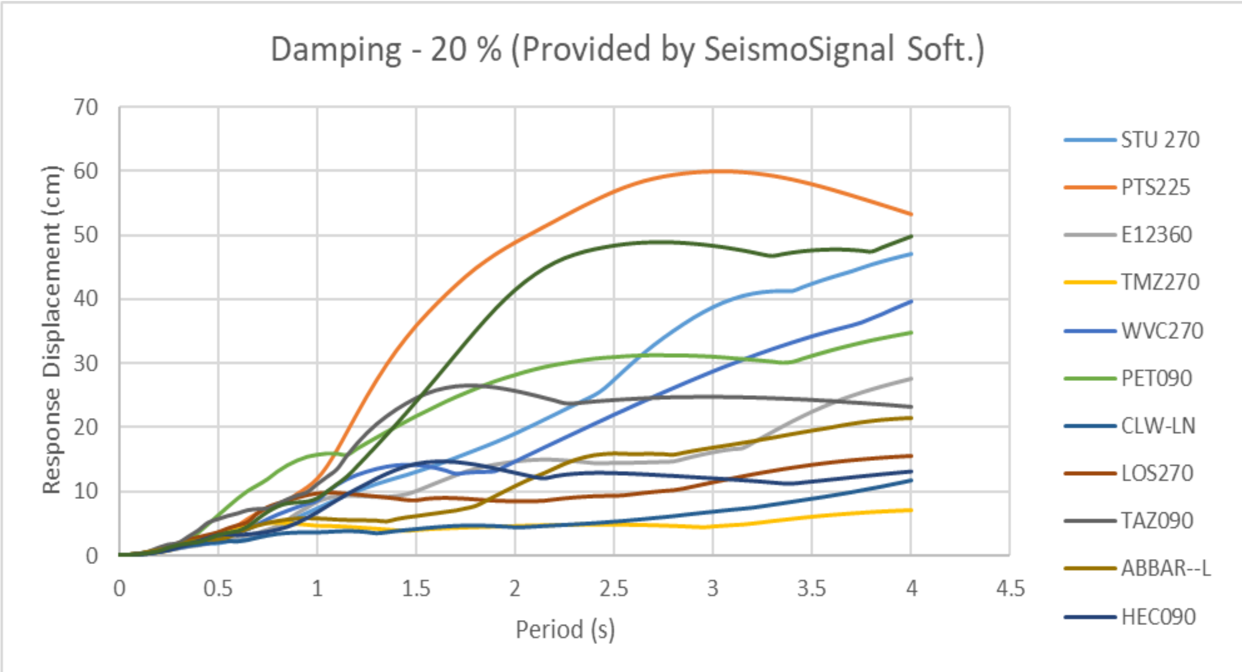

Figure 54: Response Displacement of earthquakes (20% Damping)

The fixed based and isolated structure periods were obtained through modal analysis. The fixed period of 1.25s was increased to a period almost 3 times after application of single frictional isolator. The analysis results show significant decrease in acceleration. As shown in above figures, these parameters decrease with increase in the structural fundamental period but in contrary to the total displacement. The con of increasing the structural period is that it may increase bearing displacements. However, the relative dispalcement of isolated rack structure between the top floor and bearing show a signifiant decrease which verifies the proper response of isolators in the structure.

Absolute maximum acceleration can be defined as the absolute peak acceleration value of an earthquake record to be excited horizontally in both negative and positive axis. Inertial forces are proportional to the accelerations, hence larger acceleration yield higher story forces. The acceleration data of both in fixed and isolated rack structure was taken and compared. a maximum reduction of 45% to 65% in acceleration for far-field and near-field ground motions were observed.

3.3.3 Hysteresis Loop (Force – Displacement Curves) of the Isolators

If we plot the force (F) acting on an object by the distance moved, we make a force-displacement graph. These are useful because we can always find the work done by (or on) a system by finding the area under a force-displacement graph. As the result, the hysteresis loops can be used to determine the energy dissipation per cycle and the effective damping provided by bearings. Hysteresis loop of FPS isolator for each earthquake is given below accordingly.

Figure 55: following figures are Force-Deformation Curves of FPS Links (Hysteresis Loop – Structure Fully loaded)

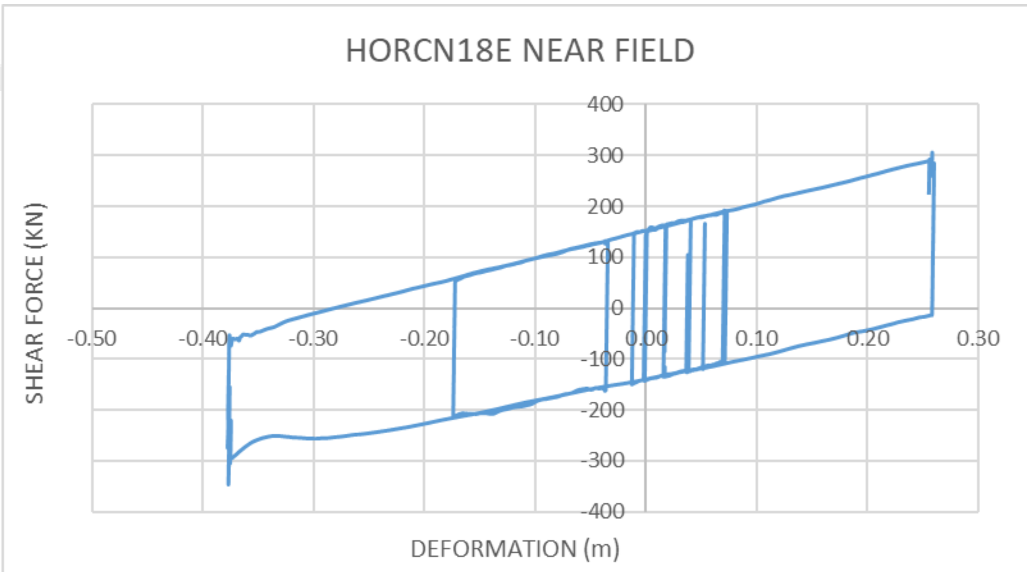

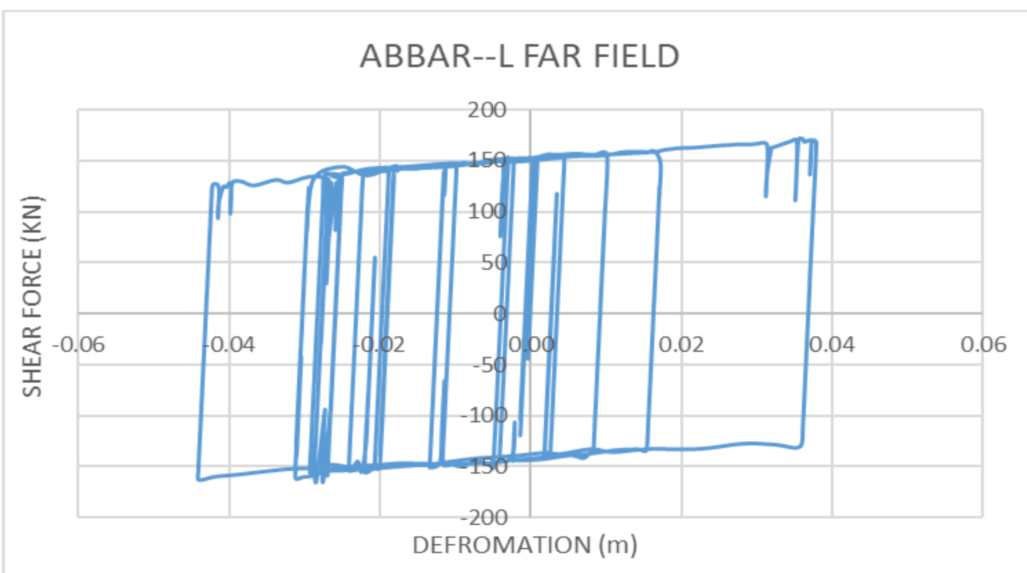

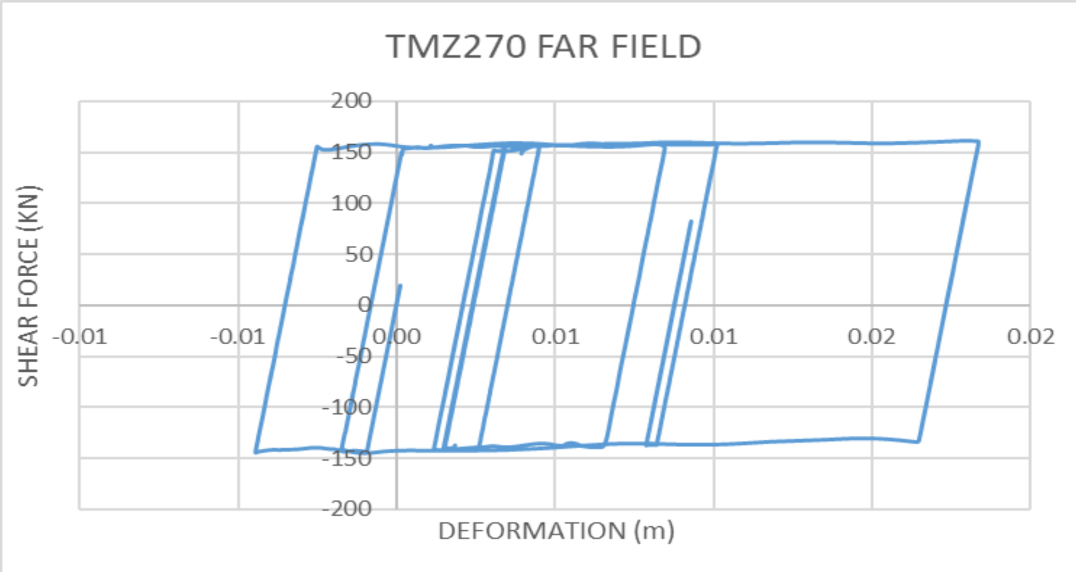
TMZ270 FAR FIELD
SHEAR FORCE (KN)
DEFORMATION (m)
200
150
100
50
0
-50
-100
-150
-200
-0.01
-0.01
0.00
0.01
0.01
0.02
0.02

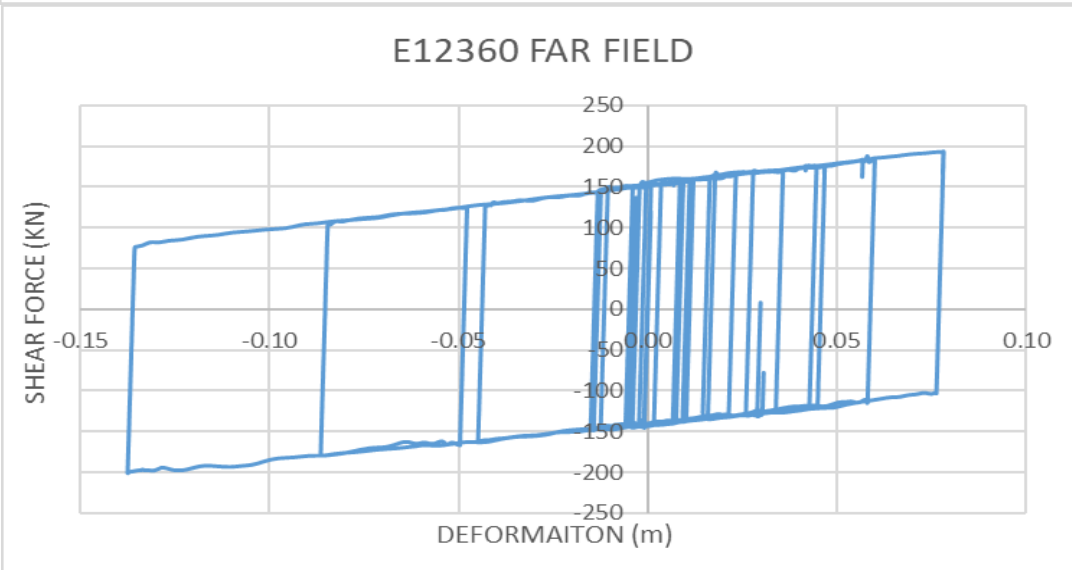
E12360 FAR FIELD
SHEAR FORCE (KN)
DEFORMAITON (m)
250
200
150
100
50
0
-50
-100
-150
-200
-250
-0.15
-0.10
-0.05
0.00
0.05
0.10

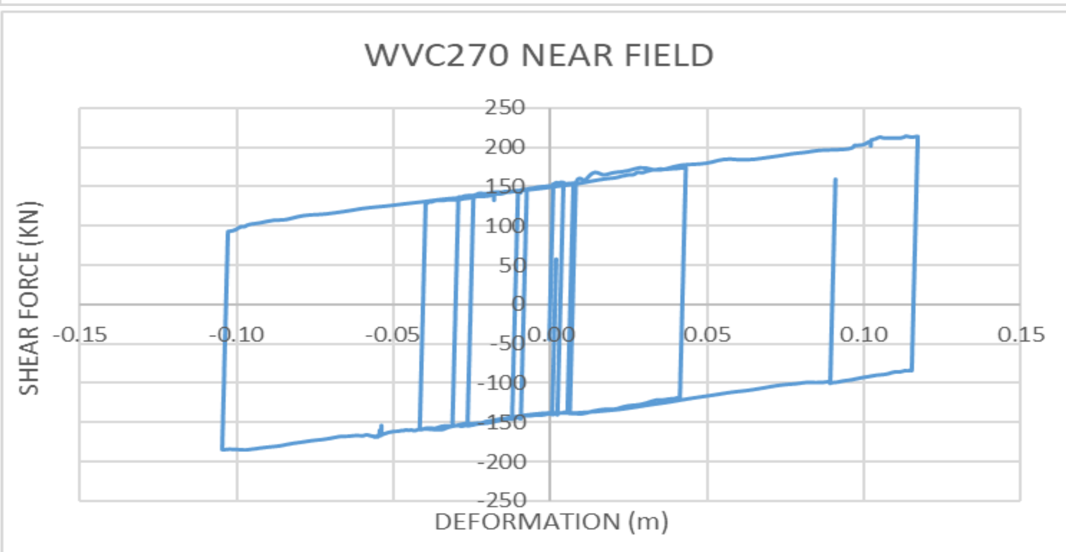
WVC270 NEAR FIELD
SHEAR FORCE (KN)
DEFORMATION (m)
250
200
150
100
50
0
-50
-100
-150
-200
-250
-0.15
-0.10
-0.05
0.00
0.05
0.10
0.15

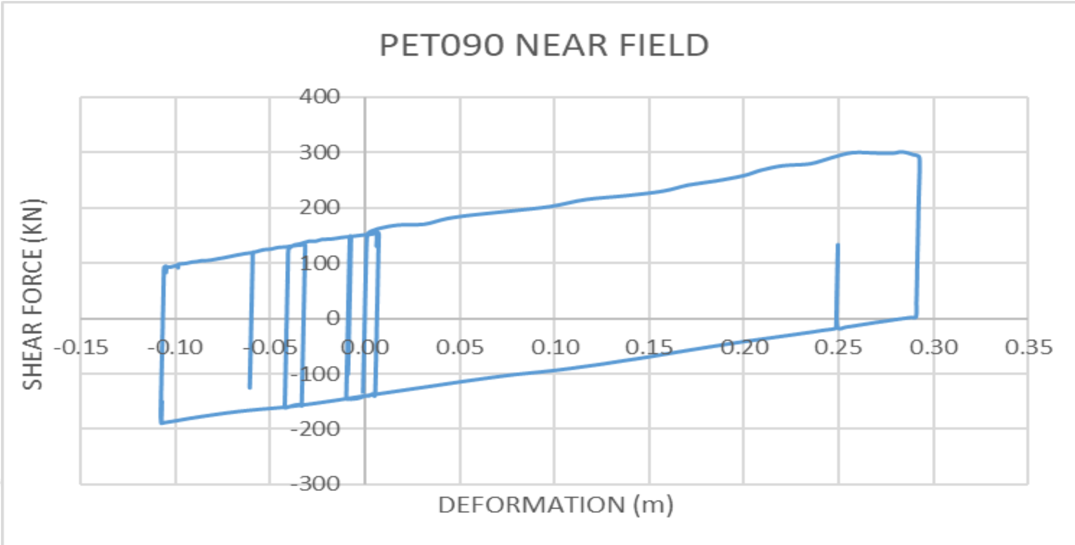
PET090 NEAR FIELD
SHEAR FORCE (KN)
DEFORMATION (m)
400
300
200
100
0
-100
-200
-300
-0.15
-0.10
-0.05
0.00
0.05
0.10
0.15
0.20
0.25
0.30
0.35

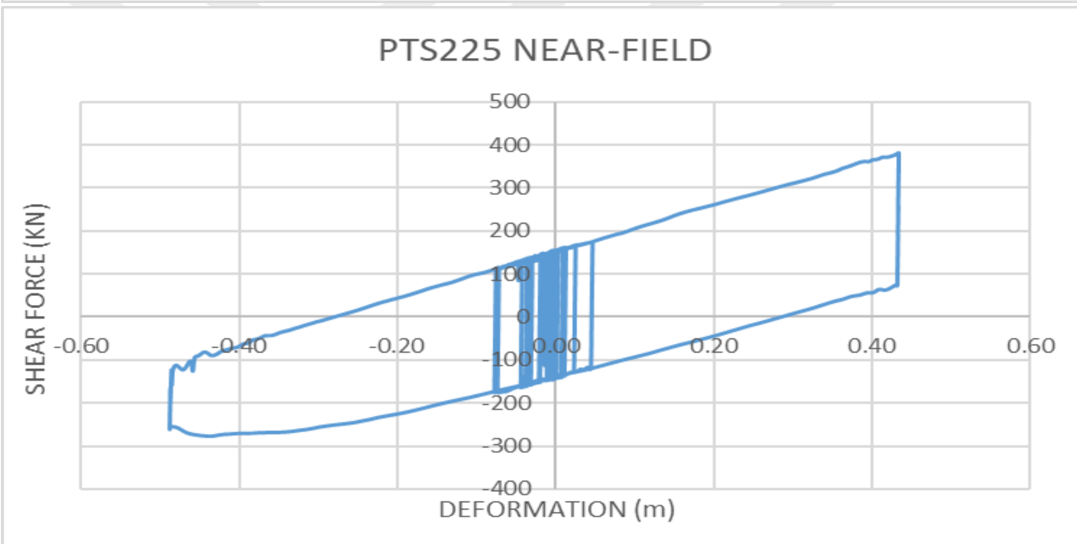
PTS225 NEAR-FIELD
SHEAR FORCE (KN)
DEFORMATION (m)
500
400
300
200
100
0
-100
-200
-300
-400
-0.60
-0.40
-0.20
0.00
0.20
0.40
0.60

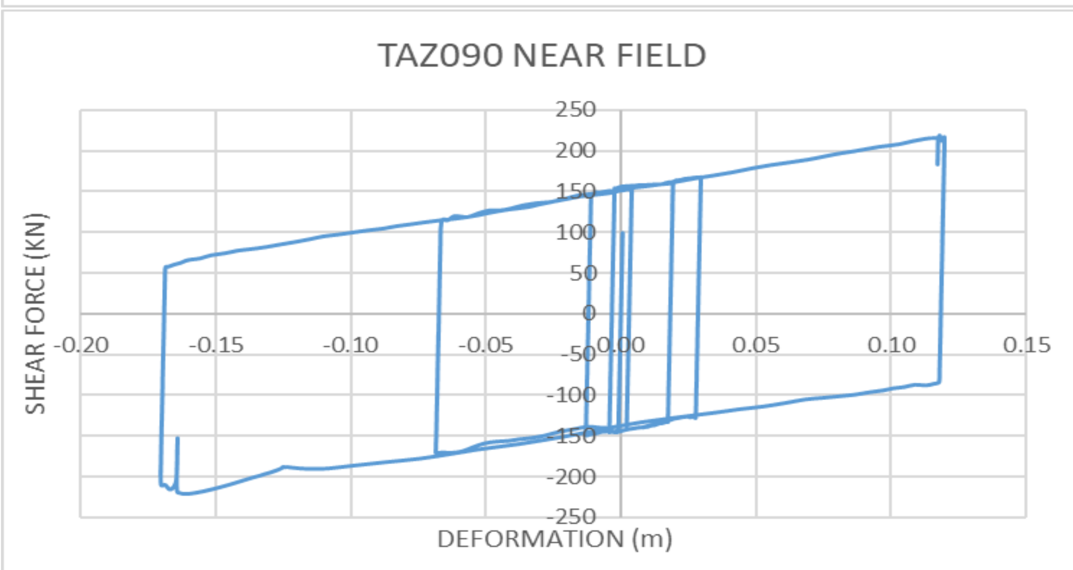
TAZ090 NEAR FIELD
SHEAR FORCE (KN)
DEFORMATION (m)
250
200
150
100
50
0
-50
-100
-150
-200
-250
-0.20
-0.15
-0.10
-0.05
0.00
0.05
0.10
0.15

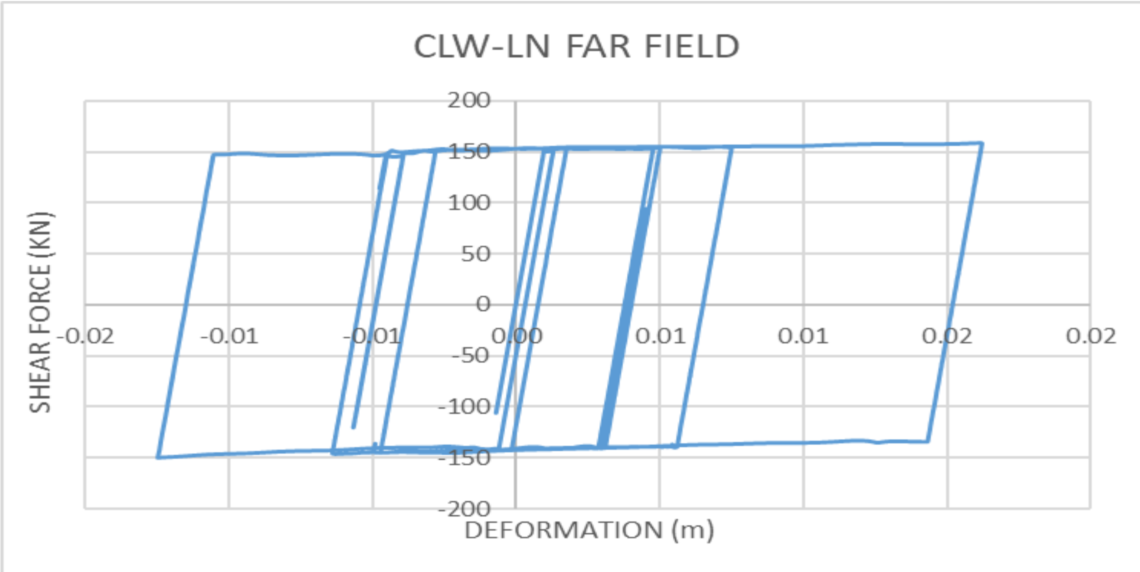

CLW-LN FAR FIELD
SHEAR FORCE (KN)
DEFORMATION (m)
200
150
100
50
0
-50
-100
-150
-200
-0.02
-0.01
-0.01
0.00
0.01
0.01
0.02
0.02

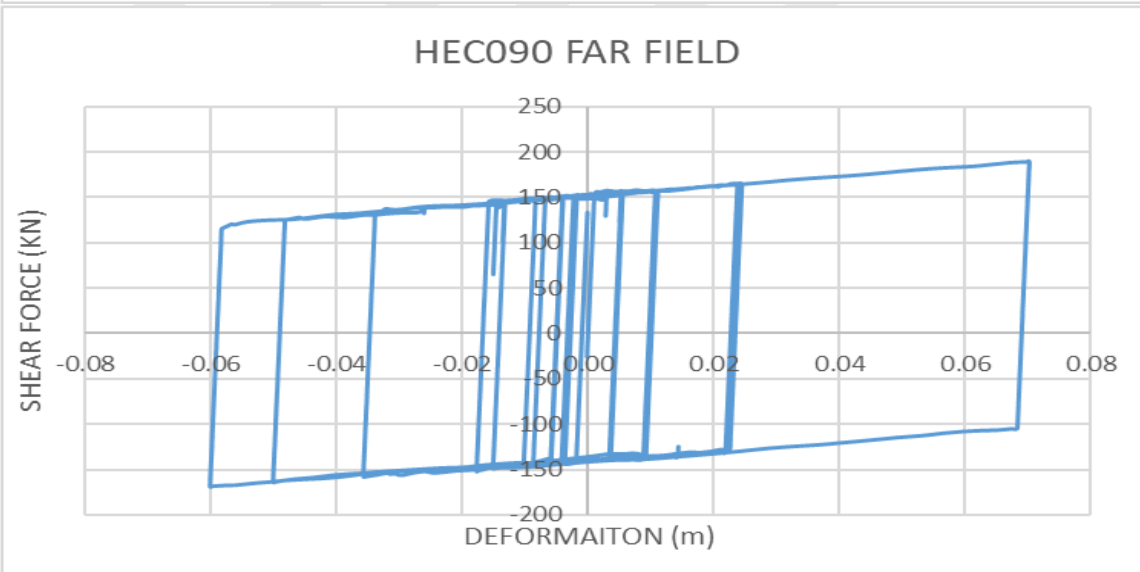

HEC090 FAR FIELD
SHEAR FORCE (KN)
DEFORMAITON (m)
250
200
150
100
50
0
-50
-100
-150
-200
-0.08
-0.06
-0.04
-0.02
0.00
0.02
0.04
0.06
0.08

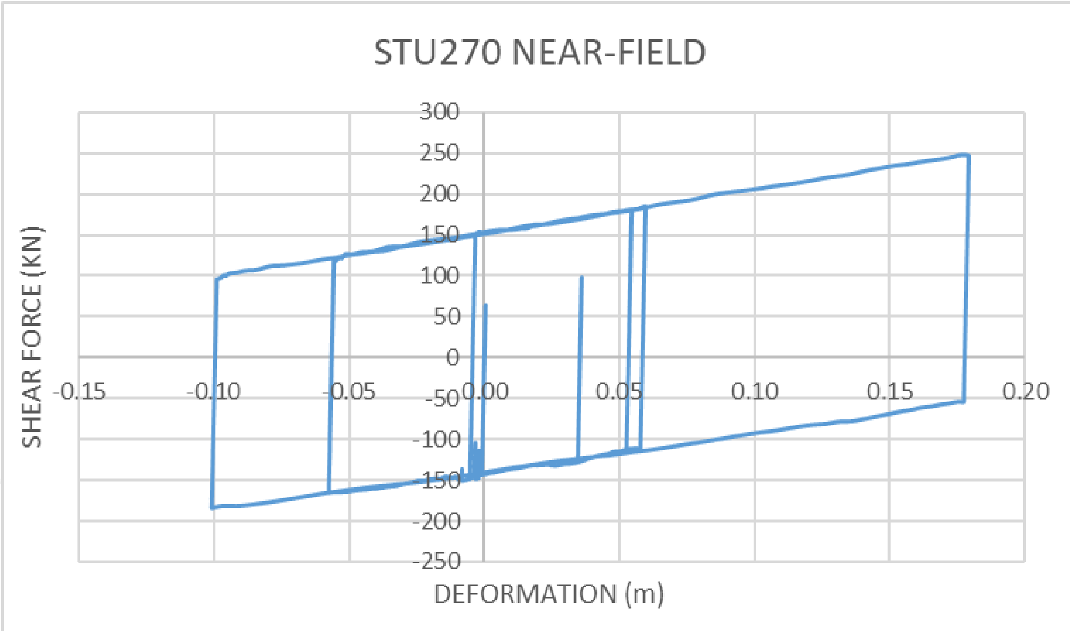
STU270 NEAR-FIELD
300
250
200
150
100
50
0
-50
-100
-150
-200
-250
-0.15
-0.10
-0.05
0.00
0.05
0.10
0.15
0.20
SHEAR FORCE (KN)
DEFORMATION (m)

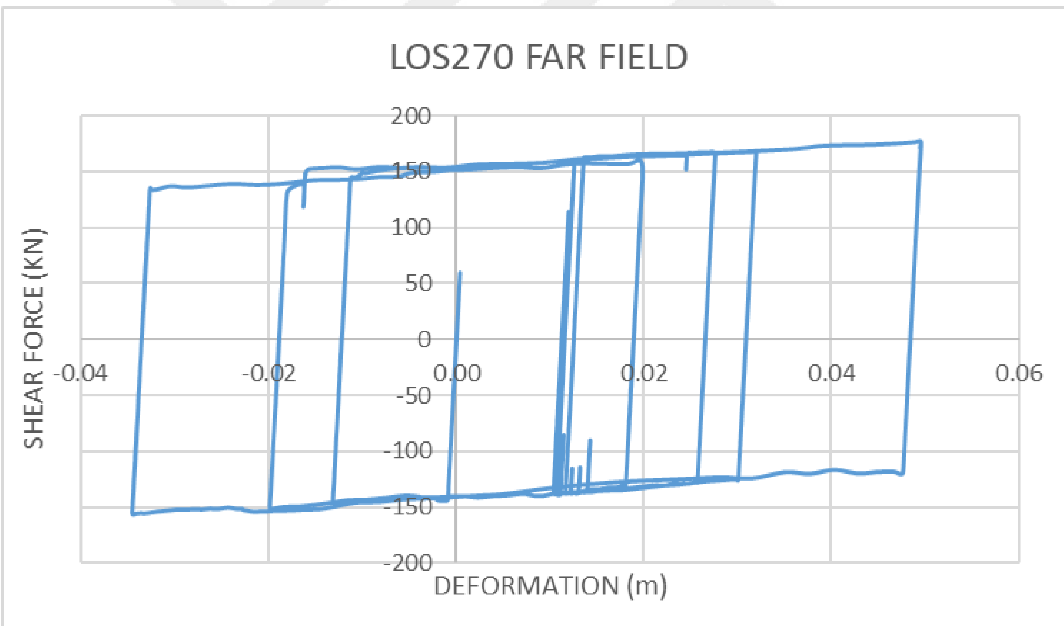
LOS270 FAR FIELD
200
150
100
50
0
-50
-100
-150
-200
-0.04
-0.02
0.00
0.02
0.04
0.06
SHEAR FORCE (KN)
DEFORMATION (m)

3.4 Study and Analysis of Various Cases of loading

As the second part of this thesis, a combined steel storage rack structure with different kinds of loadings was investigated. Four of the same rack structures were placed on a concrete slab with 2 meters distance from each other. During analysis four cases of loadings were investigated, Case 1 – all four racks were fully loaded, Case 2- only one rack out of four racks was fully unloaded, Case 3 – only two racks out of four racks were fully unloaded and finally Case 4 – three racks out of four racks were fully unloaded. Each case was carefully investigated and the behavior of rack structures and effects of it on the contents during earthquake is summarized. Also, single friction isolators were applied under concrete slab at the bearings and real earthquakes data were used for time history analysis. To find out the behavior of steel storage racks with various cases of loadings under seismic ground motions, the structure rotational displacement during earthquake was observed at two joints at the bearings. The two observed joints were in opposite positions of concrete slab, the first observed joint was at the loaded corner of the concrete slab and the second observed joint was at the unloaded corner of the concrete slab.

Time History Analysis (FNA) is done with 6 near-field and 6 far-field earthquakes. Details of earthquakes records are already given at table 4. When the structure is rotating during given ground motions, each joints displacement at bearing in the same exact time is investigated. The results show that loaded side of structure shows more displacement during the given ground motions excitations and in some cases unloaded side of structure has a significant displacement difference with the loaded side of the structure. But after unloading one or two racks of the structure, there is an increase of displacement observed in loaded side of structure comparing to structure displacement when all four racks are fully loaded.

All cases design pictures from Sap2000 are presented respectively for a better understanding of results, following displacement data of all cases at both joints. The behavior of rack structures in all cases are also explained accordingly.

3.4.1 Case one

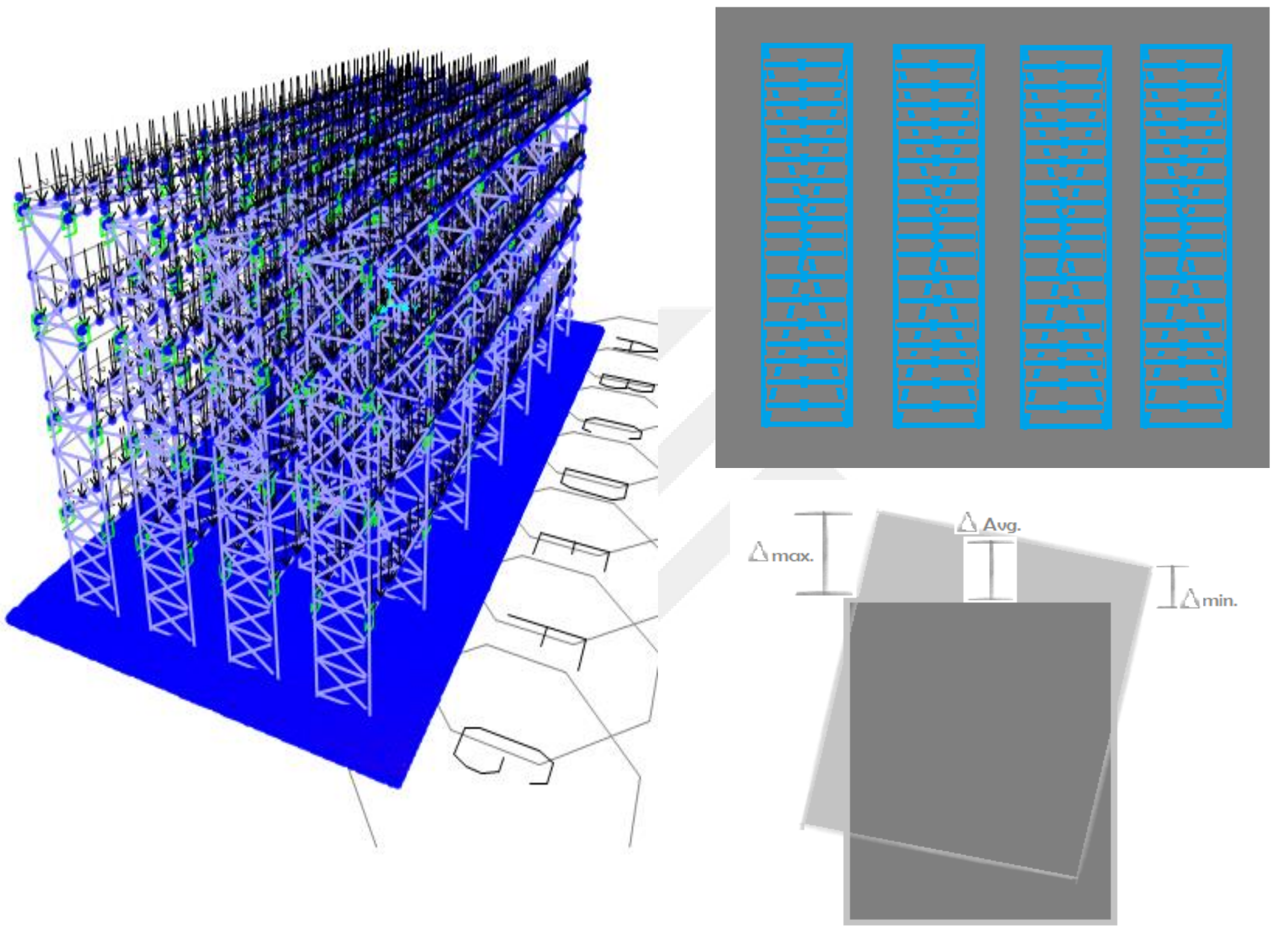

Figure 56: 3D-View of Rack Structure for case one

Displacement at the bearing of structure in case one is almost the same or identical in all positions and all joints. Since all four racks are fully loaded with the same amount of weight and all isolators are working under the same applied force on them, center of mass plus center of weight will be positioned at the center of structure and equally distributed to all joints at the bearing. Hence, not so much displacement difference is seen between both joints. As mentioned, the displacement difference between both joints in all earthquakes results are very minor or the same which might cause a minor structural rotation during earthquake excitation and shedding of storage rack contents from pallets can be negligible.

Table 6: Case One Results

CASE ONE - FOUR RACKS LOADED				
Earthquake	Δmax. (m)	Δmin. (m)	Δavg. (m)	Δmax./Δavg. Ratio
Darfield New Zealand - HORC	0.61	0.6	0.605	1.009
Loma Prieta -Saratoga	0.43	0.42	0.425	1.011
Cape Mendocino - Petrolia	0.356	0.351	0.353	1.007
Parachute Test Site	0.47	0.46	0.465	1.01
Irpina - Sturno	0.4	0.4	0.4	1
Kobe Japan - Takarazuka	0.145	0.141	0.143	1.013
Landers - Coolwater	0.197	0.191	0.194	1.015
Northridge - Canyon Country WLC	0.1	0.1	0.105	1.047
Manjil Iran - Abbar	0.17	0.17	0.175	1
Firuli, Italy - Tolmezzo	0.05	0.05	0.05	1
Hector Mine - Hector	0.1	0.09	0.095	1.052
El Mayor-Cucapah - El Centro	0.581	0.58	0.580	1

3.4.2 Case Two

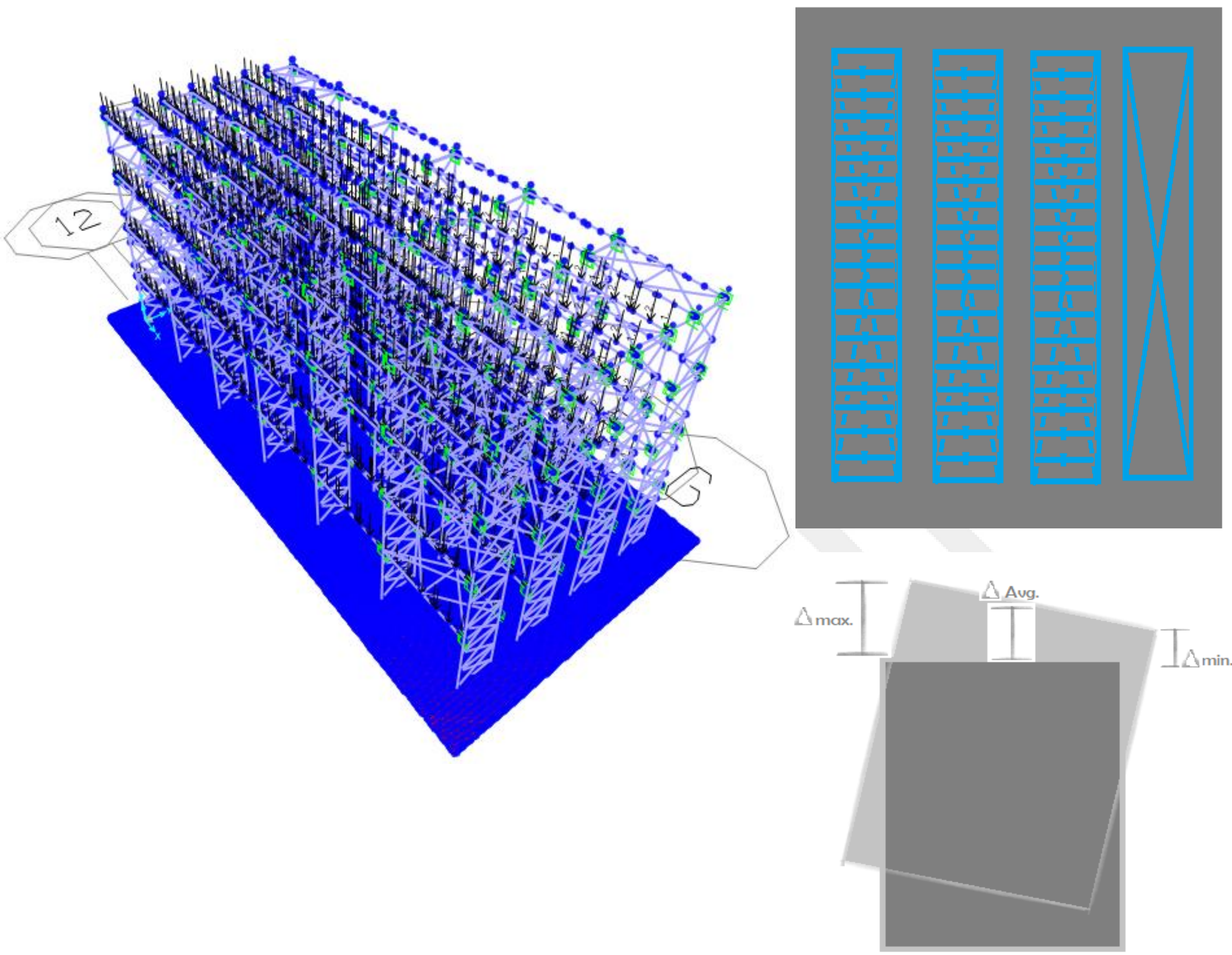

Figure 57: 3D View of Rack Structure for case two

Displacement at the bearing of rack structure in case two between joints from loaded and unloaded corner of structure shows a minor difference. Since three racks are fully loaded in the structure and the remaining one rack is fully unloaded, center of mass plus center of weight is mostly concentrated at the loaded side of structure. Hence, a minor displacement difference can be observed between both joints. In case Four and three the displacement difference between both joints in all earthquakes are considerably enough for structural rotation of rack structure during earthquake excitations than case One and Two. Also, it is to mention that a minor displacement difference between both joints can be seen in case two which can be enough for structural rotation during earthquake excitation but shedding of storage rack contents from pallets can be controllable.

Table 7: Case Two Results

CASE TWO - THREE RACKS LOADED				
Earthquake	Δmax. (m)	Δmin. (m)	Δavg. (m)	Δmax./Δavg. Ratio
Darfield New Zealand - HORC	0.78	0.69	0.735	1.06
Loma Prieta -Saratoga	0.44	0.43	0.435	1.01
Cape Mendocino - Petrolia	0.39	0.34	0.365	1.06
Parachute Test Site	0.62	0.5	0.56	1.107
Irpina - Sturno	0.44	0.38	0.41	1.07
Kobe Japan - Takarazuka	0.17	0.14	0.155	1.09
Landers - Coolwater	0.19	0.18	0.185	1.02
Northridge - Canyon Country WLC	0.13	0.1	0.115	1.13
Manjil Iran - Abbar	0.17	0.15	0.16	1.06
Firuli, Italy - Tolmezzo	0.06	0.05	0.055	1.09
Hector Mine - Hector	0.13	0.1	0.115	1.13
El Mayor-Cucapah - El Centro	0.62	0.6	0.61	1.01

3.4.3 Case Three

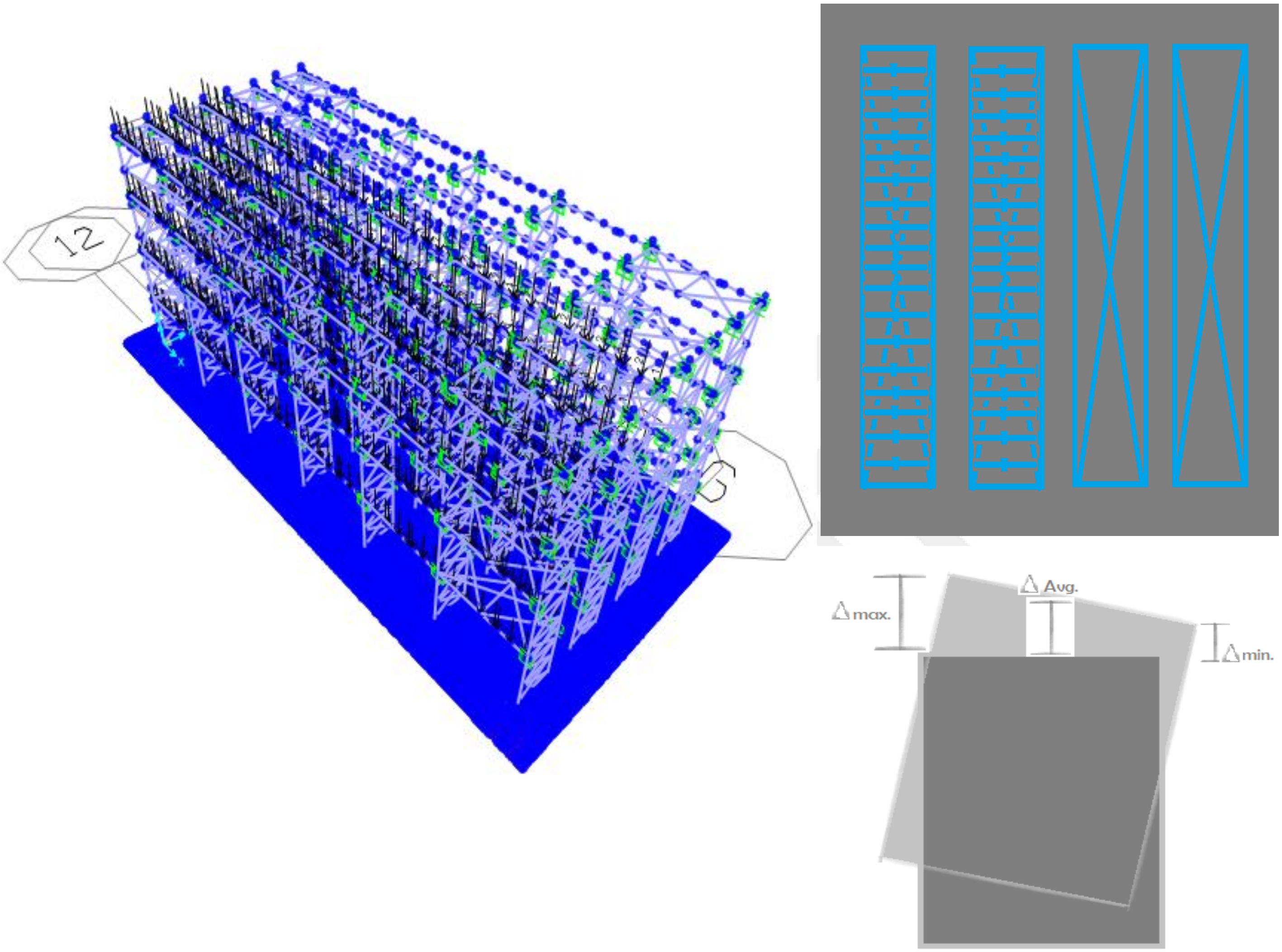

Figure 58: 3D View of Rack Structure for case three

Displacement at the bearing of rack structure in case three between joints from loaded and unloaded corner of structure shows a considerable difference too. Since only two rack is fully loaded in the structure and the remaining two racks are fully unloaded, center of mass plus center of weight is mostly concentrated at the loaded side of structure. Hence, displacement difference is seen between both joints.

Table 8: Case Three Results

CASE THREE - TWO RACKS LOADED				
Earthquake	Δmax. (m)	Δmin. (m)	Δavg. (m)	Δmax./Δavg. Ratio
Darfield New Zealand - HORC	0.73	0.66	0.695	1.05
Loma Prieta -Saratoga	0.45	0.41	0.43	1.04
Cape Mendocino - Petrolia	0.39	0.34	0.365	1.06
Parachute Test Site	0.57	0.48	0.525	1.08
Irpina - Sturno	0.45	0.38	0.415	1.08
Kobe Japan - Takarazuka	0.14	0.12	0.13	1.07
Landers - Coolwater	0.18	0.17	0.175	1.02
Northridge - Canyon Country WLC	0.12	0.09	0.105	1.14
Manjil Iran - Abbar	0.16	0.15	0.155	1.03
Firuli, Italy - Tolmezzo	0.063	0.049	0.056	1.12
Hector Mine - Hector	0.11	0.08	0.095	1.15
El Mayor-Cucapah - El Centro	0.61	0.59	0.6	1.01

3.4.4 Case Four

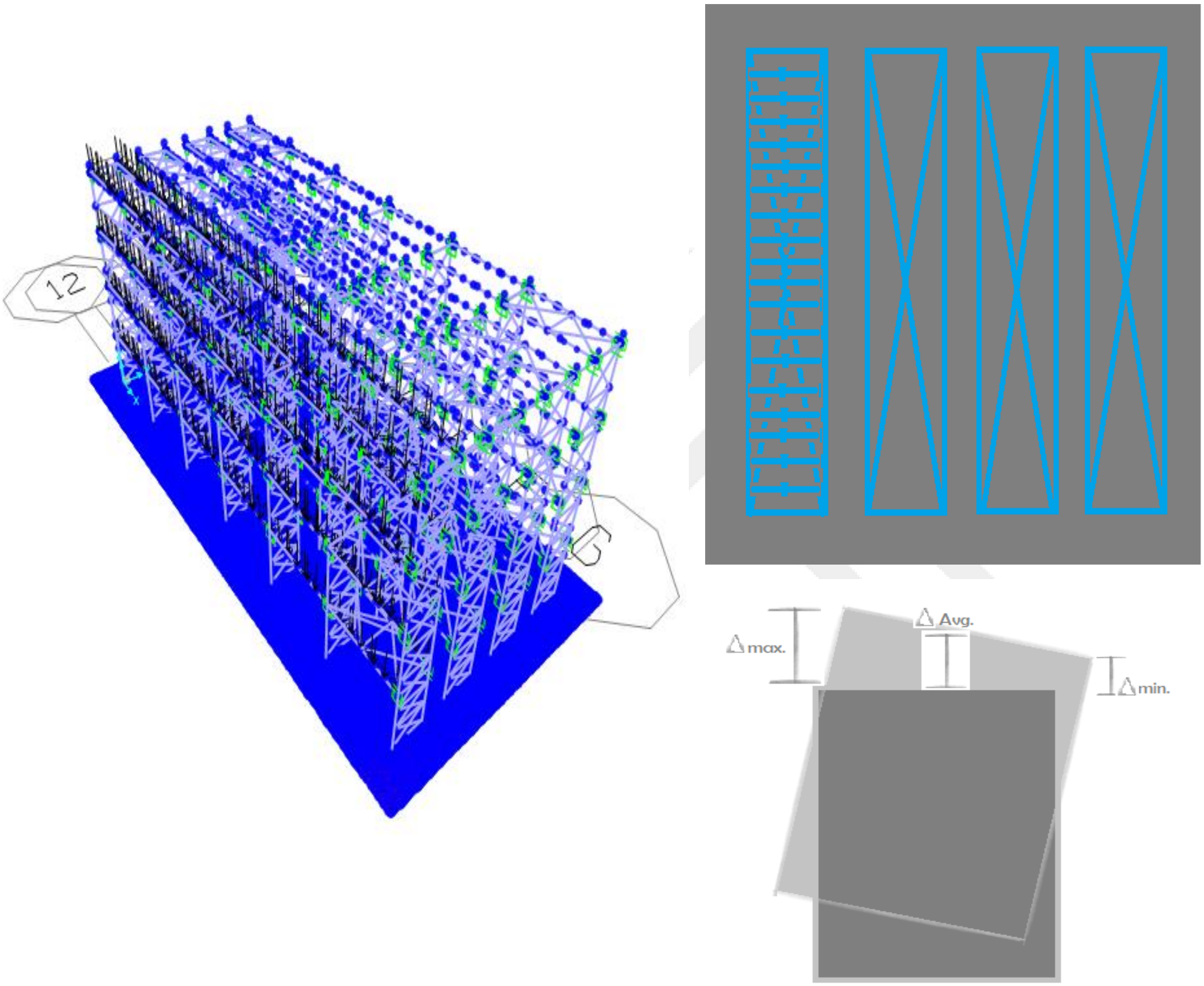

Figure 59: 3D View of Rack Structure for case four

Displacement at the bearing of rack structure in case four between joints from loaded and unloaded corner of structure shows a significant difference. Since only one rack is fully loaded in the structure and the remaining three racks are fully unloaded, center of mass plus center of weight is mostly concentrated at the loaded side of structure. Hence, displacement difference is seen between both joints.

Table 9: Case Four Results

CASE FOUR - ONE RACKS LOADED				
Earthquake	Δmax. (m)	Δmin. (m)	Δavg. (m)	Δmax/Δavg. Ratio
Darfield New Zealand - HORC	0.74	0.51	0.625	1.18
Loma Prieta -Saratoga	0.46	0.27	0.365	1.26
Cape Mendocino - Petrolia	0.4	0.31	0.355	1.12
Parachute Test Site	0.53	0.33	0.43	1.23
Irpina - Sturno	0.31	0.11	0.21	1.47
Kobe Japan - Takarazuka	0.16	0.09	0.125	1.28
Landers - Coolwater	0.2	0.14	0.17	1.17
Northridge - Canyon Country WLC	0.13	0.08	0.105	1.238
Manjil Iran - Abbar	0.155	0.127	0.141	1.099
Firuli, Italy - Tolmezzo	0.039	0.067	0.053	0.735
Hector Mine - Hector	0.17	0.11	0.14	1.21
El Mayor-Cucapah - El Centro	0.65	0.49	0.57	1.14

3.5 Variation of Friction Coefficient (Structure Fully loaded)

Analysis for variation of coefficient of friction showed that by increase of coefficient of friction an increase will also happen in acceleration of structure meanwhile a decrease in displacement.

Figure 60: Following figures are Bearing Displacement & Acceleration for various friction Coefficient:

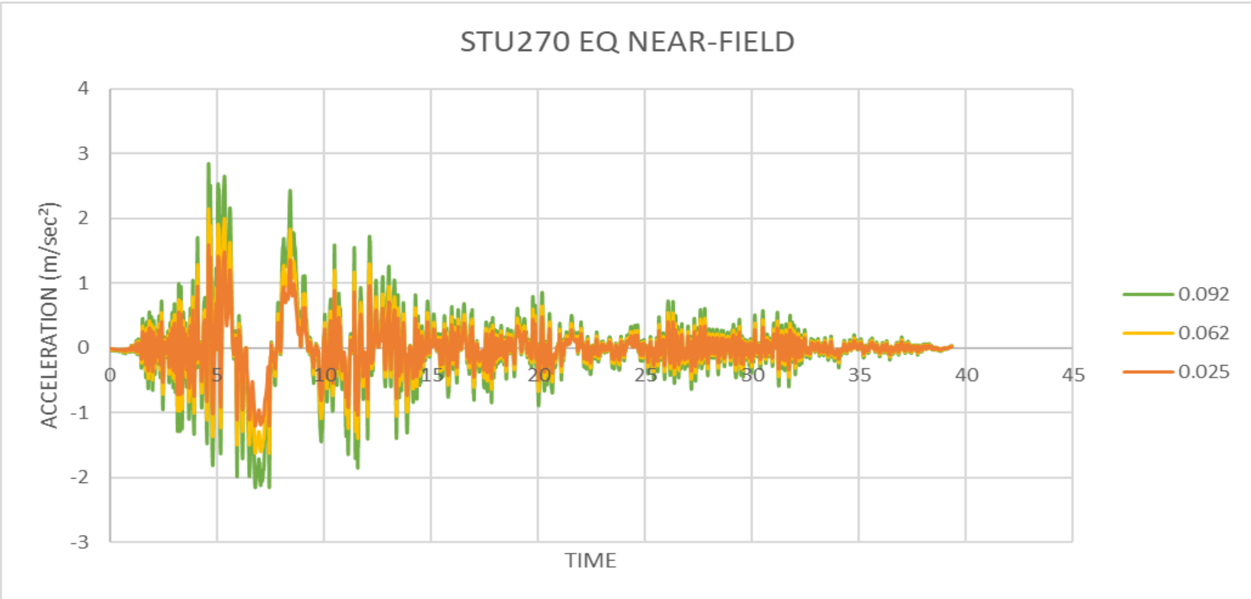

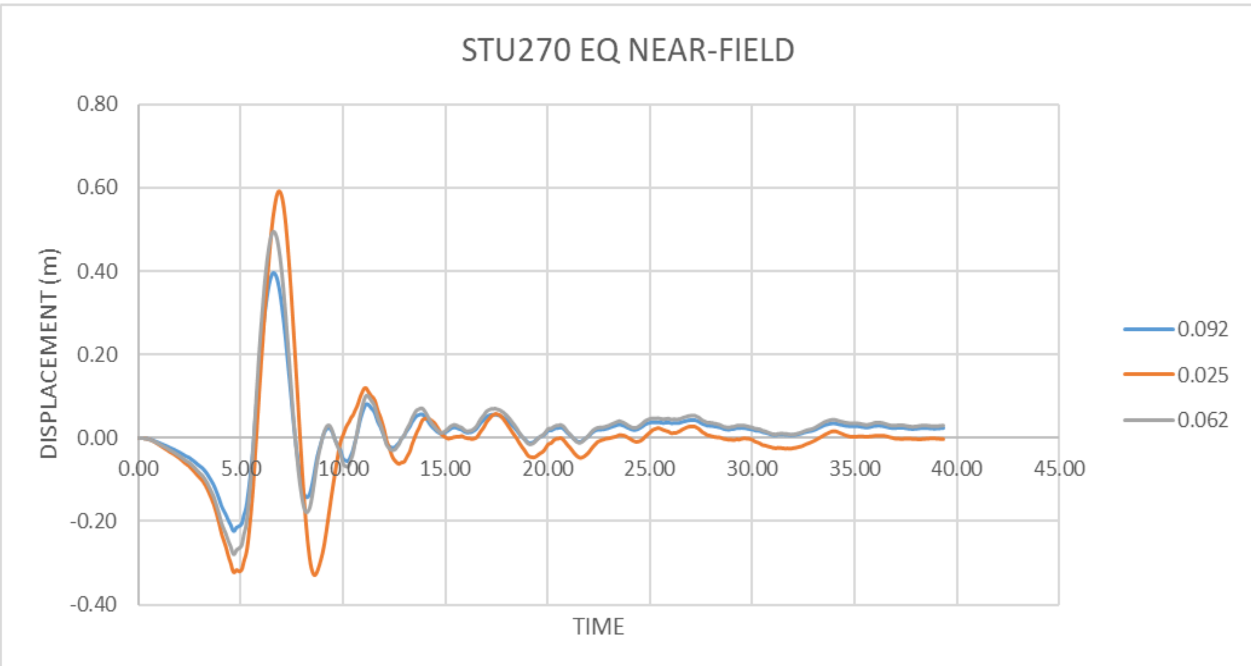

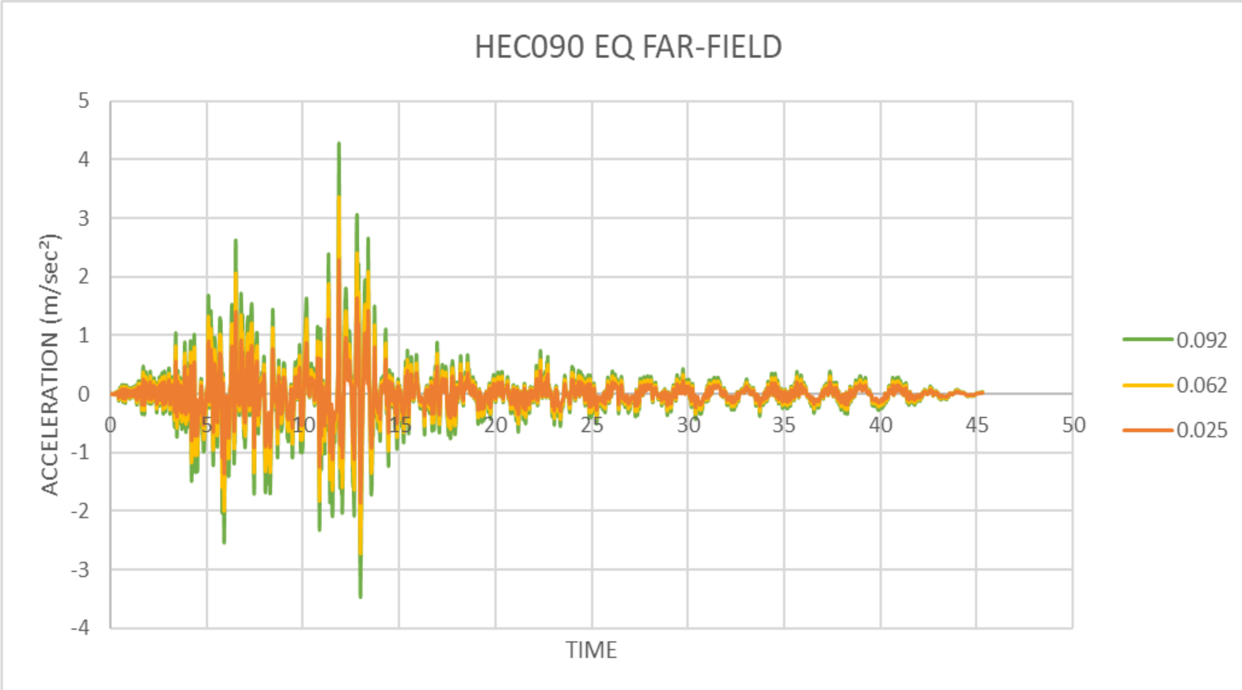
HEC090 EQ FAR-FIELD
ACCELERATION (m/sec²)
TIME
0.092
0.062
0.025

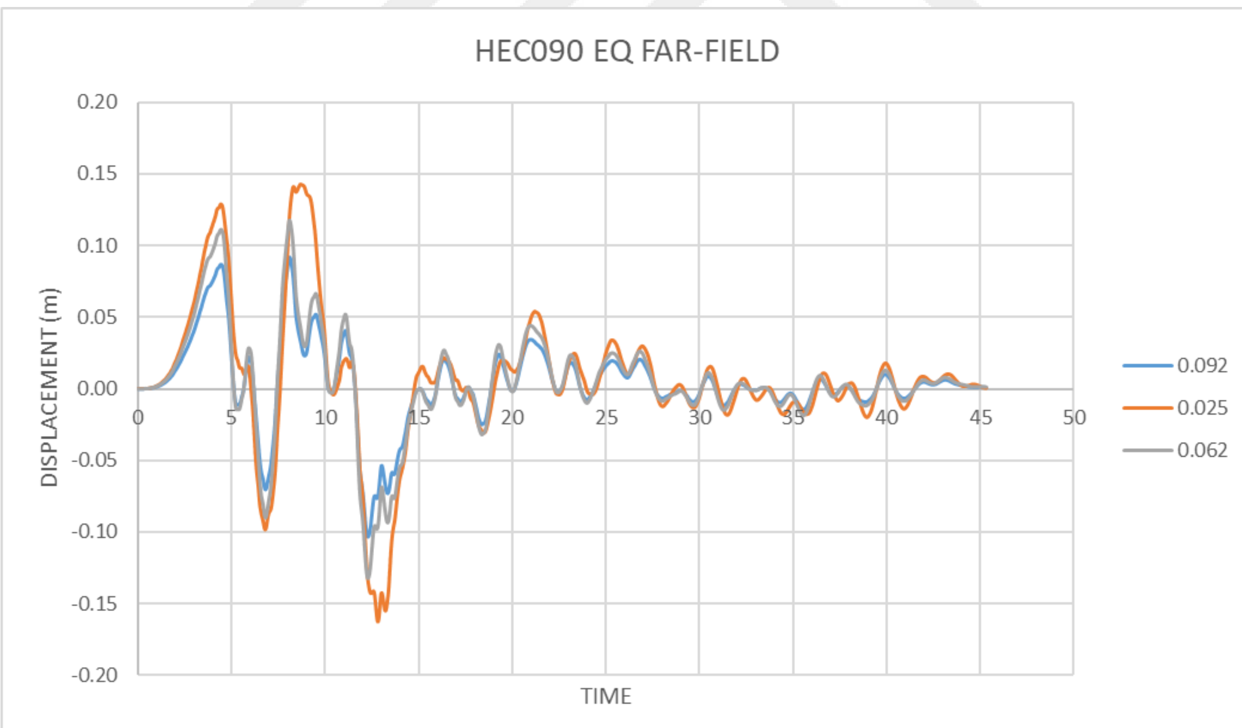
HEC090 EQ FAR-FIELD
DISPLACEMENT (m)
TIME
0.092
0.025
0.062

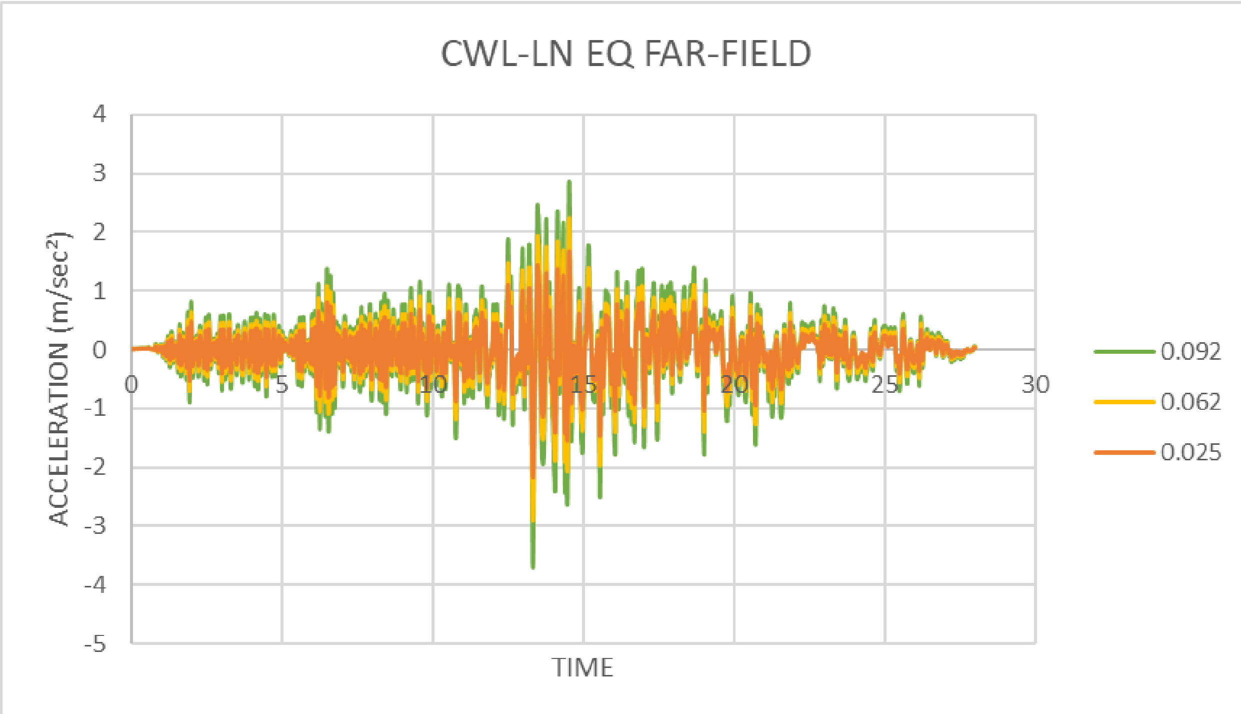
CWL-LN EQ FAR-FIELD
ACCELERATION (m/sec²)
TIME
0.092
0.062
0.025

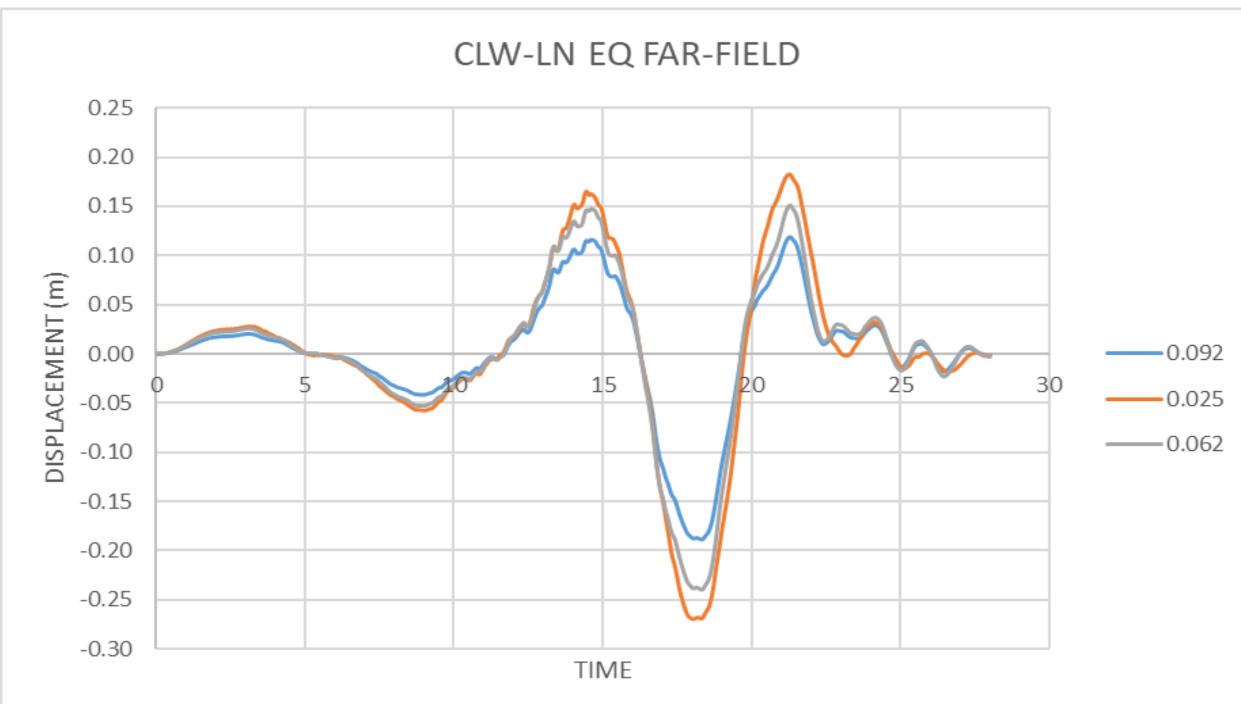
CLW-LN EQ FAR-FIELD
DISPLACEMENT (m)
TIME
0.092
0.025
0.062

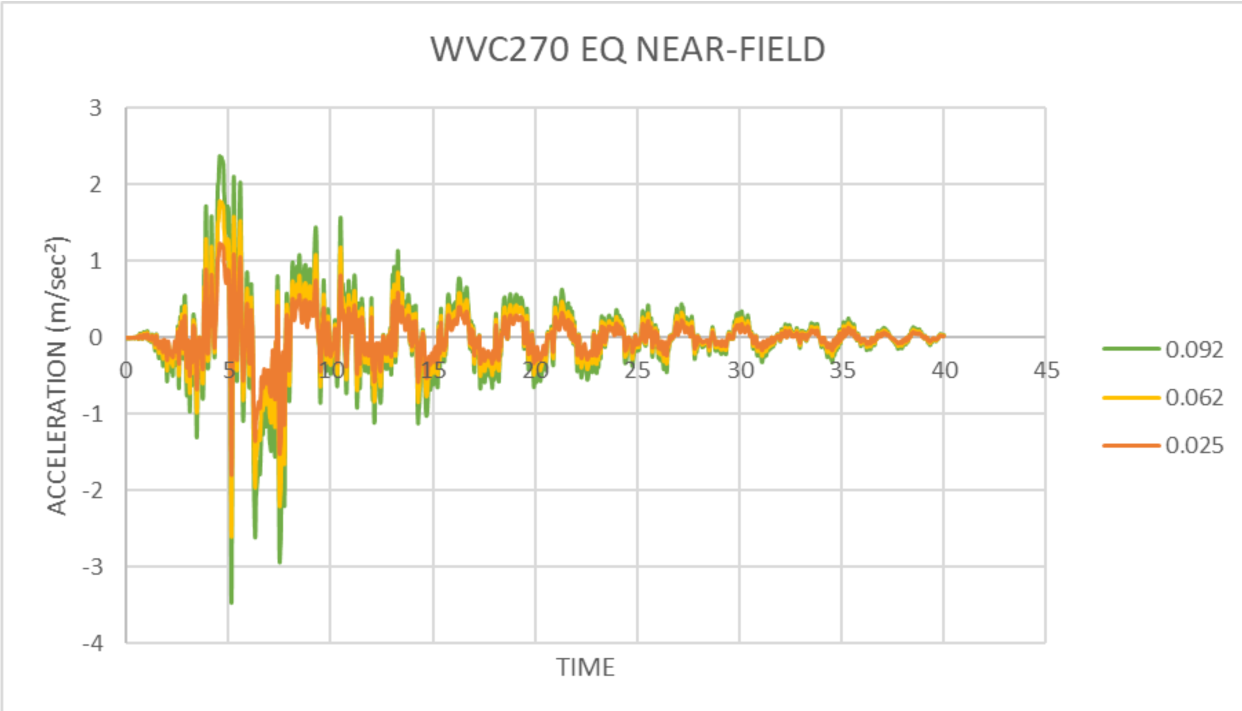
WVC270 EQ NEAR-FIELD
ACCELERATION (m/sec²)
TIME
0.092
0.062
0.025

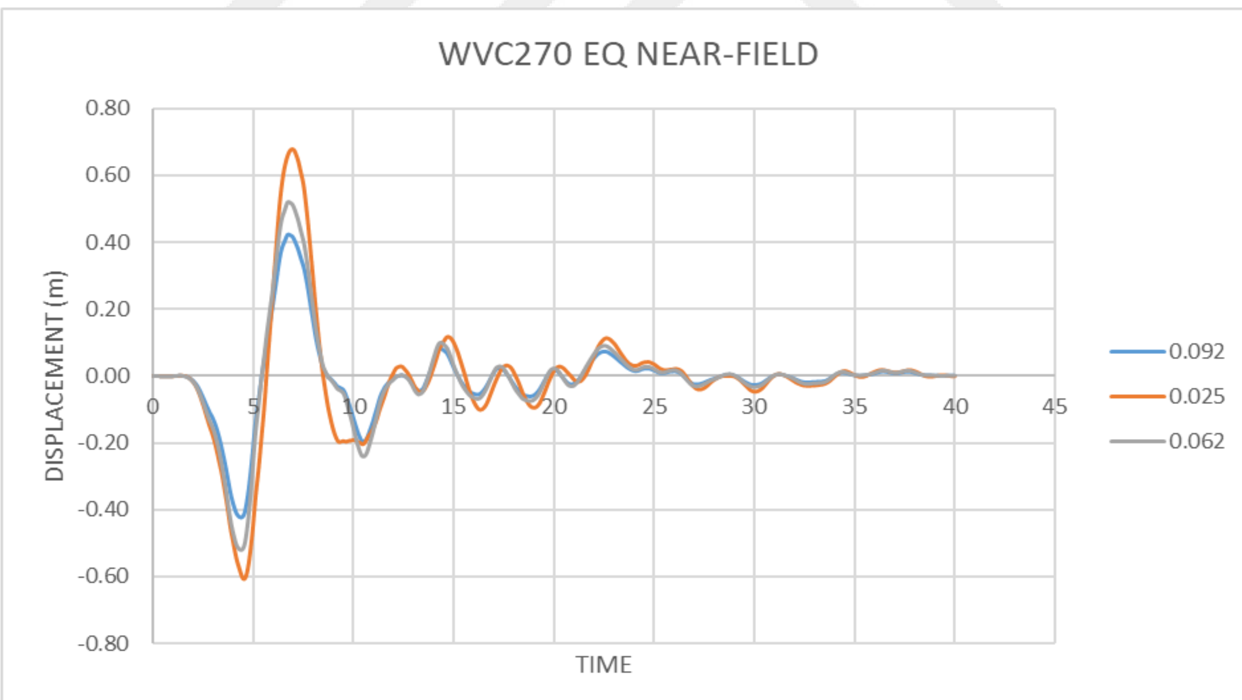
WVC270 EQ NEAR-FIELD
DISPLACEMENT (m)
TIME
0.092
0.025
0.062

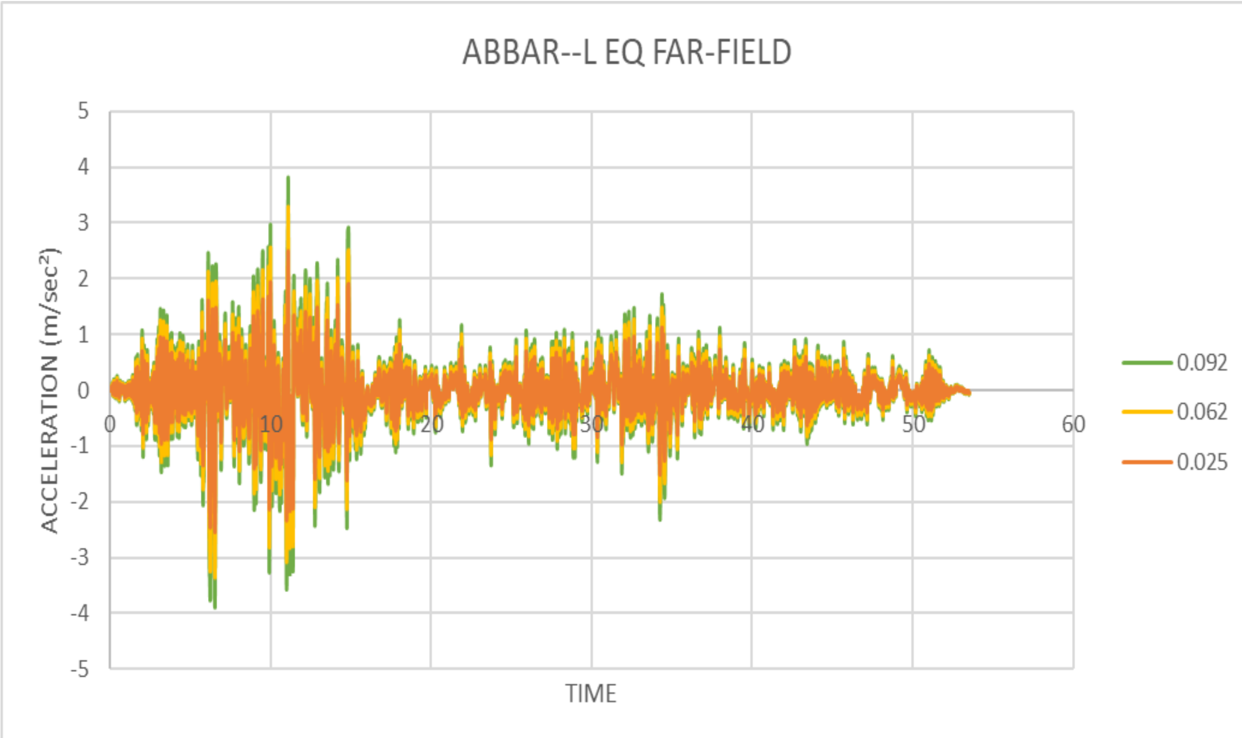
ABBAR--L EQ FAR-FIELD
ACCELERATION (m/sec²)
TIME
0.092
0.062
0.025
5
4
3
2
1
0
-1
-2
-3
-4
-5
0
10
20
30
40
50
60

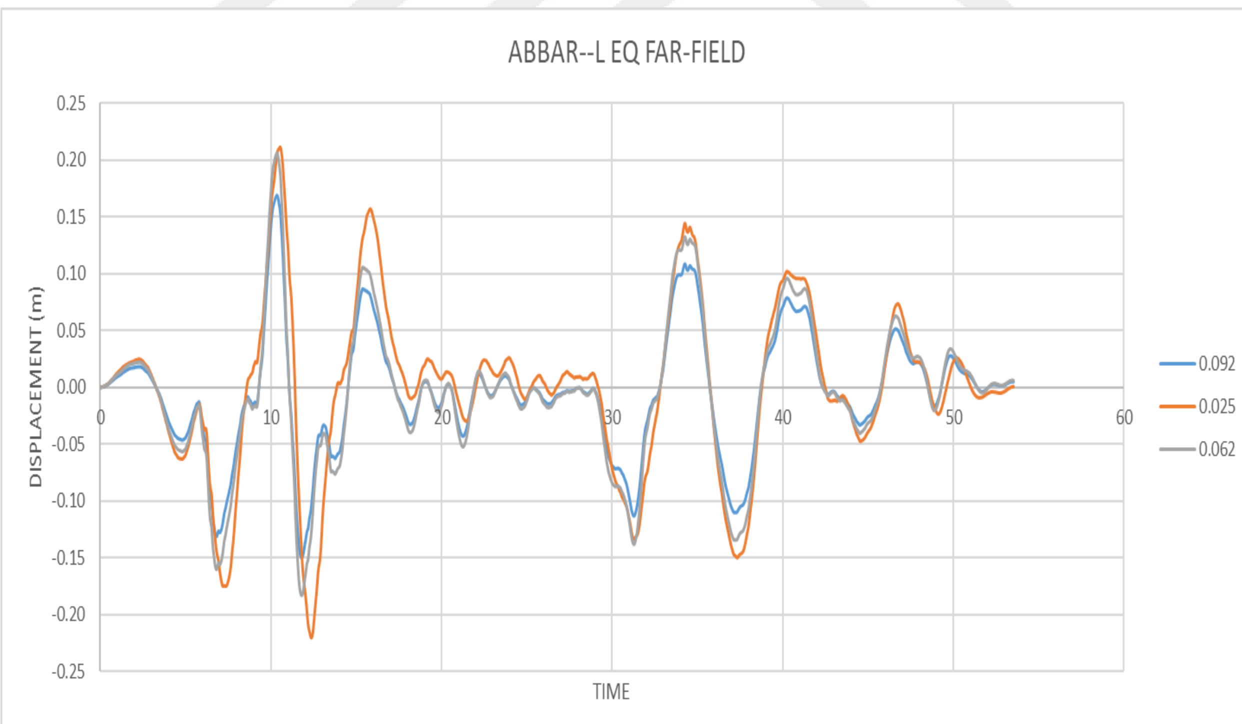
ABBAR--L EQ FAR-FIELD
DISPLACEMENT (m)
TIME
0.092
0.025
0.062
0.25
0.20
0.15
0.10
0.05
0.00
-0.05
-0.10
-0.15
-0.20
-0.25
0
10
20
30
40
50
60

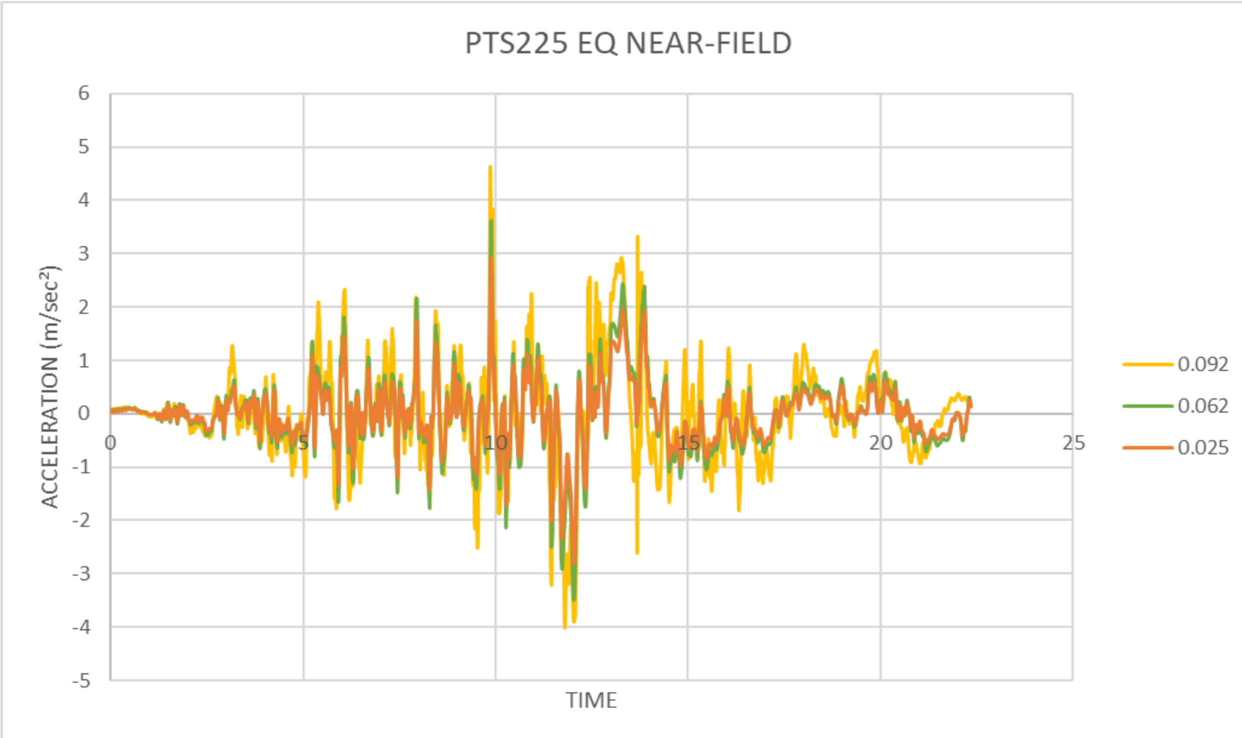
PTS225 EQ NEAR-FIELD
ACCELERATION (m/sec²)
TIME
0.092
0.062
0.025

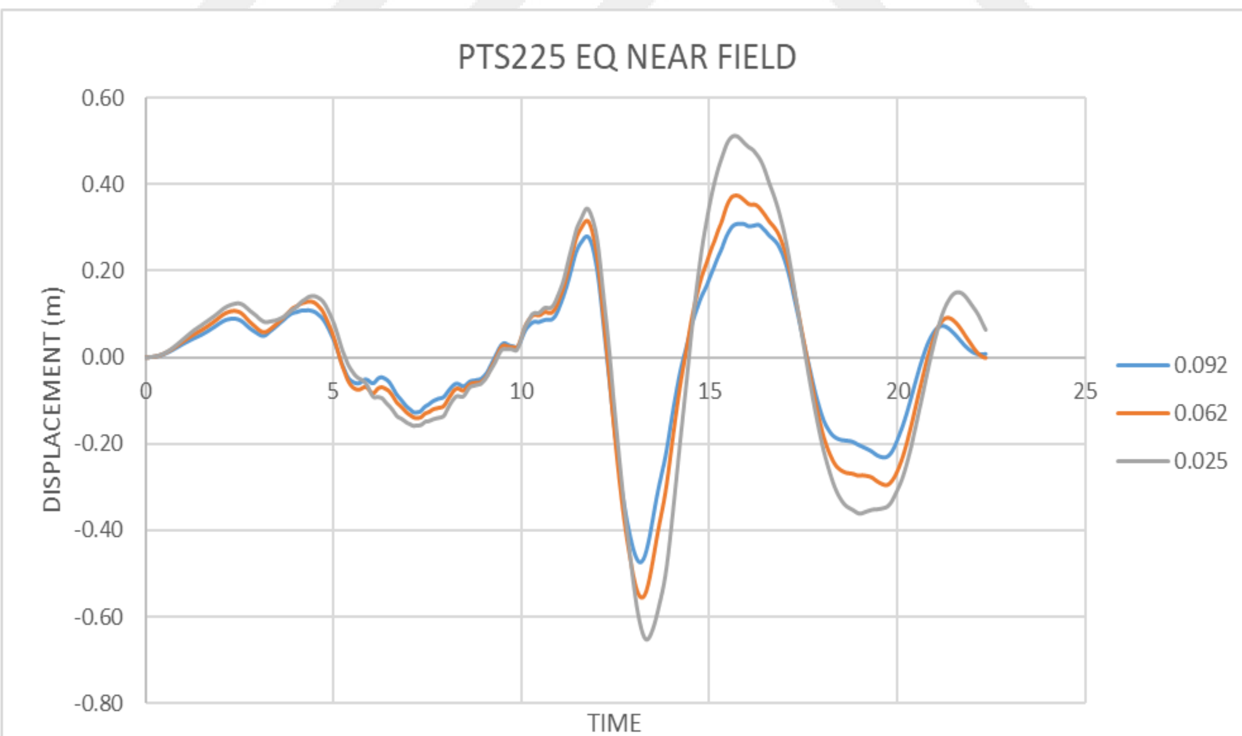
PTS225 EQ NEAR FIELD
DISPLACEMENT (m)
TIME
0.092
0.062
0.025

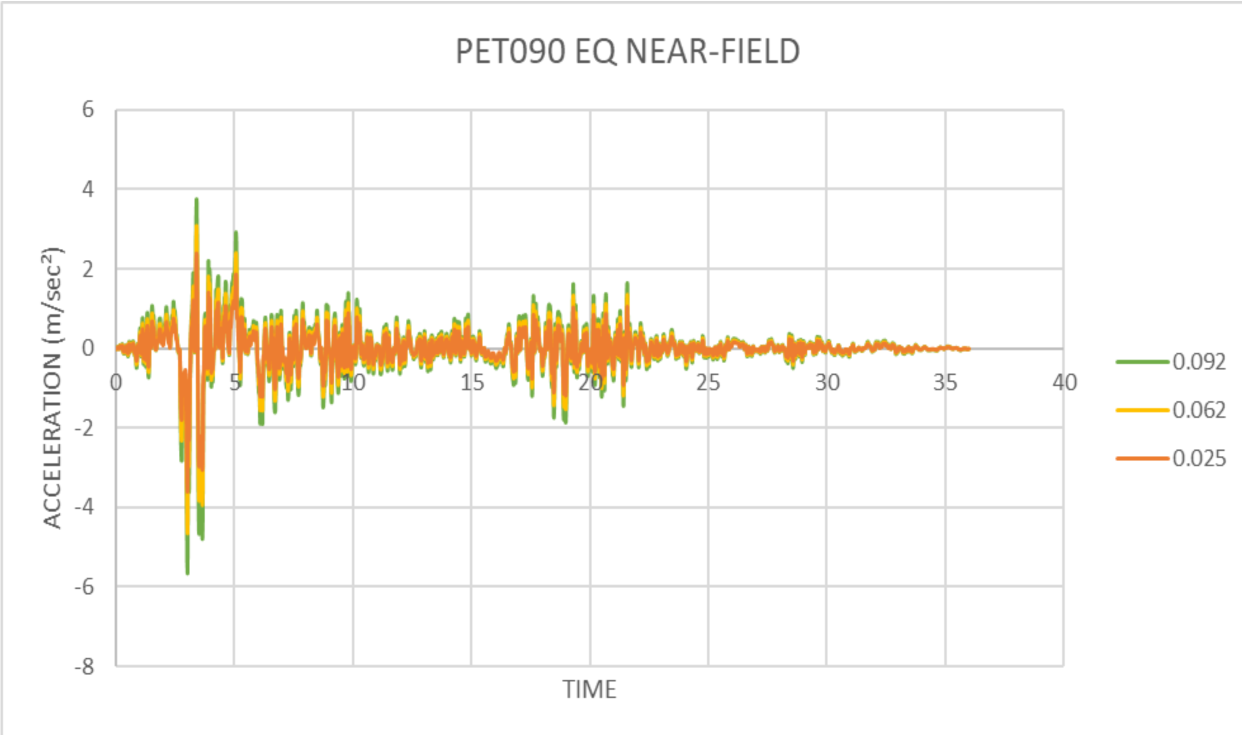
PET090 EQ NEAR-FIELD
ACCELERATION (m/sec^2)
TIME
6
4
2
0
-2
-4
-6
-8
0
5
10
15
20
25
30
35
40
0.092
0.062
0.025

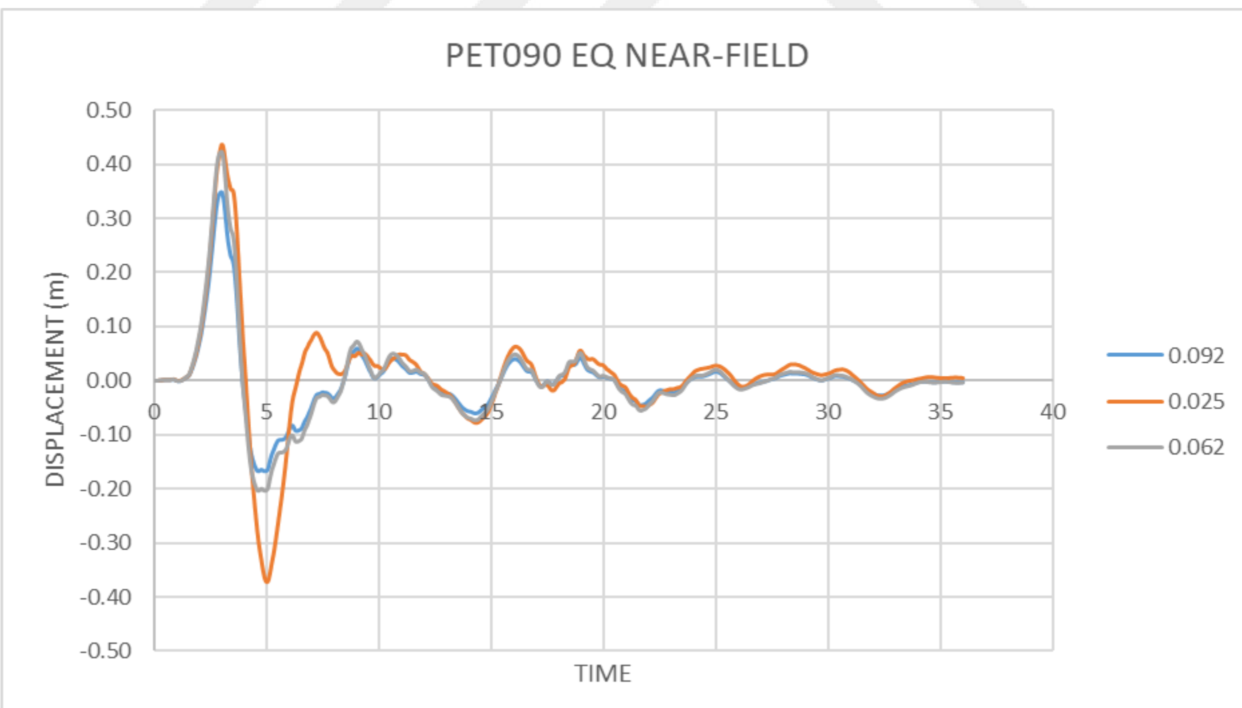
PET090 EQ NEAR-FIELD
DISPLACEMENT (m)
TIME
0.50
0.40
0.30
0.20
0.10
0.00
-0.10
-0.20
-0.30
-0.40
-0.50
0
5
10
15
20
25
30
35
40
0.092
0.025
0.062

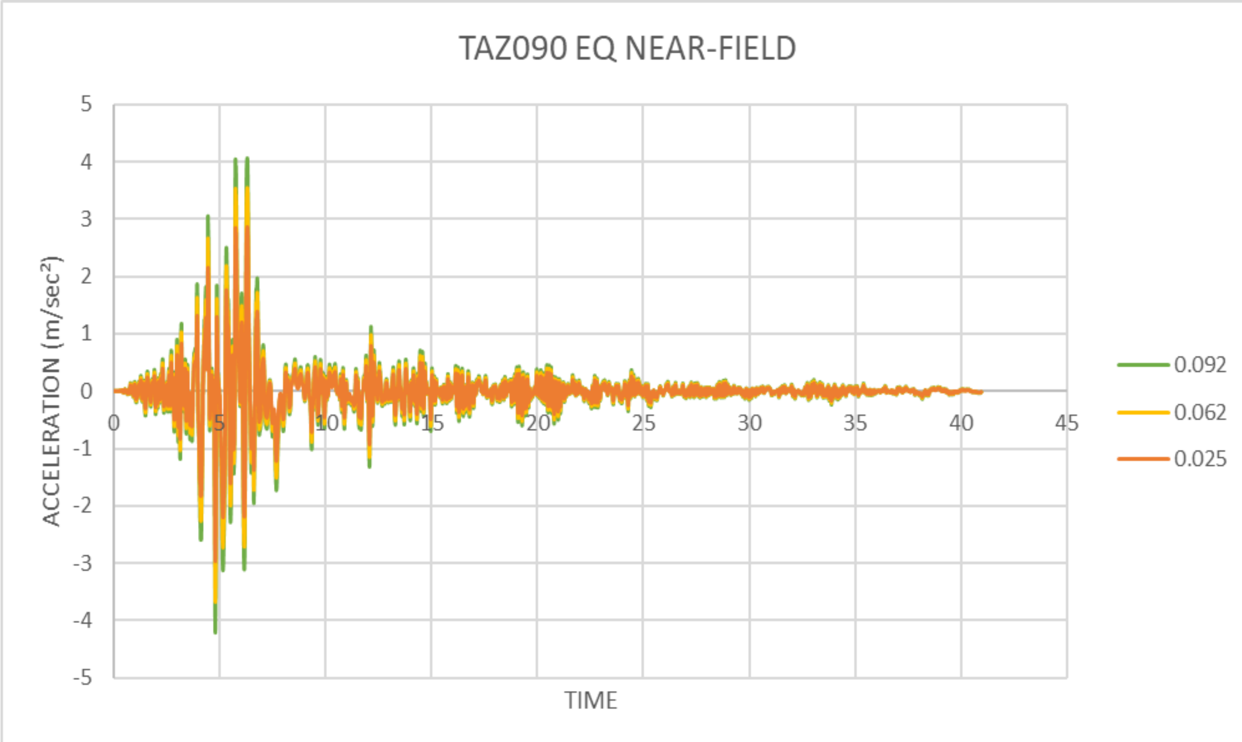
TAZ090 EQ NEAR-FIELD
ACCELERATION (m/sec²)
TIME
0.092
0.062
0.025

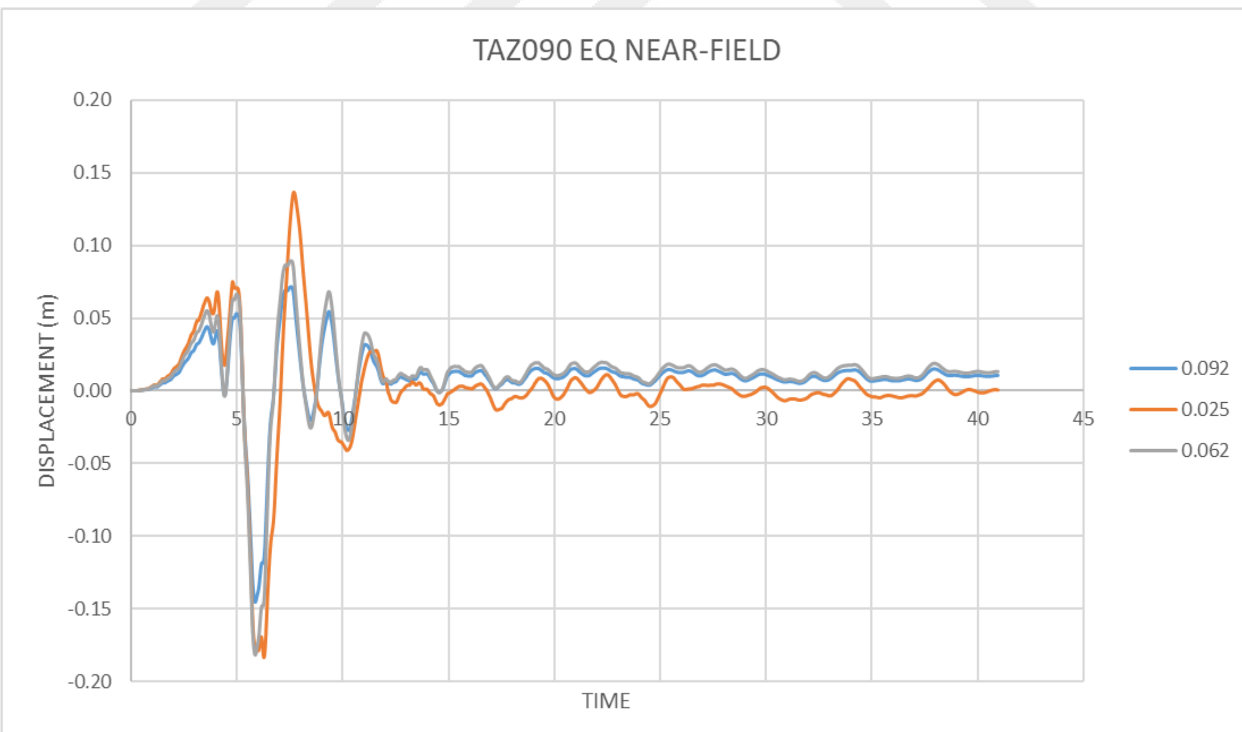
TAZ090 EQ NEAR-FIELD
DISPLACEMENT (m)
TIME
0.092
0.025
0.062

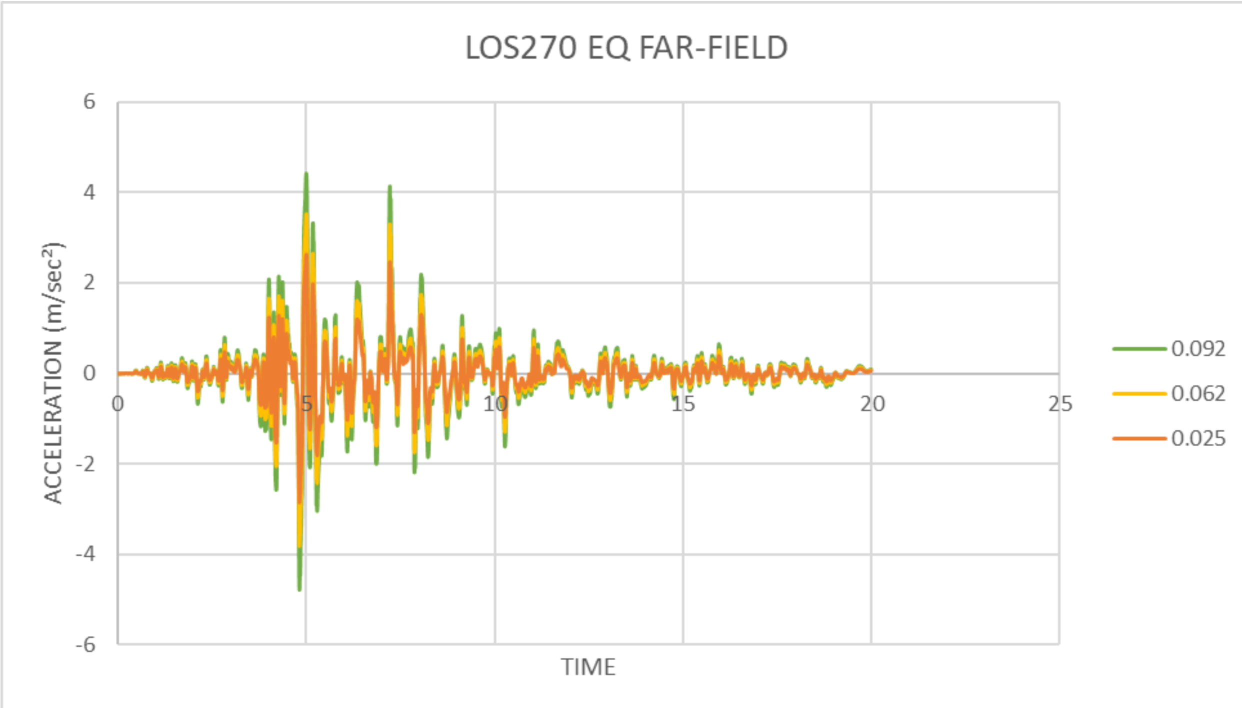

LOS270 EQ FAR-FIELD
ACCELERATION (m/sec²)
TIME
0.092
0.062
0.025

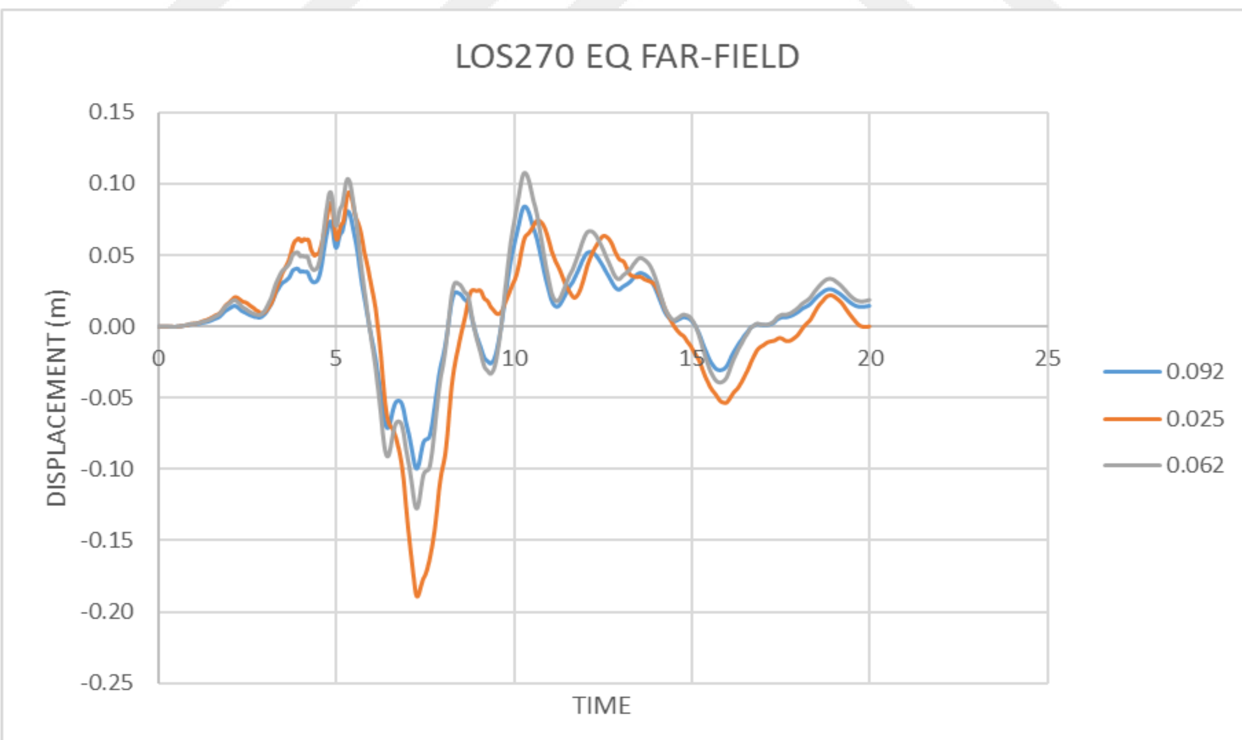

LOS270 EQ FAR-FIELD
DISPLACEMENT (m)
TIME
0.092
0.025
0.062

4. Summary and Conclusion

In this thesis, Seismic protection of storage rack system with base isolation is studied. the effect of single friction isolators in steel storage rack structure and their advantages in comparison to the fixed based steel storage rack structures are shown and discussed. Additionally, as the main focus of this thesis the behavior of storage rack structures with various cases of loading under seismic isolators has been investigated and presented. The purpose behind seismic isolation is prevention of contents shedding from pallets and a more controlled structural behavior of steel storage rack system. Since the design of steel storage rack was not the primary concern of this thesis, the important specifications of rack's components are obtained from SEISRACK 2 project models. Furthermore, fixed and isolated storage rack structures natural frequency period was analyzed and time history analysis under six far-field and six near-field ground motions. The analyses performed conclude that;

a. After seismic isolation system was performed under real earthquake excitations. The reduction reached up to 45% to 65% in acceleration, 40% to 50% in relative displacement. Furthermore, period of isolated base rack structure increased almost 3 times in comparison to the fixed base rack structure.
b. Structural rotation or floor twist during earthquake can cause shedding of contents from pallets and since FPS reduce acceleration of structure and may increase total displacement at the bearing, equally distributed loadings in storage rack system is found to have lesser displacement at the bearing and a very minor rotational behavior.
c. Out of 4 various loading cases, case four and three showed larger displacement difference between joints at the bearing, seems to be the worst case during an earthquake. Case one and two showed lesser displacement difference between joints at the bearing, seems to be a more controlled rack system. The main consequence of floor twist is an unequal demand of lateral displacement in the elements of the structure; Hence, it is suggested to keep the storage rack system always equally loaded.
d. Analysis of variation of coefficient of friction showed that by increase of coefficient of friction an increase will also happen in acceleration of structure meanwhile a decrease in displacement and vice versa.
e. The results of this thesis are in agreement with Kilar et al. (2011) [46] investigation on asymmetry of fixed and isolated steel storage rack structures.

More studies need to be done in this regard. For further studies it is suggested to investigate the perforation on the uprights, shedding of the contents during motion and friction between pallets and beams of rack structure. Friction of pallets play an important role in shedding of goods from beams. Therefore, it is always advised to use wood pallets instead of plastic or steel pallets.

References

[1] ANSI (American National Standard Institute) MH16.1: 2008 (a revision of MH16.1: 2004) Specification for the Design, Testing and Utilization of Industrial Steel Storage Racks.

[2] FEMA-460 2005, section 6.2.1

[3] Jeff Crosier, Mark Hannah and David Mukai. DAMAGE TO STEEL STORAGE RACKS IN INDUSTRIAL BUILDINGS IN THE DARFIELD EARTHQUAK. University of Canterbury, Christchurch, New Zealand, 2010.

[4] EUROCODE 8, Section 6.2.1

[5] Degee, H., Rossi, B. & Jehin, D. 2011, 'GEOMETRICALLY NONLINEAR ANALYSIS OF STEEL STORAGE RACKS SUBMITTED TO EARTHQUAKE LOADING', International Journal of Structural Stability and Dynamics, vol. 11, no. 05, pp. 949-67

[6] Lingfeng Yina, Gan Tangb, Zhanjie Lic, Min Zhanga, Bo Feng, 2012 'Responses of cold-formed steel storage racks with spine bracings using speed-lock connections with bolts I: Static elastic-plastic pushover analysis', School of Civil Engineering, Southeast University, SiPaiLou 2, Nanjing 210096, China

[7] Kenny Martens, Experimental and numerical study of storage racking systems in earthquake situation, Faculty of Engineering and Architecture of Ghent University 2012-2013.

[8] C.A. Castiglioni - Politecnico di Milano, Milano, Italy. P. Carydis - National Technical University, Athens, Greece. P. Negro Joint Research Center, Ispra, Italy. L. Calado Instituto Superior Tecnico, Lisboa, Portugal. H. Degée University of Liege, Liege, Belgium. I. Rosin ACAI, Milano, Italy. Seismic behavior of steel storage racking systems. 2009.

[9] N. Baldassino and R. Zandonini, PERFORMANCE OF BASE-PLATE CONNECTIONS OF STEEL STORAGE PALLET RACKS, University of Trento. 2014.

[10] A.M.S. Freitas, M.S.R. Freitas, F.T. Souza, Analysis of steel storage rack columns, Department of Civil Engineering, School of Mines, Federal University of Ouro Preto, Brazil 2005.

[11] Robert Michaela, James A. Courtwrightb, Ernie Ferroc, Andre Filiatraultd, Peter S. Higginse, and Assawin Wanitkorkulf., DEVELOPMENT OF A NEW BASE ISOLATION SYSTEM FOR SEISMIC ISOLATION OF STEEL PALLET STORAGE RACKS. Department of Civil, Structural and Environmental Engineering, University at Buffalo, 2010.

[12] John B. Pellegrino, James A., Robert Michael. STORAGE RACK VIBRATION ISOLATORS AND RELATED STORAGE RACKS. United States Patent Pellegrino et al. Patent N0*: US 7,263,806 B2 Date of Patent: Sep. 4, 2007.

[13] P. Agarwal, Shrikhande M., Earthquake resistant design of structures, Prenttice Hall of India, New Delhi, 2006

[14] Zayas V. Earthquake protective column support. US patent 4644714; Feb. 24, 1987.

[15] Zayas V, Low S, Mahin S. The FPS earthquake resistant system. Experimental report UC Berkeley; 1987. (Report No. UCB/EERC-87/01).

[16] Zayas VA, Low S, Mahin S. A simple pendulum technique for achieving seismic isolation. Earthq Spectra 1990;6(2):317–33.

[17] Paolo M. Calvia, Gian Michele Calvi, Historical development of friction-based seismic isolation systems, Department of Civil and Environmental Engineering, University of Washington, Seattle, WA, USA and Scuola Universitaria Superiore, IUSS, Pavia, Italy, 2018.

[18] Tessy Thomas, Dr. Alice Mathai, Civil Engineering Department, Mar Athanasius College of Engineering/ Mahatma Gandhi University, India, 2016.

[19] Tessy Thomas, Dr. Alice Mathai, Civil Engineering Department, Mar Athanasius College of Engineering/ Mahatma Gandhi University, India, 2016.

[20] Markazi FD, Beale RG, Godley MHR. Experimental analysis of semi-rigid boltless connectors. Thin-Walled Structures 1997.

[21] C. Bernuzzi, C. A. Castiglioni. Experimental analysis on the cyclic behaviour of beam-to-column joints in steel storage pallet racks. Thin-Walled Structures 2001.

[22] KM Bajoria, RS Talikoti. Determination of flexibility of beam to column connectors used in thin walled cold formed steel pallet racking systems. Thin-Walled Structures 2006.

[23] Xianzhong Zhao, Tuo Wang, Yiyi Chen, K.S. Sivakumaranc. Flexural behavior of steel storage rack beam-to-upright connections. Journal of Constructional Steel Research 99 (2014) 161–175.

[24] Saverio Giordanoa, Federico Gusella, Giovanni Lavacchinib, Maurizio Orlandoa, Paolo Spinellia, Experimental tests on beam-end connectors of cold-formed steel storage pallet racks, University of Florence, Dept. Civil and Environmental Engineering, Italy, 2014.

[25] N. ASAWASONGKRAM, P. CHOMCHUEN and P. PREMTHAMKORN, SEISMIC PERFORMANCE EVALUATION OF STEEL STORAGE RACKS USING EXPERIMENTAL RESULTS OF BEAM-TO-COLUMN CONNECTION, 2014.

[26] Paweá A. Królab, Magdalena Papadopoulos-WoĨniaka, Jarosáaw Wójt, Experimental Tests on Semi-Rigid, Hooking-Type Beam-to-Column Double-Sided Joints in Sway-Frame Structural Pallet Racking Systems, Warsaw University of Technology, Faculty of Civil Engineering, Institute of Building Engineering, Al. Armii Ludowej 16, 00-637 Warsaw, Poland, Auburn University, Samuel Ginn College of Engineering, Department of Civil Engineering, 213A Ramsay Hall, 261 W. Magnolia Ave., Auburn, AL. 36849, USA (within PL-US Fulbright Commission Program), 2014.

[27] Nadia Baldassino, Claudio Bernuzzi, Riccardo Zandonini, PERFORMANCE OF JOINTS IN STEEL STORAGE PALLET RACKS, Department of Mechanical and Structural Engineering, University of Trento, Department of Structural Engineering, Politecnico di Milano, 2014.

[28] Bajoria, K. & Talikoti, R. 2006, 'Determination of flexibility of beam-to-column connectors used in thin walled cold-formed steel pallet racking systems', Thin-walled structures, vol. 44, no. 3, pp. 372-80.

[29] N. Baldassino and R. Zandonini, PERFORMANCE OF BASE-PLATE CONNECTIONS OF STEEL STORAGE PALLET RACKS, University of Trento, Trento, Italy, 2013.

[30] A.M.S. Freitas, M.S.R. Freitas, F.T. Souza, Analysis of steel storage rack columns, Department of Civil Engineering, School of Mines, Federal University of Ouro Preto, Campus Morro do Cruzeiro, Brazil, 2005.

[31] Gilbert, B., & Rasmussen, K. J. R. (2011). Determination of the base plate stiffness and strength of steel storage racks. Journal of Constructional Steel Research, 67(6), 1031–1041,

[32] Filiatrault & Wanitkorkul, Seismic behavior of Steel Storage Pallet Racking System, University of Buffalo, 2004.

[33] Timoshenko, S. P. and Gere, J. M. “Theory of Elastic Stability”, McGraw-Hill Book Company, New York, NY, Second Edition.

[34] Rao, S.S., Beale, R. & Godley, 'Shear stiffness of pallet rack upright frames', Seventeenth international specialty conference on cold-formed steel structures., Missouri S&T (formerly the University of Missouri-Rolla), 2004.

[35] Lingfeng Yina, Gan Tangb, Zhanjie Lic, Min Zhanga, Bo Feng, Responses of cold-formed steel storage racks with spine bracings using speed-lock connections with bolts I: Static elastic-plastic pushover analysis, aSchool of Civil Engineering, Southeast University, SiPaiLou 2, Nanjing 210096, China, 2018.

[36] Gilbert, B.P., Rasmussen, K.J., Baldassino, N., Cudini, T. & Rovere, L. 2012, 'Determining the transverse shear stiffness of steel storage rack upright frames', Journal of Constructional Steel Research, vol. 78, pp. 107-16.

[37] Alireza Kamrava, Seismic Isolators and their Types, Department of Environment and Cvil engineering, Campus of Shiraz University of Technology, Shiraz, Iran, 2015.

[38] Feng, M.Q., Shinozuka, M. & Fujii, S. 1993, 'Friction-controllable sliding isolation system', Journal of engineering mechanics, vol. 119, no. 9, pp. 1845-64.

[39] Madden, G.J., Symans, M.D. & Wongprasert, N. 2002, 'Experimental verification of seismic response of building frame with adaptive sliding base-isolation system', Journal of Structural Engineering, vol. 128, no. 8, pp. 1037-45.

[40] Robert Michaela, James A. Courtwrightb, Ernie Ferroc, Andre Filiatraultd, Peter S. Higginse, and Assawin Wanitkorkulf, DEVELOPMENT OF A NEW BASE ISOLATION SYSTEM FOR SEISMIC ISOLATION OF STEEL PALLET STORAGE RACKS, Structural Engineering and Earthquake Simulation Laboratory (SEESL) at the University at Buffalo.

[41] Civil Engineering SAP2000 Software Book, Prof. Dr. Ahmet Can ALTUNISIK, Prof. Dr. Sevket ATES, Prof. Dr. Suleyman ADANUR, page 709, Trabzon, Turkey, 2018.

[42] Seismic performance of steel pallet racks, Avgerinou Stella, National Technical University of Athens-Laboratory of Metal Structures, Athens, 2012.

[43] FEMA P695 / June 2009

[44] Symans, M.D. and Constantinou, M.C. 1999. Semi-active control systems for seismic protection of structures: a state-of-the-art review. Engineering Structures, Vol. 21, No. 6, pp. 469-87

[45] Filiatrault, A. Higgins, P.S. Wanitkorkul, A., Courtwright, J.A. and Michael, R. 2008, Experimental seismic response of base isolated pallet-type steel storage racks, Earthquake Spectra, vol. 24, no. 3, pp. 617-39

[46] Kilar, V., Petrovcic, S., Koren, D. and Silih, S. 2011, Seismic analysis of an asymmetric fixed base and base isolated high rack steel structure. Engineering Structures, vol. 33, No. 12, pp. 3471-82

[47] D. Cardone, G. Gesualdi, P. Brancato, 2015, Restoring Capability of friction pendulum seismic isolation systems, University of Basilicata, Potenza, Italy

[48] RMI first edition 1964, Professor George winter of Cornel University, Minimum Engineering Standards for industrial steel storage Racks.

[49] ANSI (American National Standard Institute) (MH16.1: 2004) Specification for the Design, Testing and Utilization of Industrial Steel Storage Racks, An Affiliated Trade Association of Material Handling Industry of America (MHIA)

[50] FEM 10.2.08 (2005) Recommendations for the Design of Static Steel Pallet Racking in Seismic Condition, Federation Europeen de la Manutention.

[51] Castiglioni et al. (2007) SEISRACKS RFSR-CT-2004-00045, Final Report, Research Program of the Research Fund for Coal and Steel RTD.

[52] Castiglioni et al. (2014) SEISRACKS2 RFSR-CT-2011-00031, Mid-term Report, Research Program of the Research Fund for Coal and Steel RTD.

[53] CSA A344, Guideline for Industrial Steel Storage Rack, Canadian Standard Associations building code for steel storage racks, 2005.

[54] AS4084, Guideline for Industrial Steel Storage Rack, first Australian Standard code for Steel Storage Racks, 2009.

[55] AS 4084 Guideline for Industrial Steel Storage Rack, Australian Standard code for Steel Storage Racks, 2012.

[56] M. Efiloglu, "Understanding the concept of base isolation," 2013

[57] Sliding Isolation Systems: State-of-the-Art Review, Malu Girish, Murnal Pranesh Ph.D. Scholar, Shivaji University, Kolhapur, India, 2012 (IOSR Journal of Mechanical and Civil Engineering (IOSR-JMCE) ISSN: 2278-1684, PP: 30-35)

[58] Malu Girish and Murnal Pranesh, Variable Coefficient of Friction: An effective VFPI parameter to control near-fault ground motion, ISET Journal of Earthquake Technology 2012.

[59] Seismic Isolation: History, Application and Performance - A world view, Lan G. Buckle, M. EERI, and Ronald L. Mayes 1990

[60] Structural Control through Base Isolation, Andrei M. Reinhorn, Bufallo University, New York. 2012.

[61] Rheological and restoring force models regarding belt tensioner dymamic behavior: Prediction & experiment, J. Bastiena , G. Michonb , L. Maninc , R. Dufourc, Laboratoire Mécatronique 3M, Équipe d'accueil A 3318 Université de Technologie de Belfort-Montbéliard, 90010 Belfort cedex, France, 2006

[62] Analysis of seismic isolation systems running on sliding friction. Fanel Dorel scheaus, university of Jos Galati, 2013.

[63] Restoring capability of friction pendulum seismic isolation systems, D. Cardone, G. Gesuladi, P. Brancato 2015

[64] Effects of Loading Characteristics on the Performance of Sliding Isolation Devices, G. Lomiento, N. Bonessio & G., Benzoni University of California, San Diego Department of Structural Engineering, 2012.

APPENDIX A

- Verification of Time History Analysis results with Seism-Signal Data:

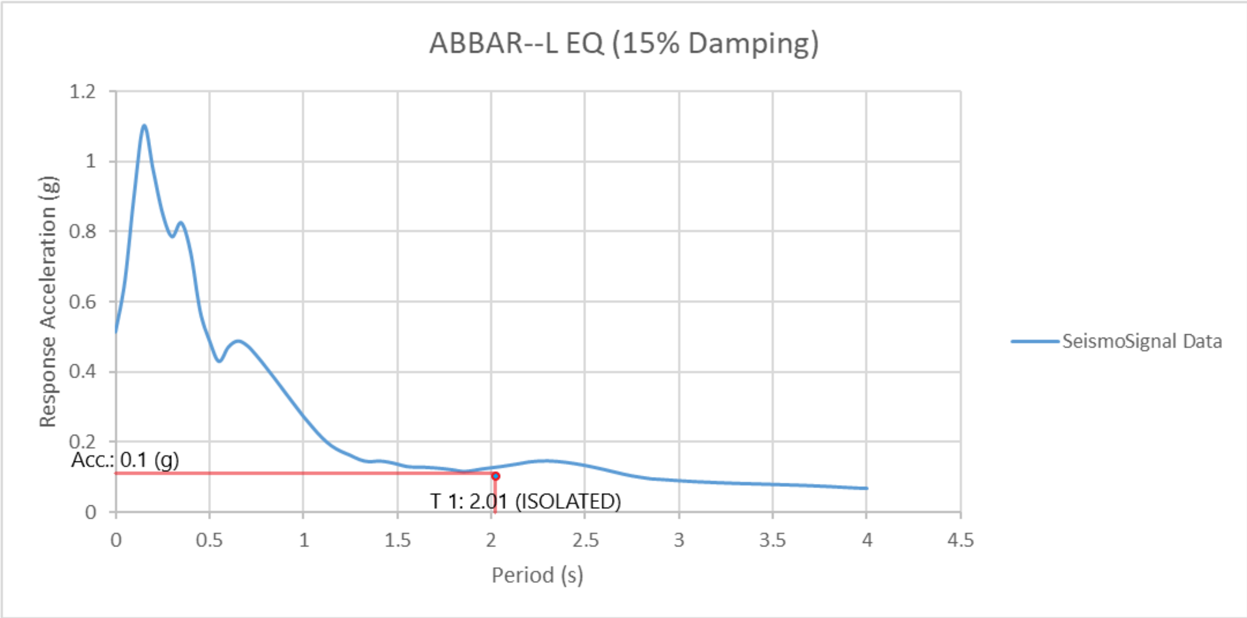

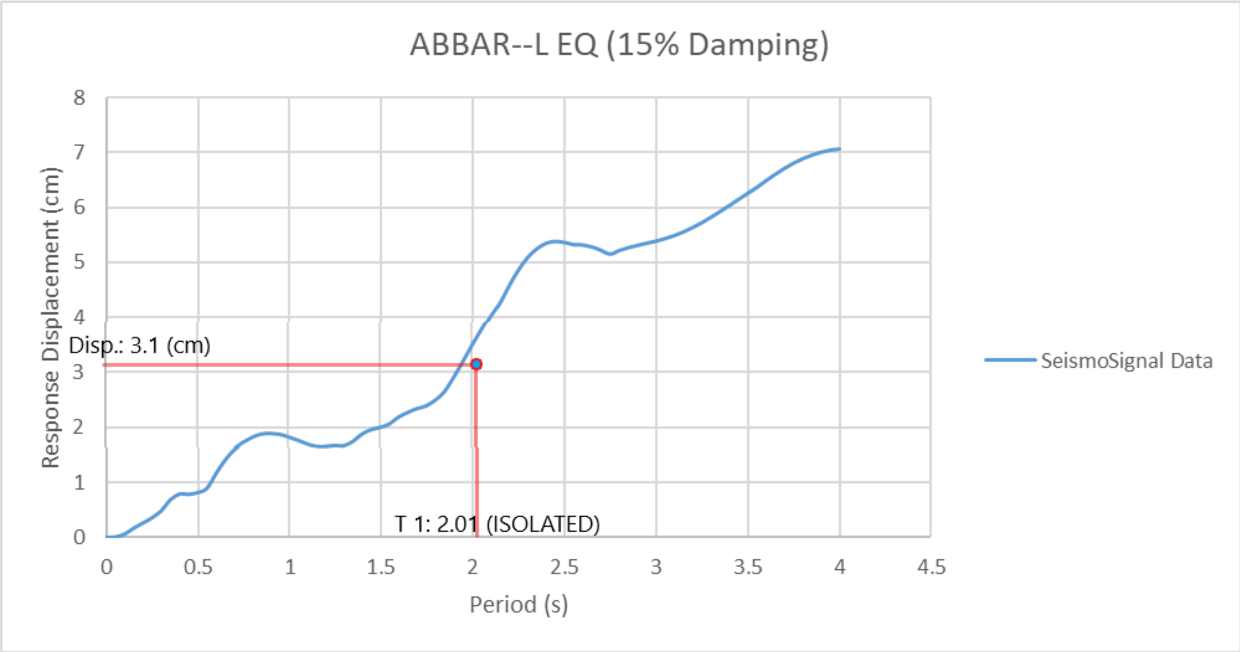

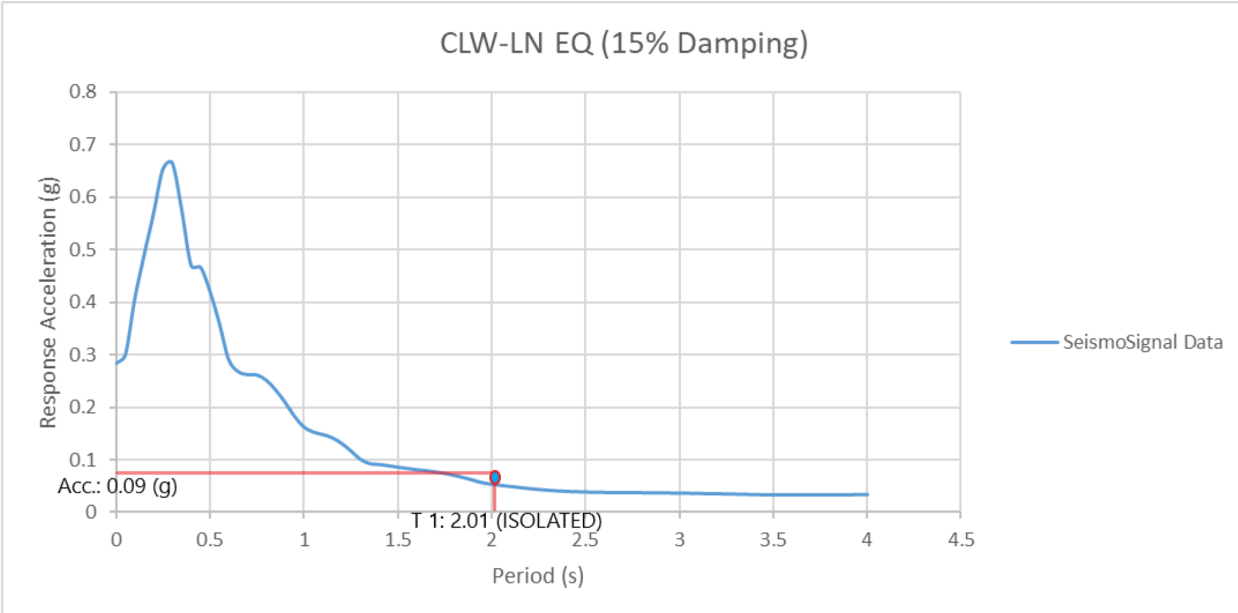
CLW-LN EQ (15% Damping)
Response Acceleration (g)
0.8
0.7
0.6
0.5
0.4
0.3
0.2
0.1
0
Acc.: 0.09 (g)
T 1: 2.01 (ISOLATED)
0
0.5
1
1.5
2
2.5
3
3.5
4
4.5
Period (s)
SeismoSignal Data

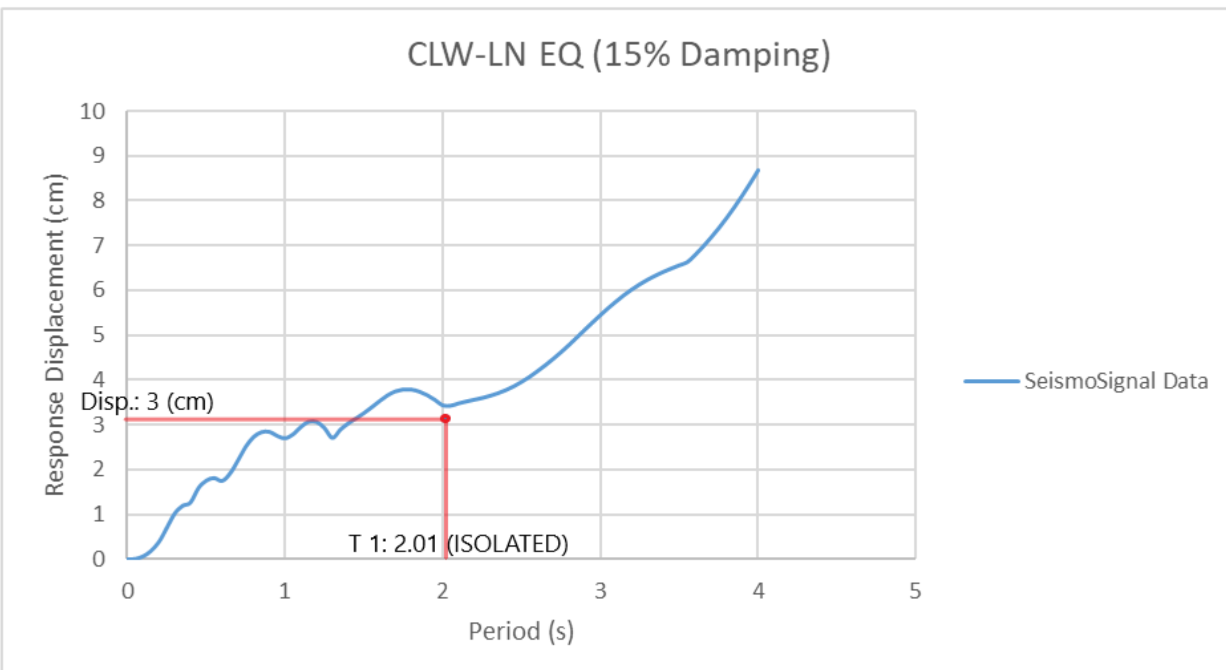
CLW-LN EQ (15% Damping)
Response Displacement (cm)
10
9
8
7
6
5
4
3
2
1
0
Disp.: 3 (cm)
T 1: 2.01 (ISOLATED)
0
1
2
3
4
5
Period (s)
SeismoSignal Data

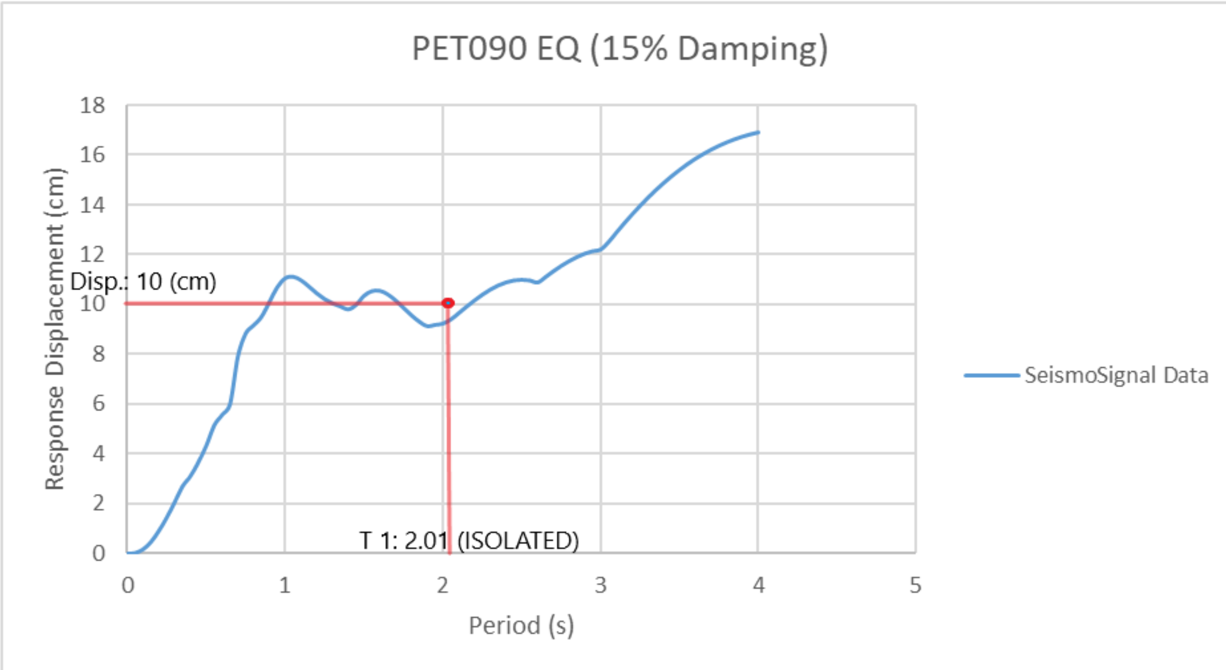
PET090 EQ (15% Damping)
Response Displacement (cm)
Period (s)
Disp.: 10 (cm)
T 1: 2.01 (ISOLATED)
SeismoSignal Data
0
2
4
6
8
10
12
14
16
18
0
1
2
3
4
5

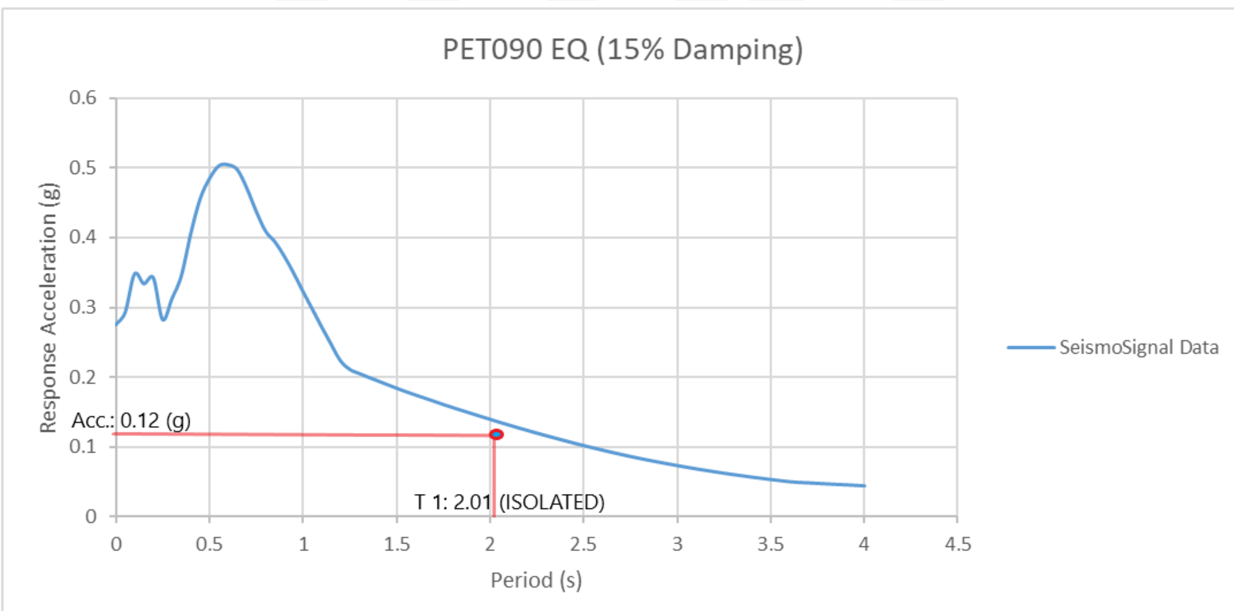
PET090 EQ (15% Damping)
Response Acceleration (g)
Period (s)
Acc.: 0.12 (g)
T 1: 2.01 (ISOLATED)
SeismoSignal Data
0
0.1
0.2
0.3
0.4
0.5
0.6
0
0.5
1
1.5
2
2.5
3
3.5
4
4.5

- Time histories, Acc. & Disp. Spectra of selected Ground Motions data presented by Seism-signal Software.

1. Cape, Petrolia Earthquake:

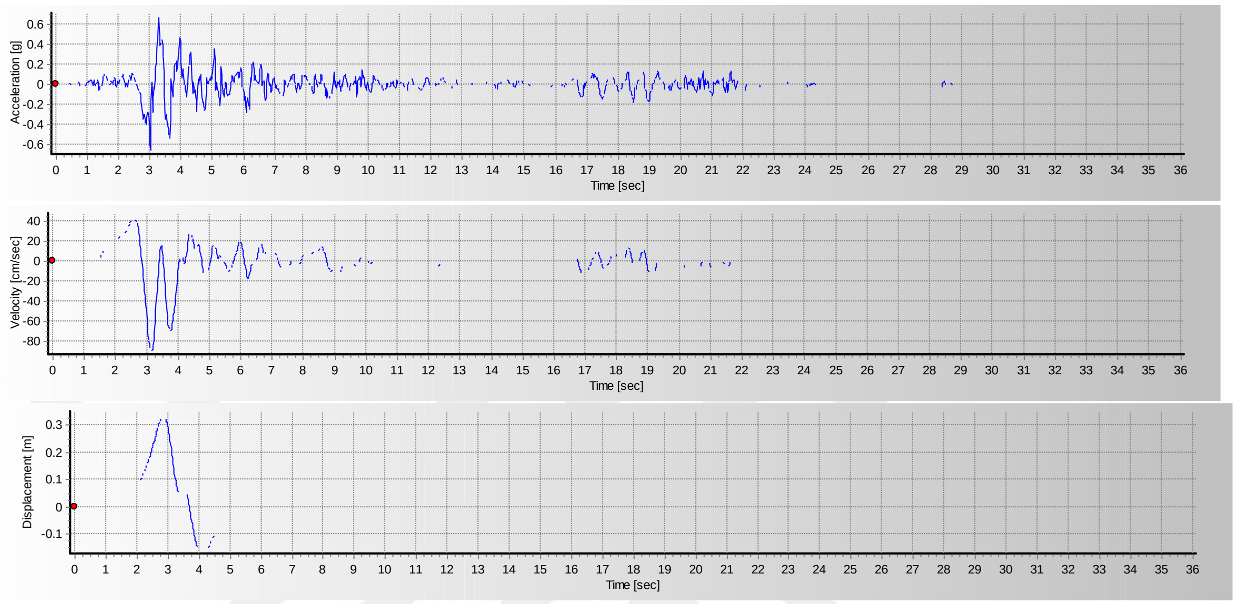

2. Darfield, HORC Earthquake:

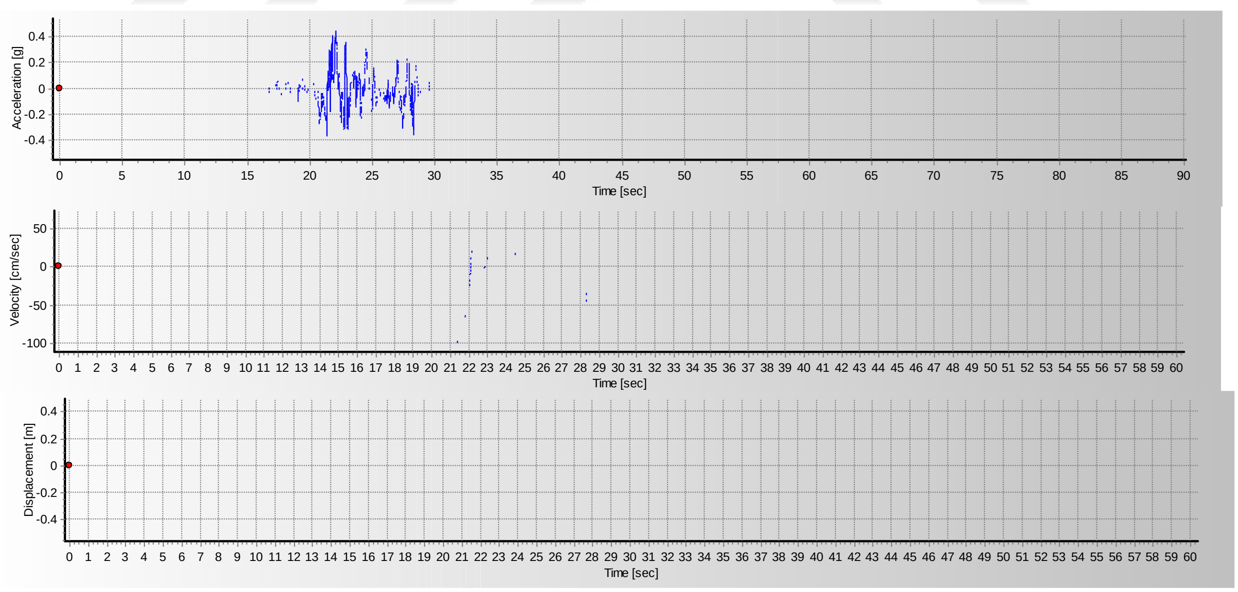

3. El Mayor, El Centro Earthquake:

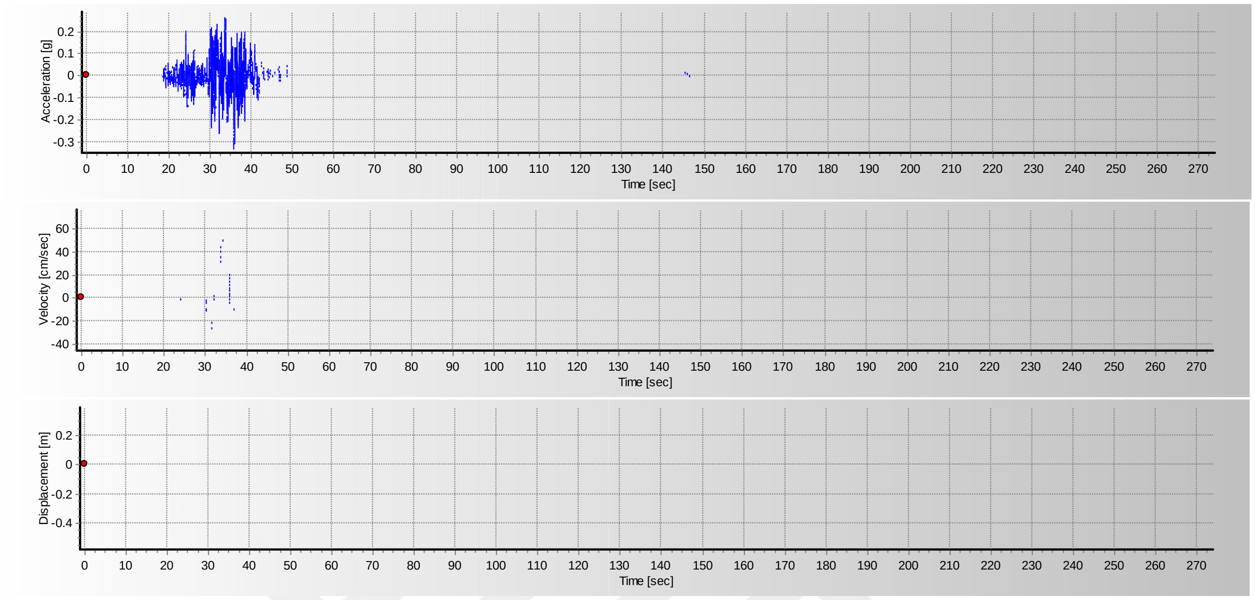

4. Firuli, Tolmezzo Earthquake:

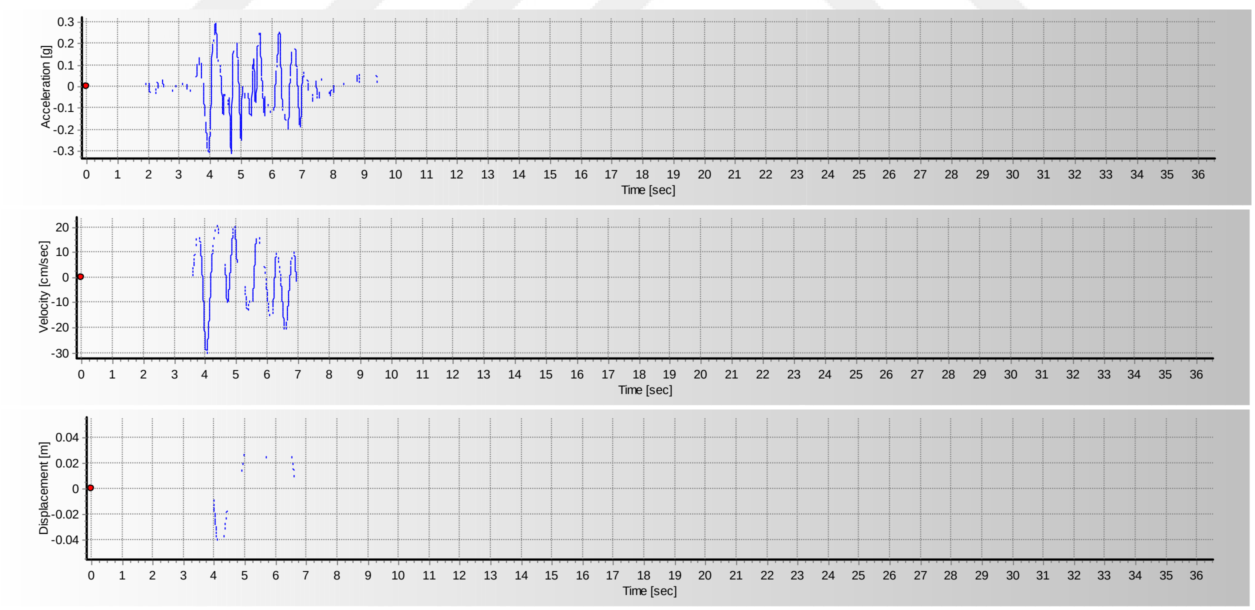

5. Hector Mine, Hector Earthquake:

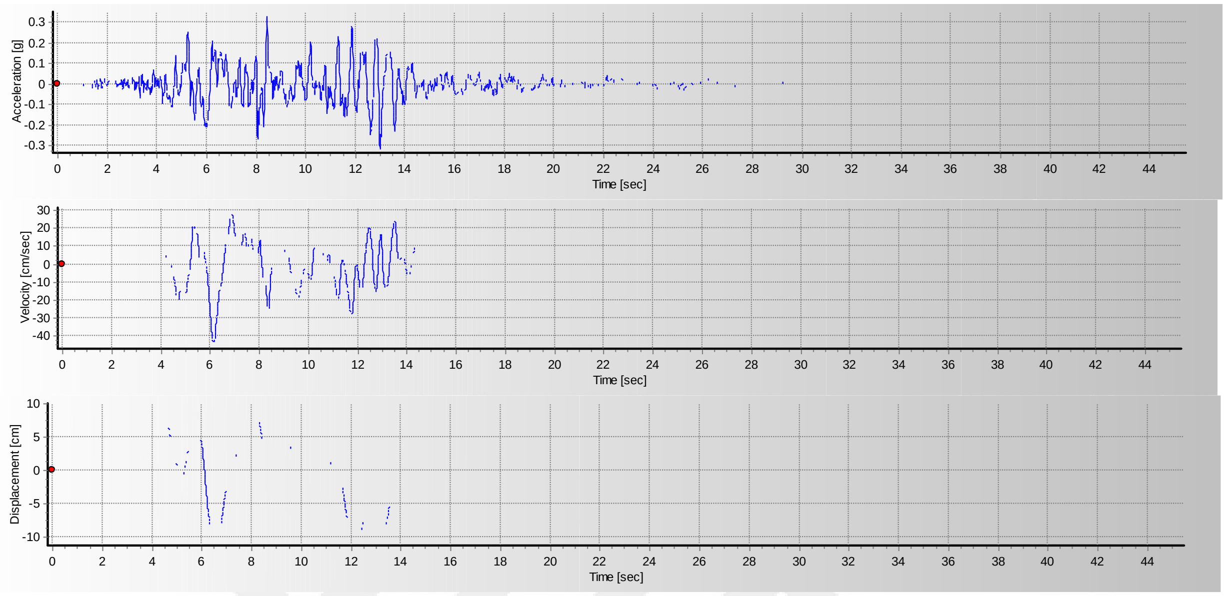

6. Kobe, Takarazuka Earthquake:

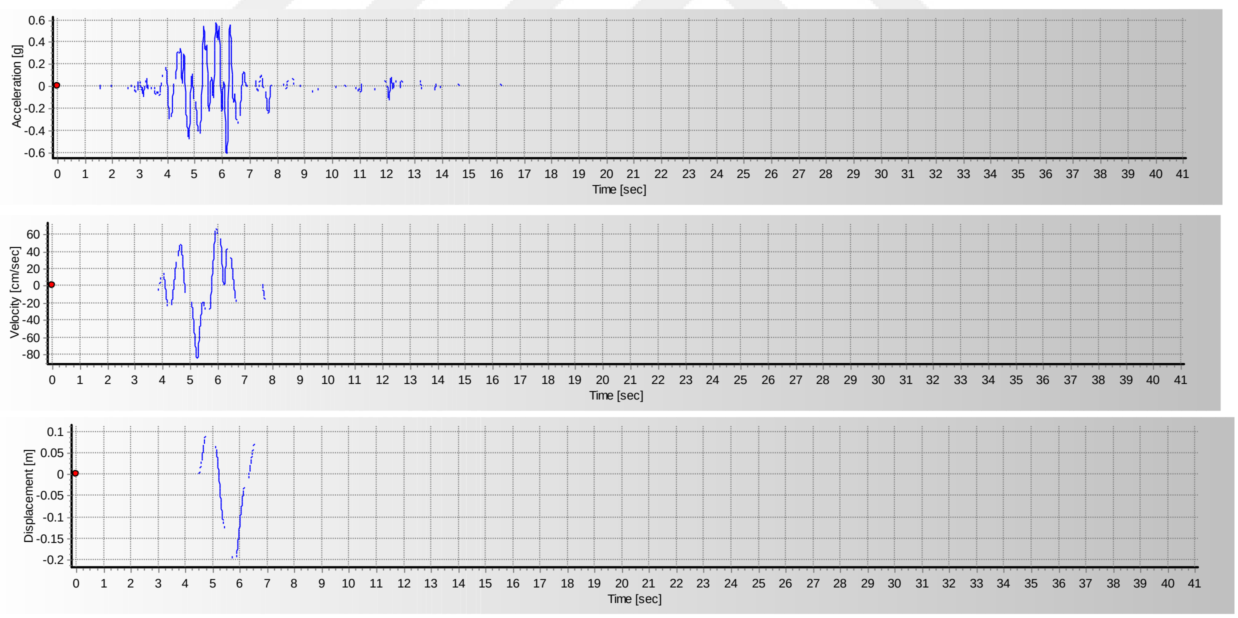

7. Landers, Coolwater Earthquake:

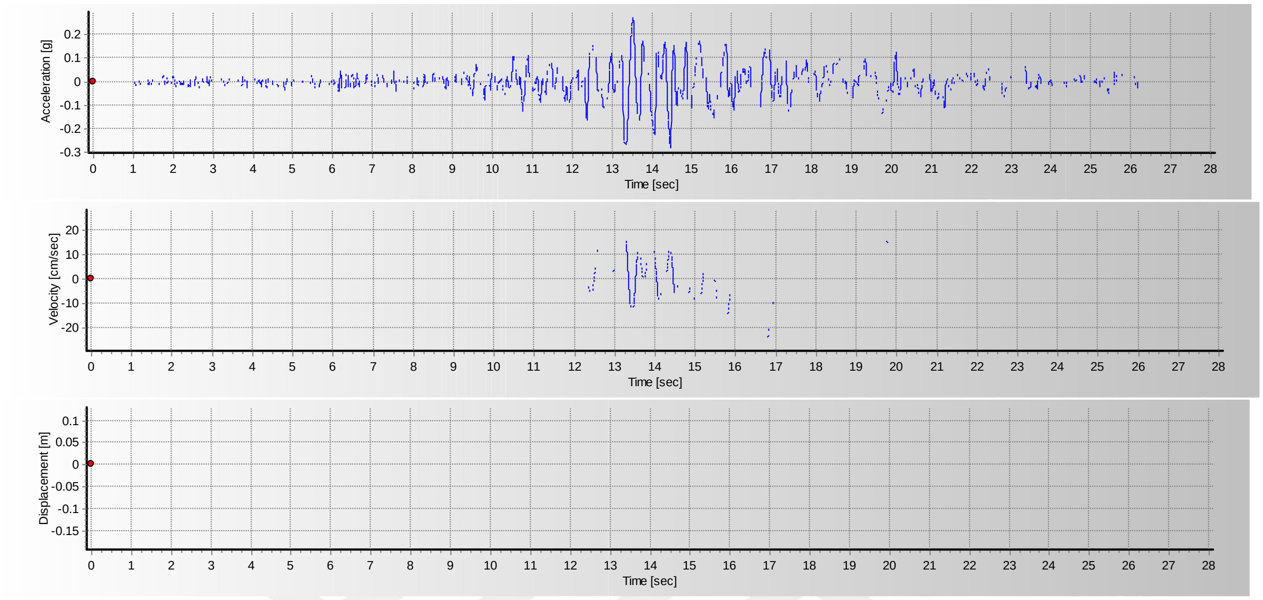

8. Loma P., Saratoga Earthquake:

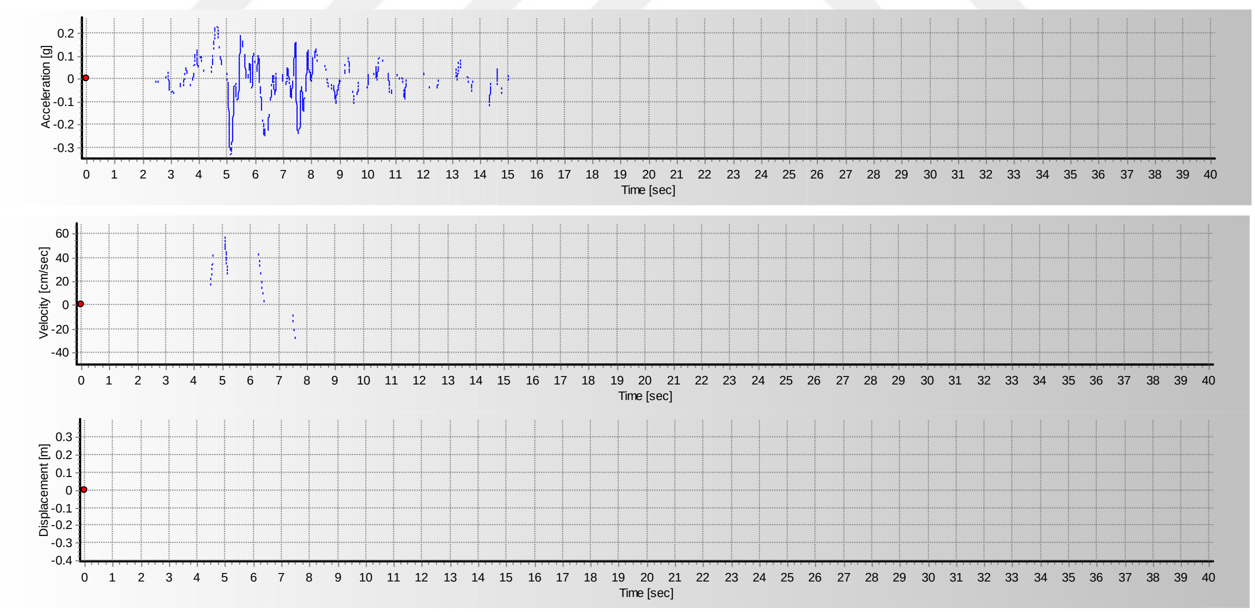

9. Manjil, ABBAR Earthquake:

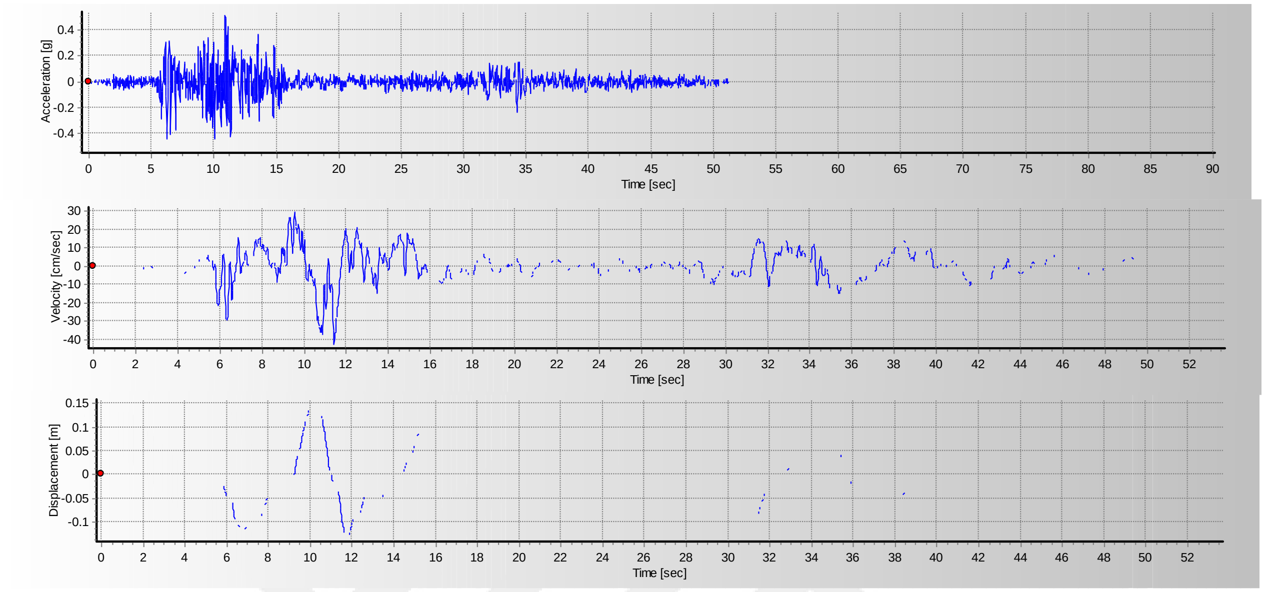

10. Northridge, Canyon Country WLC Earthquake:

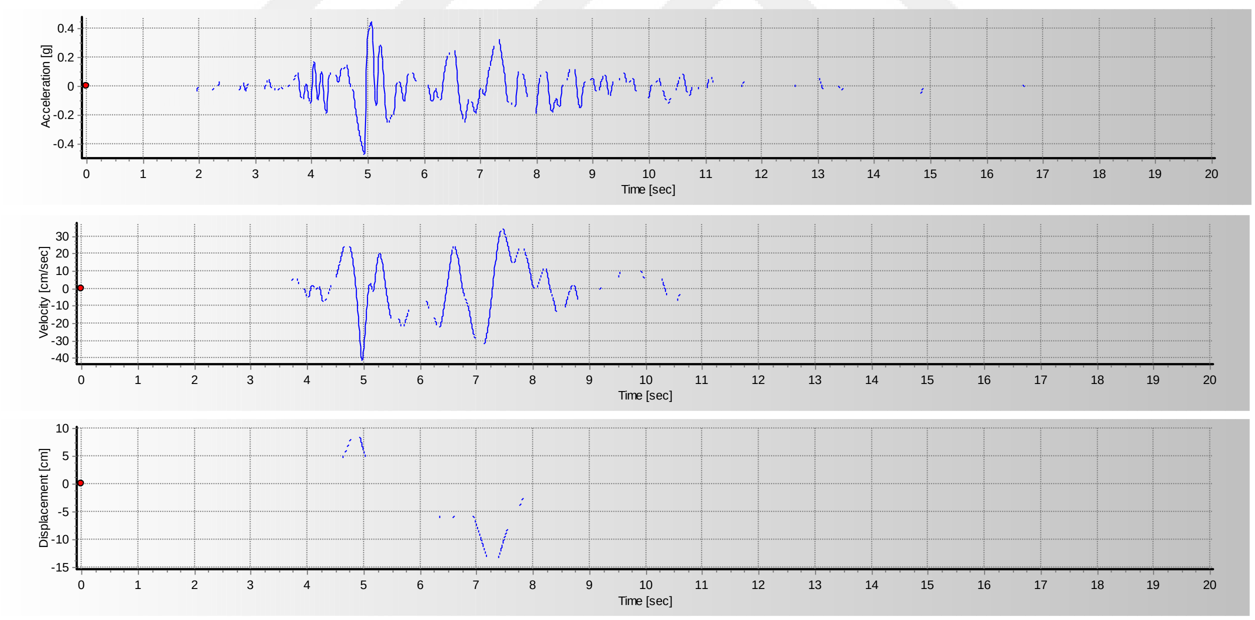

11. Hills - Parachute Test Site Earthquake: